Atmospheric behaviors and control measures of persistent organic pollutants: case studies on polybrominated diphenyl ethers and pentachlorophenol

Nguyen Thanh Dien

Table of contents

List of Tables

List of Figures

Chapter 1 Introduction

1.1 Background

The presence of toxic compounds such as persistent organic pollutants (POPs) in the environment, wildlife, and humans, poses a serious public health and environmental problems even at low levels. POPs have been identified as persistent, bioaccumulative, and toxic (so-called PBT properties) together with long-range transport (LRT) [1]. National, regional and global control actions have been made to restrict and eliminate the production, use and emission of POPs. Among the agreements and treaties, the Stockholm Convention (SC) on POPs, a global treaty under UNEP, entered into force in 2004 with the objective to protect human health and the environment from hazardous, long-last chemicals [2]. The SC has promoted various aspects of the implementation frameworks for sound management of chemical wastes, namely, national implementation plan (NIP), emission inventory guidance, best available techniques (BAT) and best environmental practices (BEP), global monitoring plan (GMP), unintentional POPs, waste management and stockpiles, persitent organic pollutant review committee (POPRC), and new POPs.

In order to examine the effectiveness of reduction policies, atmospheric levels of POPs have been monitored at multiple stations throughout the world. In addition, by analyzing the extensive air data and corresponding meterological data for different seasons, we can gain insight into the atmospheric behavior of POPs (e.g., seasonality). In other aspects, estimation in-use stock of POPs and air emission inventory can assist to explore their exposure pathway. This can help selecting the technological control measure regarding BAT and BEP, and drafting the policy measure in order to reduce and deplete POPs in society. By the means of substance flow and modeling study, we can deal with the environmental emission and behavior, draft the policy and technological control measures for POPs. In this thesis, we applied these methods for penta-brominated diphenyl ether (penta-BDE), octa-brominated diphenyl ether (octa-BDE), and pentachlorophenol (PCP) as regards the new POPs and deca-brominated diphenyl ether (deca-BDE) as regards the candidate POP. This study plays an important role in enhancing integrated framework for waste prevention of these compounds based on the scientific ground, in adapting to the Stockholm Convention.

Polybrominated diphenyl ethers (PBDEs) are some of the most widely used brominated flame-retardants (BFRs), and include three major PBDE technical mixtures, namely, penta-BDE, octa-BDE, and deca-BDE. PBDEs have been applied extensively to electronics, textiles, furniture, automotive interiors, and electronic and electric devices. PBDEs can be released to the environment during every step of their life cycle, starting with releases during production, leaching/losses from products during usage, and inappropriate disposal (e.g., incineration, land-filling, and e-waste disposal) [3]. The indicated widespread and persistent occurrence of

PBDEs in the indoor and outdoor environments poses a potential risk to animals and humans [4]. PBDEs have the potential for adverse human health effects, particularly neurotoxicity and thyroid hormone metabolism disruption [5,6]. Kiciński et al. [5] investigated the neurobehavioral effects of brominated flame retardants in humans in the large samples of biomonitoring program. They found that low-level PBDE exposure (0.18 pg/mL (or 180 ppt) for BDE-99; 0.15 pg/mL (or 150 ppt) for BDE-100) was associated with changes in the motor function and serum levels of FT3 (free triiodothyronine) and TSH (thyroid stimulating hormone). Leijs et al. [6] found that the thyroid hormone system in Dutch adolescents was influenced by current background levels of PBDEs (mean: 10.5 ng/g lipid).

Because of their apparent toxicity, penta- and octa-BDEs were phased out worldwide and were listed as persistent organic pollutants (POPs) under the 2009 Stockholm Convention [7]. In 2012, the European Chemicals Agency (ECHA) identified deca-BDE as a substance of extremely high concern [8]. The Agency has specified deca-BDE as being extremely bioaccumulative, and has stipulated the substance as persistent, bioaccumulative, and toxic (PBT). In 2013, Norway tabled a proposal to list deca-BDE as a POP under the Convention [9]. Recently, the Persistent Organic Pollutants Review Committee (POPRC) has recommended that the Stockholm Convention consider listing and specifying the control measures relevant to deca-BDE in its Annex A (with the specific exemption of various critical legacy spare parts used in the automotive and aerospace industries that still need to be defined) [10].

In Japan, limiting the domestic demand for commercial penta-, octa-, and deca-PBDEs had started decades earlier with penta- and octa-BDEs being phased out in 1990 and 1999, respectively. Although deca-BDE is still in use in Japan, the domestic demand has been declining gradually from 10,000 ton in 1990 to only 900 ton in 2013) [11]. Even though POP-PBDEs (penta- and octa-BDEs) and deca-BDE were phased out and restricted, as mentioned above, the main challenge to eliminate the substances is identifying the existing in-use stocks of PBDE-containing products and disposing of PBDE-containing waste [12,13]. Therefore, estimating the amounts of PBDE contained in products at present and in the near future is important. Such understanding is clearly a significant factor in the drafting of policy measures to reduce PBDE emissions.

In order to examine the effectiveness of reduction policies, the Japan Ministry of Environment (JMOE) has performed semiannual surveys (in warm and cold seasons from 2009−2012) on atmospheric PBDE congeners presented in gas plus particle phase concentrations [14,15]. However, one-third or more samples of PBDE congeners failed to reach the limit of detection (LOD). This causes inappropriate to apply linear regression analysis to see the time trend of atmospheric PBDEs over the period 2009−2012. Therefore, it is essential to apply advanced analysis to deal with the missing values (also called as non-detect values or

censored values).

The seasonality on atmospheric PBDEs was often observed in outdoor air. Previous studies have consistently agreed that BDE-47 and -99 were higher in warm season, suggesting a seasonal effect on less-brominated PBDEs [16,17]. Up to now, many articles [18-21] found that BDE-209 concentrations in outdoor air were higher in cold season than in warm season. However, their explanation on this tendency was unclear since the environmental fate and behavior of BDE-209 were not fully understood and still need to be clearly addressed.

Pentachlorophenol (PCP) was widely used in agricultural and industrial applications as wood preservative, herbicide, pesticide, fungicide and broad-spectrum biocide over the world [22]. According to the International Register of Potentially Toxic Chemicals (IRPTC), 90,000 ton PCP per year was produced globally in 1983 [23]. By the 1990s, the widespread use of PCP was discontinued in the most countries. Its use has declined due to its high toxicity and slow biodegradation. In 2015, the Conference of the Parties (COPs) adopted amendments to Annex A to the Stockholm Covention to list PCP and its salts and esters as the new POPs [24]. The POPRC and COPs have concluded that PCP its salts and esters are likely, as a result of their long-range environmental transport, to lead to significant adverse human health and environmental effects such that global action is warranted. PCP poses a serious health effects including acute effects, chronic effects, reproductive/developmental effects, and cancer risk [24]. Recently in 2016, the Japan Ministry of Economy, Trade and Industry (METI) has announced the decision to include PCP (its salts and esters) in Class I Specified Chemical Substances and to prohibit the importation of products containing such substances [25]. Under the new amendments, PCP (salt or ester) cannot be imported as preservatives, wood antiseptic, and glue.

Domestic use, such as indoor application of wood preservatives and paints on PCP or PCP-treated indoor wood panels and boards, may lead to high concentration in the indoor atmosphere. The ban on use of PCP for this purpose has been considered in most developed countries. Many countries have restricted the agricultural use and use in fabric as well. In Japan in 1990, the registration of all products containing PCP as agricultural chemical was withdrawn. Then, in 2003, the use of PCP as an agricultural chemical was banned [26]. PCP is currently used as wood preservative in the industry market in the United Nations Economic Commission for Europe (UN-ECE) region [27]. PCP and its microcontaminants (dioxins, furans, and hexachlorobenzene) are released into the environment during the production, use, in-use products, and disposed waste of PCP. Wood preservation and hazardous waste handling are the most important sources of PCP emissions. In the U.S., approximately 2,600 kg PCP was released in 2008, of which 172 kg (7%) was released to air, 513 kg (20%) to water and 1,865 kg (72%) was land filled [28].

PCP is released to the air by evaporation from treated wood surfaces and factory waste

disposal (chemical manufacturing plants and wood preservation plants). It enters surface water and groundwater from factories, wood-treatment facilities, and hazardous waste sites. It also enters the soil as a result of spills, disposal at hazardous waste sites, and its use as a pesticide. The physical and chemical properties of PCP suggest that not much PCP will evaporate into the atmosphere and that most of it will move with water and generally stick to soil particles. As a result, the monitoring data shows that PCP were found higher concentrations in soil, sediment, and sludge than that in the air [26,29]. The soils close to the sawmill or former production facilities remain highly contaminated. Kitunen et al. [30] found that there was no significant decrease of PCP in soil around the wood preserving sites up to five years after the last use of technical PCP. In the U.S, several PCP-contaminated sites have been classified as superfund sites. Also, the An-Shun site (Southern Taiwan) has been known for its extremely high concentration of PCP (0.312–110 μg/g) and polychlorinated dibenzo-p-dioxins and dibenzofurans, in brief, dioxins or PCDD/Fs (36 ng I-TEQ/g) in soil [31]. These high concentrations in the soil around the site of an old factory are related to the former industrial production of chlorophenols (CPs). There is, therefore, considerable interest in the remediation of this site. Various methods have been promoted for the remediation of PCP contaminated soil such as biodegradation, thermal treatment, nanomaterial, etc [32]. Among these current methods, nanomaterial was considered as one of the effective technologies to recover the soil from PCP contamination [33,34].

1.2 The aim of this study

The main objectives of this thesis were (1) to quantify the atmospheric emissions and behavior of PBDEs using the statistical analysis, (2) to investigate how the policy and technological control measure, using substance flow analysis, can help reduce PBDEs in society, and (3) to provide a technological control measure dealing with PCP-contaminated soil. The specific objectives was as follows:

(i) To determine the factors influencing atmospheric concentrations of PBDEs with focusing on meteorological parameters (atmospheric boundary layer height, temperature, and rainfall rate) and human activities (yearly trend and population density)

(ii) To estimate the amount and time trend of in-use stocks of PBDEs at present and near future and their atmospheric emissions

(iii) To treat PCP-contaminated sandy soil, bimetallic iron (BioCAT as a commercial product) was applied as one of the technological control measures.

1.3 Structure of the thesis

Figure 1.1 presents the structure of thesis covering five main chapters as briefly describing as follow:

Chapter 1 outlines the background of polybrominated diphenyl ethers (PBDEs) and pentachlorophenol (PCP) studies and determines the aim and scope of study.

Chapter 2 presents factors influencing atmospheric behaviors of PBDEs, that were relied on the long-term monitoring of atmospheric PBDEs across 50 sampling sites during 2009–2012 in Japan (using Tobit regression analysis)

Chapter 3 presents how the estimation of in-use PBDE stock can help drafting the policy and technological control measure in order to reduce and deplete PBDEs in society (using population balance model)

Chapter 4 presents bimetallic iron material as one of the technologies to recover the soil from PCP contamination (using microcosm test)

Chapter 5 draws the conclusions and recommendations for future research

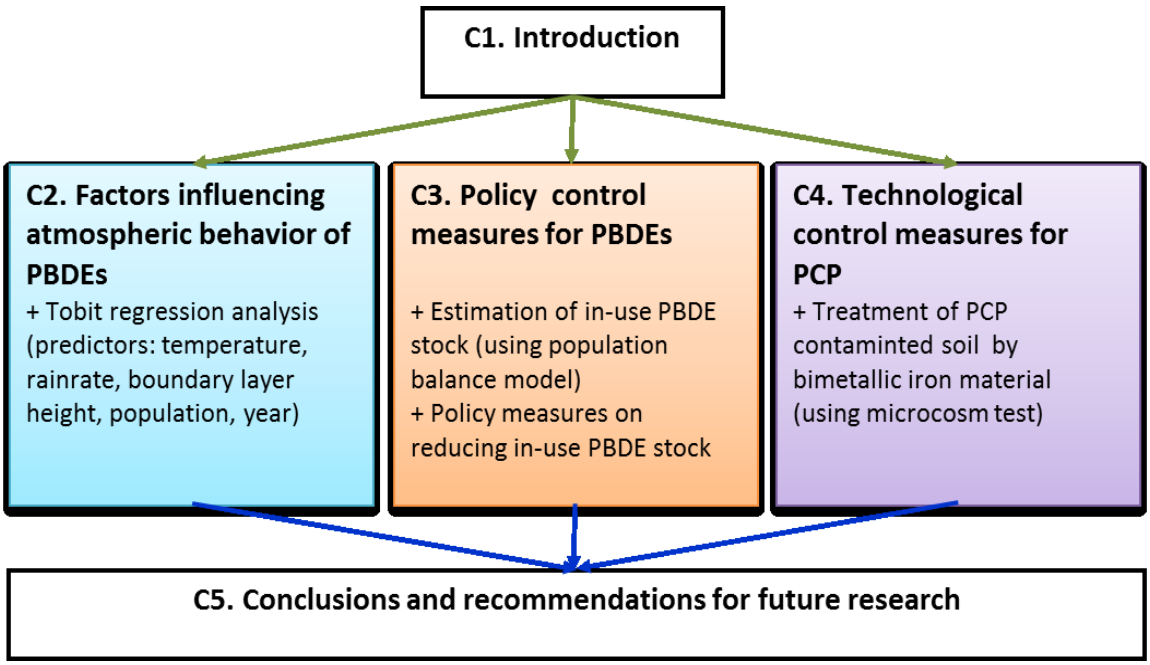

Figure 1.1 Structure of the thesis

References

1. Scheringer M (2009) Long-range transport of organic chemicals in the environment. Envi Toxico Chem 28: 677–690

2. UNEP. Stockholm Convention on persistent orgarnic pollutant. http://chm.pops.int/Home/tabid/2121/Default.aspx

3. Sakai S, Hirai Y, Aizawa H, Ota S, Muroishi Y (2006) Emission inventory of deca-brominated diphenyl ether (DBDE) in Japan. J Mater Cycles Waste Manag 8: 56–62

4. Besis A, Samara C (2012) Polybrominated diphenyl ethers (PBDEs) in the indoor and outdoor environments − A review on occurrence and human exposure. Environ Pollut 169:217–229

5. Kiciński M, Viaene MK, Den Hond E, Schoeters G, Covaci A, Dirtu AC, Nelen V, Bruckers L, Croes K, Sioen I, et al. (2012) Neurobehavioral function and low-level exposure to brominated flame retardants in adolescents: a cross-sectional study. Environ Health 11: 86

6. Leijs MM, ten Tusscher GW, Olie K, van Teunenbroek T, van Aalderen WMC, de Voogt P, Vulsma T, Bartonova A, Krayer von Krauss M, Mosoiu C, et al. (2012) Thyroid hormone metabolism and environmental chemical exposure. Environ Health 11: S10

7. UNEP (2009) Stockholm Convention on Persistent Organic Pollutants (POPs): the new POPs under the Stockholm Convention. http://chm.pops.int/TheConvention/ThePOPs/TheNewPOPs/tabid/2511/Default.aspx . Accessed 18 February 2015

8. European Chemicals Agency (ECHA) (2012) Agreement of the member state committee on the identification of bis (pentabromophenyl) ether [decabromodiphenyl ether] as a substance of very high concern (adopted on 29 November 2012)

9. UNEP (2013) Proposal to list decabromodiphenyl ether (commercial mixture) in Annexes A, B and/or C to the Stockholm Convention on Persistent Organic Pollutants. UNEP/POPS/PORC.9/2

10. UNEP (2015) Report of the Persistent Organic Pollutants Review Committee (POPRC) on the work of its eleventh meeting. Rome, Italy. 19–23 October 2015

11. Japan Ministry of Environment (JMOE) (2014) PBDE demand in Japan.

http://www.env.go.jp/chemi/dioxin/chosa/result_h26.pdf (in Japanese). Accessed 26 September 2014

12. UNEP (2015) Guidance on best available techniques and best environmental practices for the recycling and disposal of articles containing PBDEs listed under the Stockholm Convention on Persistent Organic Pollutants

13. Abbasi G, Buser AM, Soehl A, Murray MW, Diamond ML (2015) Stocks and flows of PBDEs in products from use to waste in the U.S and Canada from 1970 to 2020. Environ Sci Technol 49:1521−1528

14. Japan Ministry of Environment (JMOE) (2013) Results of the environmental monitoring. http://www.env.go.jp/chemi/kurohon/2013/sokutei/pdf/03_04_14.pdf (in Japanese). Accessed 26 September 2014

15. UNEP (2015) Global monitoring plan under the Stockholm Convention: The 2nd POPs monitoring report Asia-Pacific region

16. Gouin T, Harner T, Daly G, Wania F, Mackay D, Jones KC (2005) Variability of concentrations of polybrominated diphenyl ethers and polychlorinated biphenyls in air: implications for monitoring, modeling and control. Atmos Environ 39:151–166

17. Venier M, Hites RA (2008) Flame retardants in the atmosphere near the Great Lakes. Environ Sci Technol 42: 4745–4751

18. He W, Qin N, He QS, Kong XZ, Liu WX, Wang QM, Yang C, Jiang YJ, Yang B, Bai ZL, Wu WJ, Xu FL (2014) Atmospheric PBDEs at rural and urban sites in central China from 2010 to 2013: residual levels, potential sources and human exposure. Environ Pollut 192: 232–243

19. Shi S, Huang Y, Wan K, Dong L, Yang Y (2013) Levels and seasonal variations of polybrominated diphenyl ethers in the urban atmosphere of Beijing. China Bull Environ Contam Toxicol 90: 296–301

20. Drage DS, Newton S, deWit CA, Harrad S (2016) Concentrations of legacy and emerging fl ame retardants in air and soil on a transect in the UK West Midlands. Chemosphere 148: 195–203

21. Okonski K, Degrendele C, Melymuk L, Landlová L, Kukučka P, Vojta Š, Kohoutek J, Čupr P, Klánová J, Vojta S, Kohoutek J, Cupr P, Klánová J (2014) Particle size distribution

of halogenated flame retardants and implications for atmospheric deposition and transport. Environ Sci Technol 48:14426–14434

22. Fisher B (1991) Pentachlorophenol: toxicology and environmental fate. J Pesticide Reform 11:1–5

23. International Registrer of Potentially Toxic Chemicals (1983) Data profile on pentachlorophenol. United Nations Environment Programme, Geneva.

24. UNEP (2015). The Conference of the Parties to the Stockholm Convention on Persistent Organic Pollutants at its seventh meeting. Decision SC‐7/13: Listing of pentachlorophenol and its salts and esters in Annex A

25. METI (2016) http://www.meti.go.jp/english/press/2016/0226_02.html. Accessed 10 June 2016

26. UNEP (2013) Report of the Persistent Organic Pollutants Review Committee on the work of its ninth meeting: risk profile on Pentachlorophenol and its salts and esters

27. van der Zande A (2010) Exploration of management options for Pentachlorophenol (PCP). Paper for the 8th meeting on the UNECE CLRTAP task force on Persistent Organic Pollutants, Montreal.

28. EPA (2010) Toxic Release Inventory. U.S. Environmental Protection Agency, available via http://www.epa.gov/triexplorer/chemical.htm)

29. Zheng W, Wang X, Yu H, Tao X, Zhou Y, Qu W (2011) Global trends and diversity in pentachlorophenol levels in the environment and in humans: a meta-analysis. Environ Sci Technol 45(11):4668–75

30. Kitunen VH, Valo RJ, Salkinoja-Salonen MS (1987) Contamination of soil around wood preserving facilities. Environ Sci Technol 21:96–101

31. Environmental Protection Bureau of Tainan City (2004) The pollution survey of two-ninth paths of Tainan City. Report Number 2004-09-25

32. Thuan NT, Dien NT, Chang MB (2013) PCDD/PCDF behavior in low-temperature pyrolysis of PCP-contaminated sandy soil. Sci Tot Env 443: 590–596

33. Morales J, Hutcheson R, Cheng IF (2002) Dechlorination of chlorinated phenols by

catalyzed and uncatalyzed Fe^0 and Mg^0 particles. J Hazard Mater B90:97–108

34. Dien NT, Windt WD, Buekens A, Chang MB (2013) Application of bimetallic iron (BioCAT slurry) for pentachlorophenol removal from sandy soil. J Hazard Mater 252–253:83– 90

Chapter 2 Factors influencing atmospheric behavior of PBDEs

2.1 Introduction

2.1.1 PBDE management in Stockholm Convention and in Japan

Polybrominated diphenyl ethers (PBDEs), including penta-BDEs and octa-BDEs, were listed as persistent organic pollutants (POPs) in the Stockholm Convention in 2009. In Japan, the use of penta-BDEs and octa-BDEs was stopped in new products in 1990 and 1999, but old products containing these flame retardants are still in use. Deca-BDE is the main form of PBDEs in Japan, but its domestic demand is gradually decreasing (from 10,000 t in FY1990 to 900 t in FY2013) [1]. PBDE-containing products are expected to decrease in abundance along with decreasing demand for them, since the average lifespan of consumer products (such as electronic products and vehicles) in Japan is around 10−15 years [2]. Sakai et al. [3] found that the largest stock of deca-BDE exists in in-use consumer products, and emissions from such products were estimated to be the largest source of deca-BDE into the air. These suggest the importance of emissions during the service life of products containing deca-BDE.

2.1.2 Long-term monitoring PBDEs in globe (literature review) and in Japan (JMOE)

To examine the effectiveness of reduction policies, environmental levels of PBDEs have been monitored at multiple stations throughout the world [4−10]. The Japan Ministry of Environment (JMOE) has performed semiannual surveys (in warm and cold seasons from 2009−2012) on atmospheric PBDE congeners presented in gas plus particle phase concentrations [11,12]. In this annual survey, 38 sites in prefectural governments across Japan were selected to monitor air samples of PBDEs using active samplers, then samples were analyzed by appointed laboratories. The 292 air samples from the JMOE survey are a valuable dataset for analysis of the temporal, spatial, and seasonal trends of atmospheric PBDEs in Japan.

2.1.3 Dealing with nd data for statistical analysis on PBDE data

In the JMOE's report, they considered only the yearly trend of PBDEs, but factoring out other parameters (such as meteorological and geographic conditions). In addition, once one-third or more samples of PBDE congeners failed to reach the limit of detection (LOD), they judged it inappropriate to apply linear regression analysis, in which cases no trend was reported. Therefore, it is essential to apply advanced analysis to determine which factors influenced concentrations of PBDEs in the missing values (also called as non-detect values or censored values) over the period 2009−2012.

When there are several observations at the limit (e.g., 0 or < LOD), this feature destroys the linearity assumption so that the linear model with simple substitutions is clearly inappropriate [13,14]. In previous studies of atmospheric PBDEs, non-detect (nd) values were assigned as a

value of zero, one-half or another fraction of the LOD [5,10,15]. However, none of these substitutions are intellectually satisfying and would lead to artificially inflated average concentrations [16]. For dependent variables in linear regression analysis, the use of substitution below the LOD may cause bias in parameters and their variances unless the proportion of assigned data is low (e.g., ≤ 10%) [17].

Helsel [18], in his 2012 statistical textbook, suggested two feasible approaches for dealing with nd values: nonparametric methods (for distribution-free procedures) and the Tobit model with maximum likelihood estimation (for procedures assuming a specific distribution). Nonparametric methods include (i) binary method-logistic regression, (ii) ordinal methods for one reporting limit, and (iii) Akritas-Theil-Sen nonparametric regression [18]. With (i) logistic regression, the response variable (Y value) is probability π, such as the probability of the concentration being greater than or equal to the reporting limit. The probability of falling below the reporting limit is then 1-π. For application, the Y value for each observation is either a 1 (nondetect) or a 0 (detect). Hence, this method is suitable when dealing with many nondetect values and binary relation in the dataset. However it may cause the loss of information when dealing with few/moderate nondetect values and multiple relation. The ordinal method for one reporting limit (ii), the alternative to the estimate of slope in linear regression, is the median of all possible slopes between pairs of data points. Both the slope and intercept are affected by any value chosen to represent censored observations, making the ordinal method invalid for censored data unless there are very few censored observations (less than 15%). A major advantage of (iii) the Akritas-Theil-Sen (ATS) slope estimator over the maximum likelihood estimator is that the ATS can be computed for doubly censored data, data where X (explanatory variable) and Y (response variable) are both censored. However, the application of ATS on multiple X variables is still being challenged. The Tobit model is well-suited to analyze data with one or multiple censoring limits [19]. This is confirmed by the better model fits for the Tobit model compared with the ordinary least squares (OLS) regression [13,14,19]. In environmental studies, the normal distribution or log-normal distribution has been widely used to describe the widespread data. The Tobit model with maximum likelihood estimation (MLE) is increasingly used in environmental studies for air quality and for geochemistry [18]. Therefore, in this study, we applied the Tobit model, requires no substitution of fabricated data, for the multiple regression analysis. The Tobit model (also called the censored regression model), first suggested in a pioneering work by Tobin [13], is a hybrid of probit analysis and multiple regression. Amemiya [14] and Schnedler [19] have proven that the maximum likelihood estimator suggested by Tobin for the censored model is consistent (which means it approaches the true value of the parameter being estimated).

2.1.4 Seasonality of PBDEs and related factors

The seasonality of atmospheric PBDEs has been observed often in the outdoor air. Previous studies have consistently pointed out that the concentrations of BDE-47 and -99 were higher during the warm season, suggesting a seasonal effect on less-brominated PBDEs [20,21]. A study by Gouin et al. [20] has found that temperature and precipitation had a significant effect on a simulated concentration of BDE-47. The atmospheric boundary layer (ABL) height (or the height of the well-mixed layer of air above the earth's surface) combined with the temperature, has been indicated as crucial controlling factors of the diel (24 h) variability of the atmospheric PBDEs and polychlorinated biphenyls (PCBs) [22,23]. A study by Moeckel et al. [23] has pointed out that temperature was the primary driving force of the diel concentration pattern observed for BDE-28. In contrast, the effect of the atmospheric mixing height (or ABL), combined with irreversible deposition on aerosol particles, could explain the diel patterns of BDE-47, -99, and -100. This study was conducted during periods of stable weather conditions (high atmospheric pressure, with scant cloudiness, and no rain) that include repetitive diel patterns of meteorological conditions. However, the effects of ABL on the long-term trends of atmospheric PBDEs (especially BDE-209) have not been determined yet.

Furthermore, research [15,24−28] has shown that the BDE-209 concentrations in the indoor and outdoor air were higher during the cold season in comparison with the warm season. The BDE-209 concentrations were relatively high during winter and autumn and low in summer and spring, consistent with the seasonal trends in the atmospheric concentrations of suspended particles [24]. In addition, the concentrations of particulate matter during the winter were two or three times higher than were those during the summer. This likely reflects the use of domestic heating in winter, a lower atmospheric boundary layer, and higher gas-to-particle conversion because of the lower temperatures [26,29].

Meteorological conditions, such as ambient temperature, boundary layer height, and rainfall, are considered important factors influencing the atmospheric concentrations of PBDEs [20,30]. Partitioning of PBDEs between atmospheric gas and particulate phases is a key factor for understanding their environmental fate and behavior [31]. Socioeconomic factors related to gross domestic product (GDP) and population density also influenced the distribution of the various PBDEs among regions [21,32]. In addition, the building volume was found to be a good predictor of urban PBDE air concentrations [33].

2.1.5 Atmospheric boundary layer height

The atmospheric boundary layer (ABL) height is an important parameter in analyzing the air quality, studying pollutant dispersion, and quantifying pollutant emissions and sources [34,35]. The ABL controls the interactions between the atmosphere and the oceans and land, and determines the air volume for the dispersion of all the atmospheric constituents emitted at the

surface of the Earth. The ABL cannot be measured directly; however, it can be estimated by an upper-air instrument [34]. Various indirect measuring techniques have been developed, such as Light Detection And Ranging (lidar) observation [35−37] and radio sounding [38]. However, there are limitations to these methods, such as an unavailable observation over the long-term at multiple sites [35].

In order to deal with the insufficient observation, the global climatology information relevant to the ABL height can be retrieved from reanalysis data, which combines the information obtained from observation with those from models. These data can provide important insight, from a global perspective, into the physics pertaining to the boundary layer. Moreover, such data can be used to evaluate weather and climate prediction models [39,40]. The Japanese global reanalysis (JRA-55) database, based on four-dimensional variational analysis (latitude, longitude, vertical level, and time), provides high-quality, long-term data (from 1958) [40]. Combining the data from the JRA-55 and the JMOE provides an opportunity to study the relationship between the ABL and the atmospheric PBDEs.

2.1.6 Mechanism of indoor PBDE emission into outdoor environment: evaporation and abrasion

The indoor emissions of PBDE-treated products are important pathways that facilitate risk assessment and control measures. A multimedia indoor model has indicated the indoor air as an emission source of PBDEs to the outdoor environment because of the volatilization of the substances from consumer products [41,42]. As regards BDE-47 and -99, characterized by high volatility and the predominance of the gas fraction, the volatilization process from treated products into the indoor air is the main transfer mechanism [43,44]. In contrast, as regards BDE-209, characterized by low volatility and the predominance of the particle fraction, the transfer mechanism from the treated products into the indoor air is mainly abrasion or weathering [45,46].

2.1.7 The aims of study

Our goals in this study are

(i) to evaluate a multiple linear regression model with simple substitutions of missing values and a Tobit model without substitution, based on atmospheric PBDEs across Japan

(ii) to confirm the yearly trend and seasonal pattern of atmospheric PBDEs

(iii) to determine factors (temperature, rainfall rate, ABL, population density, and year) influencing the atmospheric PBDE concentrations

2.2 Materials and methods

2.2.1 Data collection

Atmospheric PBDE congener concentrations (presented in gas plus particle phases) and concurrent ambient air temperatures were measured by JMOE (2013) from 38 sites across Japan during four years (2009−2012). For each site, sampling was conducted twice a year, in warm season (around August, September, October) and cold season (around November, December, January). Air samples (n=292) were collected using active samplers with medium volume (MV) or high volume (HV) equipped with a series of quartz microfiber filter (QMF), polyurethane foam (PUF), and activated carbon fiber (ACF). The sampling period was three or seven days per atmospheric sample. The total air volumes were approximately 1000 m^3 for MV, and 3000 m^3 for HV, per atmospheric sample [11,12].

Rainfall rate data were obtained from the Japan Meteorological Agency [47]. Melymuk et al. [33] found that building volume, rather than population density, was the better predictor of urban PBDE air concentrations. However, it is difficult to evaluate the building volume for 38 sites across Japan. Hence, we used the population density as one of the predictors in this study. The latitude and longitude information from 38 sampling sites were used to collect the mesh codes on 1 × 1 km grid cells, and data on population density were obtained from the Portal Site of the Statistics Office of Japan [48]. Details of location, location ID, active sampling method, PBDE congener concentration, population density, temperature, and rainfall rate are described by Dien et al. [49]. The percentage of non-detect samples and the variations of LODs with time for PBDE congeners are presented in Table 2.1.

Table 2.1 Number of non-detect samples for light and heavy BDE congeners [11]

	Year 2009		Year 2010		Year 2011		Year 2012		Total	Non
	nd/obs	LOD [pg·m^{-3}]	nd/obs	LOD [pg·m^{-3}]	nd/obs	LOD [pg·m^{-3}]	nd/obs	LOD [pg·m^{-3}]	nd/obs	detection (%)
BDE-47	1/74	0.03	1/74	0.05	3/72	0.07	15/72	0.1	20/292	7
BDE-99	8/74	0.04	9/74	0.05	14/72	0.06	22/72	0.06	53/292	18
BDE-153	46/74	0.06	32/74	0.04	40/72	0.05	65/72	0.1	183/292	63
BDE-154	37/74	0.03	46/74	0.06	33/72	0.04	47/72	0.04	163/292	56
BDE-183	41/74	0.1	33/74	0.1	42/72	0.1	68/72	0.2	184/292	63
BDE-209	18/74	5.0	43/74	9.1	12/72	4.0	27/72	5.0	100/292	34

Notes: obs is the number of observation; nd is the number of non-detectable concentration measurements

In this study, site-specific and time-dependent ABL data relevant to PBDE sampling (the latitude and longitude information and the sampling times) were estimated by using the JRA-55,

with the horizontal resolution being ca. 55 km, and the vertical levels being the surface and 60 levels up to 0.1 hPa. Kobayashi et al. [40] have presented a comprehensive report on the JRA-55, outlining the general specifications and basic characteristics. We collected three types of data from the JRA-55 database, including model-level analysis fields (*anl_mdl*), surface analysis fields (*anl_surf*), and constant fields (*TL319*). We collected data on the geopotential height, u-component of the wind, v-component of the wind, temperature, and the specific humidity from *anl_mdl*. The collection was done every six hours at 9 AM, 3 PM, 9 PM, and 3 AM (Japan time zone, equal to UTC+9) at 60 vertical levels. For *anl_surf*, data on the surface pressure, surface potential temperature, temperature, and specific humidity at the 2 m level were also collected every six hours at (local time) 9 AM, 3 PM, 9 PM, and 3 AM. Furthermore, geopotential and land cover (1=land, 0=sea) information was collected from *TL319*. The data were extracted with the OpenGrADS (version 2.0.2.oga.2), developed by Center for Ocean-Land-Atmosphere Studies (COLA) and Institute of Global Environment and Society (IGES). The Python open source program (version 2.7) (Python Software Foundation, Delaware, USA) was used to extract the meteorological data, which are encoded in GRIdded Binary format (GRIB, Edition 1) (World Meteorological Organization [WMO], Commission for Basic System [CBS]).

2.2.2 Estimating atmospheric boundary layer (ABL) height

Based on the above-metioned parameters, the height of the ABL was estimated from the maximum value obtained with the parcel method (PM) and the bulk Richardson number (Ri_b) method. The PM defines the ABL as the elevation to which an air parcel with ambient surface temperature can rise adiabatically from the ground by convection [34]. The ABL is set to the height z, where the potential temperature $\theta(z)$ (refer to Eq 1) is equal to that of the surface $\theta(z_0)$. To apply the PM, the condition $\theta(z_1) < \theta(z_0)$, with $z_1 > z_0$, corresponding to an unstable θ vertical profile, has to be fulfilled. The altitude range from start to end of this lift is considered statically unstable [50].

$$\theta(z) = T(z) \cdot (P_0/P(z))^{0.286} \qquad \textbf{Eq 1}$$

where T(z) is the temperature at height z (K), P(z) is the pressure at height z (Pa), P_0 is the reference pressure (100000 Pa), and z is the geopotential height above ground (m).

The Ri_b is a dimensionless parameter, combining the potential temperature and the vertical wind shear. The Ri_b is used to identify regions of dynamically unstable air [50]. The air compartment has variable heights to account for the formation of the convective mixed layer at daytime, and the nocturnal boundary layer and residual layer at nighttime [50]. During the day, ascending air from the heating ground drives convective mixing. At night, air layers near the surface cool much faster leading to a temperature inversion, which prohibits convective mixing. We considered a value for the critical Richardson number of 0.22 under unstable condition

(convective mixed layer in daytime) and a value of 0.33 under stable condition (nocturnal boundary layer in nightime) [34,51,52]. The Richardson number (Ri_b) is defined by

$$Ri_b = \left(\frac{g}{\Theta vs}\right) \cdot \frac{\Theta v(z) - \Theta vs}{u(z)^2 + v(z)^2} \cdot z \quad \textbf{Eq 2}$$

where g is the acceleration because of gravity (9.81 $m \cdot s^{-2}$), Θvs is the virtual temperature near the surface, $\Theta v(z)$ is the virtual potential temperature at height z, and v(z) and u(z) are the horizontal components of the velocity at z. Therefore, the virtual potential temperature, mixing ratio, and virtual temperature near the surface were calculated as shown in Eqs 3−5

$$\Theta v(z) = T(z) \cdot \frac{w(z) + 0.622}{0.622 \cdot (1 + w(z))} \cdot (P_0/P(z))^{0.286} \quad \textbf{Eq 3}$$

$$w(z) = Hs(z)/(1 - Hs(z)) \quad \textbf{Eq 4}$$

$$\Theta vs = T(2m) \cdot (1 + 0.61 \cdot Hs(2m)) \quad \textbf{Eq 5}$$

where w(z) is the mixing ratio, Hs(z) is the specific humidity, Hs(2m) is the specific humidity at 2 m, and T(2m) is the temperature at 2 m (K).

Subsequently, the ABLs calculated by Ri_b and PM were subtracted from the geopotential height of the surface to estimate properly the effective height of the mixing air that dilutes the air pollutants. Since atmospheric PBDEs were continuously monitored for three or seven days per sample, the relevant ABL values were estimated as the average of the daytime and nighttime for a sampling period, and were subsequently used in regression analysis.

2.2.3 Multiple linear regression model

2.2.3.1 Replacing nd with LOD and 1/2 LOD (without ABL)

The multiple linear regression model was applied to elucidate the atmospheric PBDE trends through the incorporation of temperature, rainfall rate, population density, time trend, and spatial variations. We applied the log-transformed data for PBDEs, which have been widely used for environmental concentration measurements [53]. We evaluated two different simple substitution methods, replacing the nd values with LODs and then with 1/2 LODs. The linear model was run by the Stata version 13 statistical software package (StataCorp, College Station, TX, USA) for panel analysis with maximum likelihood random effect.

$$\ln C_{i,y,s} = a + b_1/T_{outdoor\ i,y,s} + b_2\, Ra_{i,y,s} + b_3\, \ln(PD + 1)_i + b_4\, Y_y + \lambda_i + \varepsilon_{i,y,s} \quad \textbf{Eq 6}$$

where C is concentration of PBDE congeners (pg m^{-3}); Ra is rainfall rate (mm·h^{-1}); PD is population density (person·km^{-2}); Y is year (2009−2012); λ is a random effect of 38 sampling sites across Japan; ε is an error term that follows normal distribution with mean 0 and variance σ^2; a is intercept; b_1, b_2, b_3, b_4 are regression coefficients; i is the sampling location; y is the year; and s is the season.

2.2.3.2 Tobit model for censored data (without ABL)

The Tobit model, a censored regression model, is designed to estimate linear relationships between variables when there is censoring in the dependent variable [13]. In environmental science, we take care of the left-censoring (censoring from below) since the trace substances in the world's air, soil, and water are usually presenting the concentrations that are lower than LOD. In principle, values that fall at or below some threshold are censored. The Tobit model uses the censored data (non-detection) and the uncensored data (detection) in a regression procedure. In this model, if the true concentration C^* is larger than the LOD value, then the observed concentration C is equal to C^*. Otherwise, if the true concentration C^* is less than the LOD value, then the observed concentration C is censored to LOD as shown below

if C* > LOD, C = C*

if C* <= LOD, C = LOD

The parameters of the model are estimated by using a maximum likelihood method. The Tobit model is subsequently based on the latent variable model:

$$\ln C^*_{i,y,s} = a + b_1/T_{outdoor\,i,y,s} + b_2\, Ra_{i,y,s} + b_3\, \ln(PD+1)_i + b_4\, Y_y + \lambda_i + \varepsilon_{i,y,s} \quad \textbf{Eq 7}$$

The definition, assumption, and maximum likelihood estimation of the Tobit model are described in detail in Appendix. In this study, Tobit model was run by the function of panel analysis on censored model with left censoring limit using the Stata 13 software (StataCorp, College Station, TX, USA).

2.2.3.3 Tobit model for censored data (with ABL)

In an updated study, we performed similar Tobit regression analysis (as presented in 2.2.3.2) by using the former predictors (temperature, rainfall rate, population density, and year) plus an ABL predictor, as follows:

$$\ln C_{i,y,s} = a + b_1/T_{outdoor\,i,y,s} + b_2 \ln(Ra+1)_{i,y,s} + b_3\, \ln(ABL)_{i,y,s} + b_4\, \ln(PD+1)_i + b_5\, Y_y + \lambda_i + \varepsilon_{i,y,s} \quad \textbf{Eq 8}$$

where C is the concentration of PBDE congeners (pg m^{-3}); $T_{outdoor}$ is the outdoor temperature (K); Ra is the rainfall rate (mm·h^{-1}); PD is the population density (person·km^{-2}); ABL is the atmospheric boundary layer height (m); Y is the year (2009−2012); λ is a random effect of 50 sampling sites across Japan; ε is an error term that follows normal distribution with mean 0 and variance σ^2; a is an intercept; $b_1, b_2, b_3, b_4,$ and b_5 are regression coefficients; i is the sampling location; y is the year; and s is the season.

2.3 Results and discussion

2.3.1 Atmospheric PBDEs

2.3.1.1 Concentrations and congener profiles

Table 2.2 summarizes the gas plus particle phases of PBDE concentrations in air in Japan during 2009−2012. The arithmetic mean and geometric mean of $\sum_6 PBDEs$ were 16.4 pg m^{-3} and 11.02 pg m^{-3}, respectively.

Table 2.2 Gas plus particle phase concentrations of PBDE congeners (pg m^{-3}) in air in Japan from 2009-2012 [11]

Compound	Min	Max	Arithmetic mean	Median	Geometric mean	% Detection
BDE-47	0.015	46	0.76	0.30	0.32	93
BDE-99	0.020	36	0.39	0.12	0.12	82
BDE-153	0.020	2.10	0.09	0.050	0.05	37
BDE-154	0.015	3.30	0.07	0.030	0.04	44
BDE-183	0.050	11	0.19	0.10	0.10	37
BDE-209	2.0	290	12.20	8.0	7.97	66
$\sum_6 PBDEs$	2.38	325.5	16.40	11.34	11.02	

Note: values below limit of detections (LOD) are treated as 1/2LOD.

JMOE data showed the spatial variation of atmospheric PBDEs regarding different sampling sites (Figure 2.1). The geometric means of atmospheric PBDE concentrations were 38.65 pg m^{-3} for the Tokyo metropolitan area (range: 21−96 pg m^{-3}) and 26.27 pg m^{-3} for Osaka city (range: 12−116 pg m^{-3}) [11].

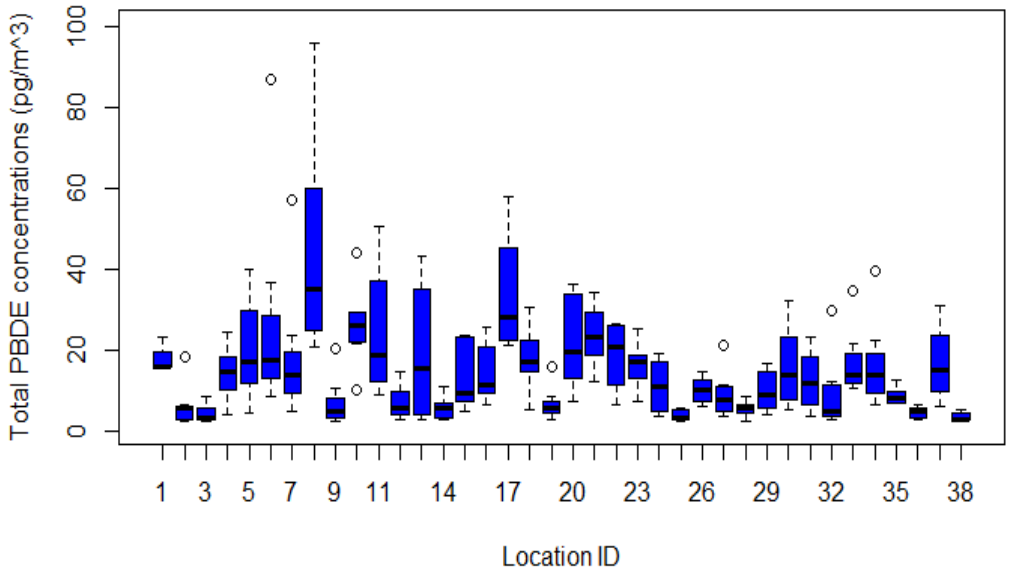

Figure 2.1 Spatial variation of PBDE concentrations across Japan

These results are comparable to the concentrations at urban sites around the Great Lakes, such as Chicago (mean: 56 pg m^{-3}) and Cleveland (mean: 77 pg m^{-3}) during 2005−2011 [9]. In the literature, high PBDE levels in air have been recently reported in Guangzhou (mean: 838 pg m^{-3}) and Beijing (mean: 781 pg m^{-3}) [25]. In the city center of Zurich, PBDE concentrations in ambient air were 17−591 pg m^{-3} in 2010−2011 and were on the upper end of concentrations reported in literature for urban sites with no point source of PBDEs [30]. In general, atmospheric PBDE concentrations in Japan were at rather low levels compared with worldwide urban locations (Table 2.3).

In JMOE data (2009−2012), PBDE data across Japan revealed the dominance of BDE-209 (87−97%), followed by BDE-47 (1−7%); then BDE-99 and BDE-183 (1−2% for each) (Figure 2.2 and Figure 2.3).

Table 2.3 Concentrations (pg m^{-3}) of PBDEs in atmosphere in literature measured by active air samplers

Location	Type	Sampling period	Number of congeners	BDE-209	∑PBDEs	References
Across Japan	Urban & rural	2009−2012	6	7.97[c] (12.20[d])	11.02[a,c] (16.40[a,d])	[11]
Tokyo (Japan)	Urban	2009−2012	6	16−78	21−96[a]	[11]
Osaka (Japan)	Urban	2009−2012	6	10−88	12−116[a]	[11]
Guangzhou (China)	Urban	2008−2009	12		838±126[a,e]	[25]
Beijing (China)	Urban	2008−2009	12		781±107[a,e]	[25]
Kuwait	Urban	2008−2010	7		57±83[b,f]	[6]
Chicago (U.S.)	Urban	2002−2003	19	1.5−878	13−980[a] (100±35[a,e])	[54]
Chicago (U.S.)	Urban	2005−2011	35	15.6[d]	56[a,d]	[9]
Cleveland (U.S.)	Urban	2005−2011	35	34.3[d]	77[a,d]	[9]
Southern Ontario (Canada)	Rural	2002	4	<3−105[g]		[55]
Toronto (Canada)	Urban	2007−2008	25		4.6−3,000[a]	[10]
Toronto (Canada)	Semi urban	2010-2011	15	0.86	38[a,d]	[56]
Across U.K	Urban & rural	2010	9		<10[b]	[5]
Izmir (Turkey)	Urban	2004−2005	7	20.7−28.7	32−82[a]	[57]
Etang de Thau (France)	Urban	2007	8	0.77−1.38	158−230[a]	[58]
Zurich (Switzerland)	Urban	2010−2011	7	3.5−314	17−591[a]	[30]
Entebbe (Uganda)	Urban & rural	2008−2010	10	2.15−20.9[d]	14.9−55.5[a,d]	[4]

Notes: [a] BDE-209 was included in the concentrations of ∑PBDEs; [b] BDE-209 was not included in the concentrations of ∑PBDEs; [c] geometric mean; [d] arithmetic mean; [e] mean with standard error; [f] mean with standard deviation; [g] particulate phase concentration

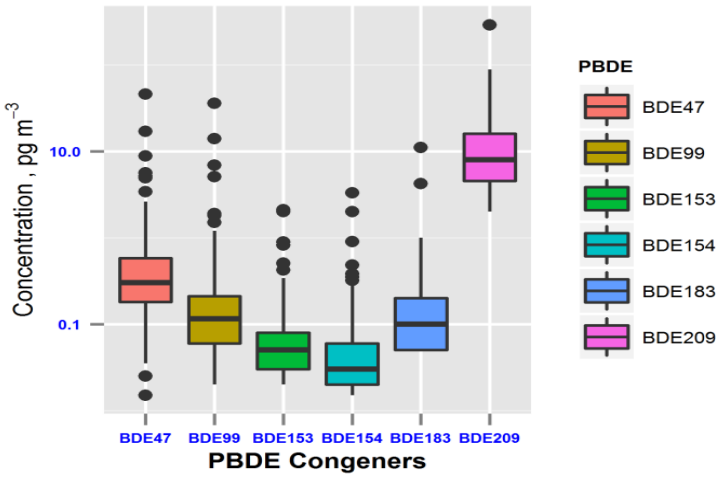

Figure 2.2 Boxplots comparing PBDE congener concentrations (pg m^{-3}) across Japan

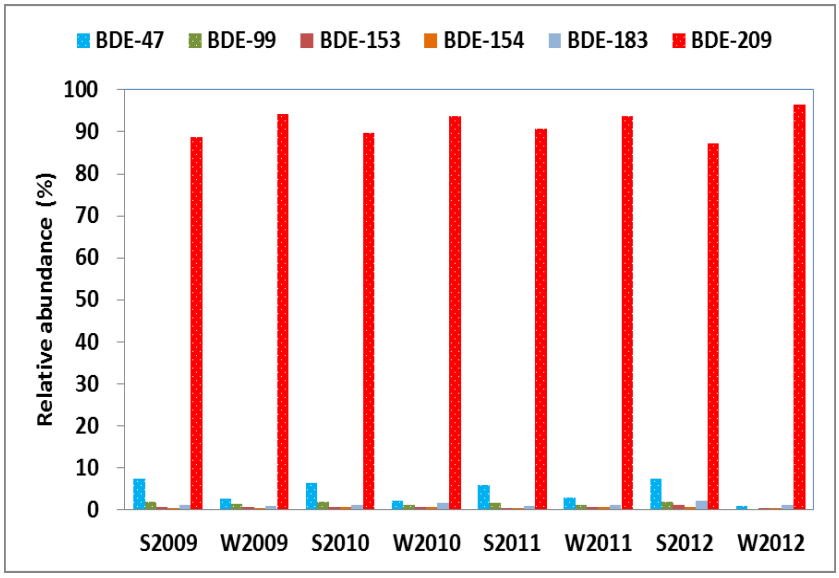

Figure 2.3 PBDE congener profiles across Japan

Notes: S represents summer, W represents winter; values below limit of detections (LOD) are treated as 1/2 LOD.

The distribution of PBDE congener profiles reflected the dominant use of BDE-209 in Japan. In the literature, BDE-209 has been recognized to occur in high concentrations and to dominate PBDE congener profiles in Southern Ontario (year 2002: Gouin et al. [55]), Zurich (years 2010−2011: Bogdal et al. [30]), and China (years 2008−2009: Yang et al. [25]).

2.3.1.2 Seasonal variations

Figures 2.4 (a) and (b) show temporal and seasonal trends for the two main dominant congeners BDE-47 and BDE-209. It seems that temporal trend of BDE-47 was declining, while

BDE-209 was stable.

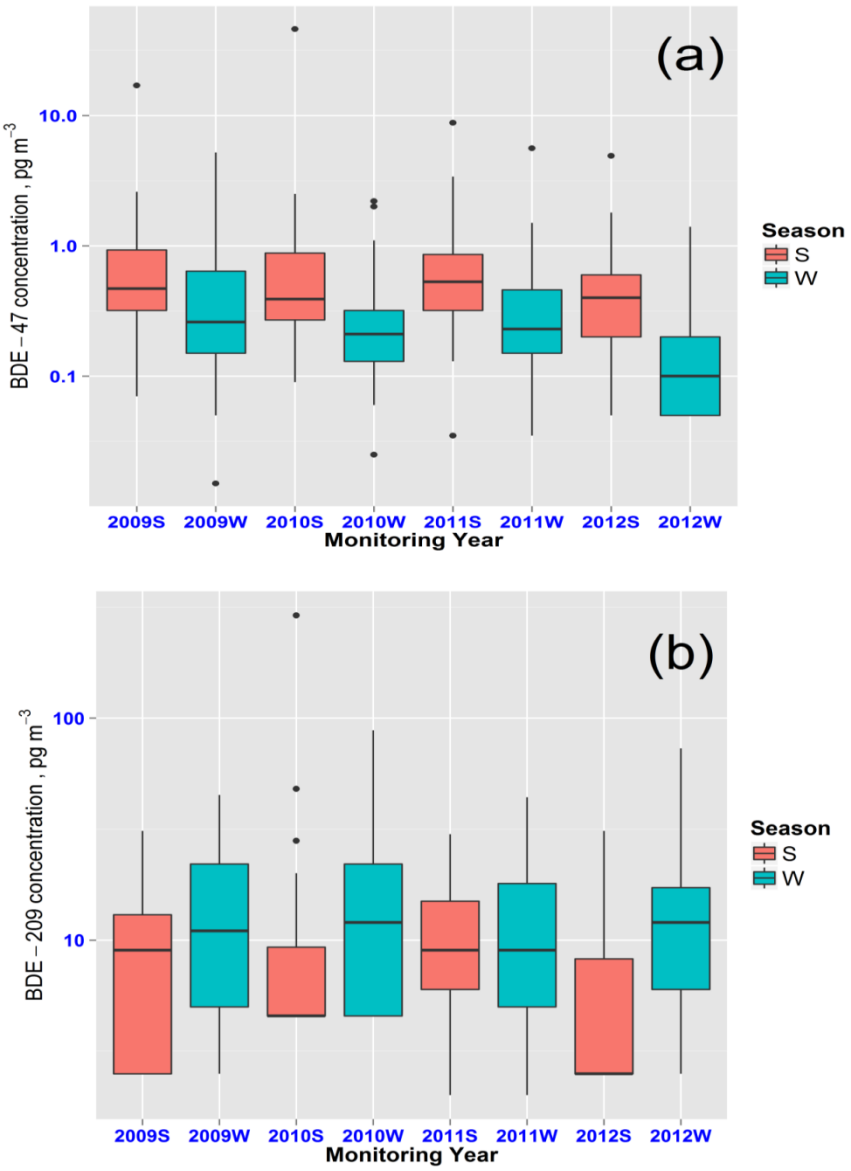

Figure 2.4 Temporal and seasonal trends of gas plus particle phase concentrations of (a) BDE-47 and (b) BDE-209 across Japan

Paired t-tests suggest that log-transformed concentrations of BDE-47 were significantly higher in summer than in winter, whereas the opposite trend was expressed for BDE-209 (details in Appendix). These behaviors of BDE-47 and -209 are in good agreement with the observed seasonality of atmospheric PBDEs in China [15,25].

To provide in-depth analysis, we performed multiple linear regression and Tobit regression to clearly elucidate the temporal and seasonal trends (using temperature as the explicit variable instead of season as the dummy variable) in atmospheric PBDE congeners (section 2.3.3).

2.3.2 Effect of the Tobit model on treatment of nd values from JMOE data

Table 2.4 Multiple regression results (without ABL) of non-censored (linear model) and censored (Tobit model) data on atmospheric PBDEs in JMOE data with n=292

Congeners	Predictors	Linear model						Tobit model		
		LOD			1/2 LOD			LOD		
		Coeff	SE	*p*-value	Coeff	SE	*p*-value	Coeff	SE	*p*-value
BDE-47	*Y*	-0.168	0.029	<0.001,***	-0.213	0.030	<0.001,***	-0.208	0.030	<0.001,***
(7% censoring	$1/T_{outdoor}$	-5018	355	<0.001,***	-5576	372	<0.001,***	-5527	376	<0.001,***
intensity)	*Ra*	-0.236	0.124	0.057	-0.252	0.130	0.053	-0.238	0.129	0.066
	ln*PD*	0.141	0.036	<0.001,***	0.156	0.037	<0.001,***	0.157	0.038	<0.001,***
BDE-99	*Y*	-0.166	0.033	<0.001,***	-0.216	0.035	<0.001,***	-0.247	0.039	<0.001,***
(18% censoring	$1/T_{outdoor}$	-1245	406	0.002,**	-1767	435	<0.001,***	-1900	473	<0.001,***
intensity)	*Ra*	-0.261	0.142	0.067	-0.374	0.152	0.014,*	-0.443	0.173	0.011,*
	ln*PD*	0.120	0.036	0.001,**	0.162	0.041	<0.001,***	0.172	0.045	<0.001,***
BDE-153	*Y*	0.080	0.028	0.004,**	0.011	0.036	0.760	-0.174	0.068	0.011,*
(63% censoring	$1/T_{outdoor}$	474	335	0.157	829	441	0.060	1430	745	0.055
intensity)	*Ra*	-0.113	0.118	0.337	-0.205	0.155	0.185	-0.579	0.283	0.041,*
	ln*PD*	0.031	0.018	0.092	0.059	0.026	0.025,*	0.166	0.057	0.004,**
BDE-154	*Y*	-0.039	0.030	0.183	-0.065	0.037	0.081	-0.121	0.057	0.033,*
(56% censoring	$1/T_{outdoor}$	162	357	0.650	582	456	0.203	1039	701	0.138
intensity)	*Ra*	-0.181	0.126	0.149	-0.377	0.160	0.019,*	-0.804	0.281	0.004,**
	ln*PD*	0.025	0.020	0.216	0.060	0.030	0.045,*	0.163	0.060	0.007,**
BDE-183	*Y*	0.096	0.029	0.001,**	0.006	0.038	0.873	-0.231	0.076	0.002,**
(63% censoring	$1/T_{outdoor}$	913	347	0.009,**	1294	459	0.005,**	2144	821	0.009,**
intensity)	*Ra*	-0.131	0.122	0.284	-0.208	0.162	0.200	-0.702	0.338	0.038,*
	ln*PD*	0.026	0.016	0.103	0.051	0.024	0.031,*	0.130	0.049	0.007,**
BDE-209	*Y*	-0.062	0.026	0.015,*	-0.065	0.032	0.042,*	-0.063	0.034	0.065
(34% censoring	$1/T_{outdoor}$	1133	314	<0.001,***	1589	394	<0.001,***	1812	424	<0.001,***
intensity)	*Ra*	-0.301	0.110	0.006,**	-0.597	0.138	<0.001,***	-0.808	0.179	<0.001,***
	ln*PD*	0.082	0.021	<0.001,***	0.123	0.028	<0.001,***	0.149	0.032	<0.001,***

Notes: Coeff is coefficient; SE is standard error; *p*-value is significance level; *** represents $p<0.001$; ** represents $p<0.01$; * represents $p<0.05$; *Y* is monitoring year; $1/T_{outdoor}$ is reciprocal outdoor temperature (K^{-1}); *Ra* is rainfall rate ($mm \cdot h^{-1}$); ln*PD* is natural logarithm of population density ($person \cdot km^{-2}$); n is number of data points.

Coefficient estimates, standard errors, *p*-values, and censoring intensity (percentage of non-detect samples) for regression analyses on PBDE congeners are shown in Table 2.4. In general, we can see the effect of different regression models by taking the ratios of means (or standard errors) between LOD (or 1/2 LOD) substitutions and Tobit model. Figure 2.5 shows that substitution method (with 1/2 LOD and LOD) and the Tobit model presented roughly similar regression coefficients and their standard errors when the censoring intensity was low (BDE-47: 7%; BDE-99: 18%).

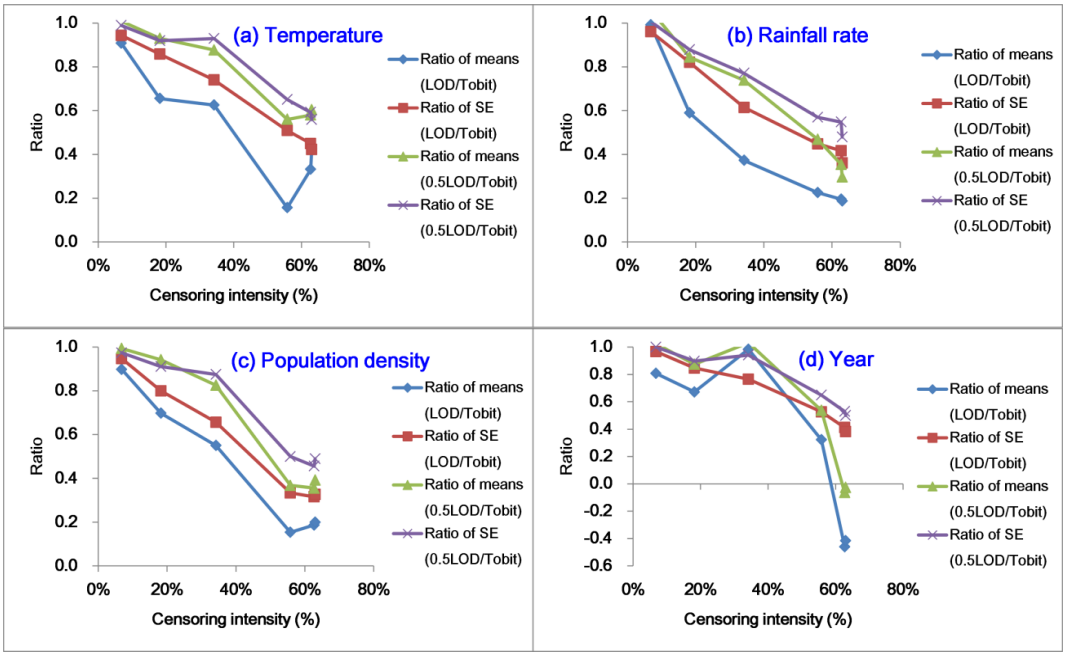

Figure 2.5 The ratio between means (standard errors) obtained by substitution method and Tobit model

The disagreement between the substitution method and the Tobit model is large when the censoring intensity is large (BDE-154: 56%; BDE-153 and -183: 63%) (Table 2.4, Figure 2.5). The similar effects between the substitution method and the Tobit regression were also derived by Zeghnoun et al. [59] for dealing with the non-detected serum dioxin data in the French Dioxin and Incinerators Study.

For rainfall rate, coefficients from the Tobit model clearly presented higher effects on heavy PBDE congeners ($p<0.05$; Table 2.4, Figure 2.6 (c)), but the coefficients from the linear model did not (Table 2.4, Figure 2.6 (a) and (b)).

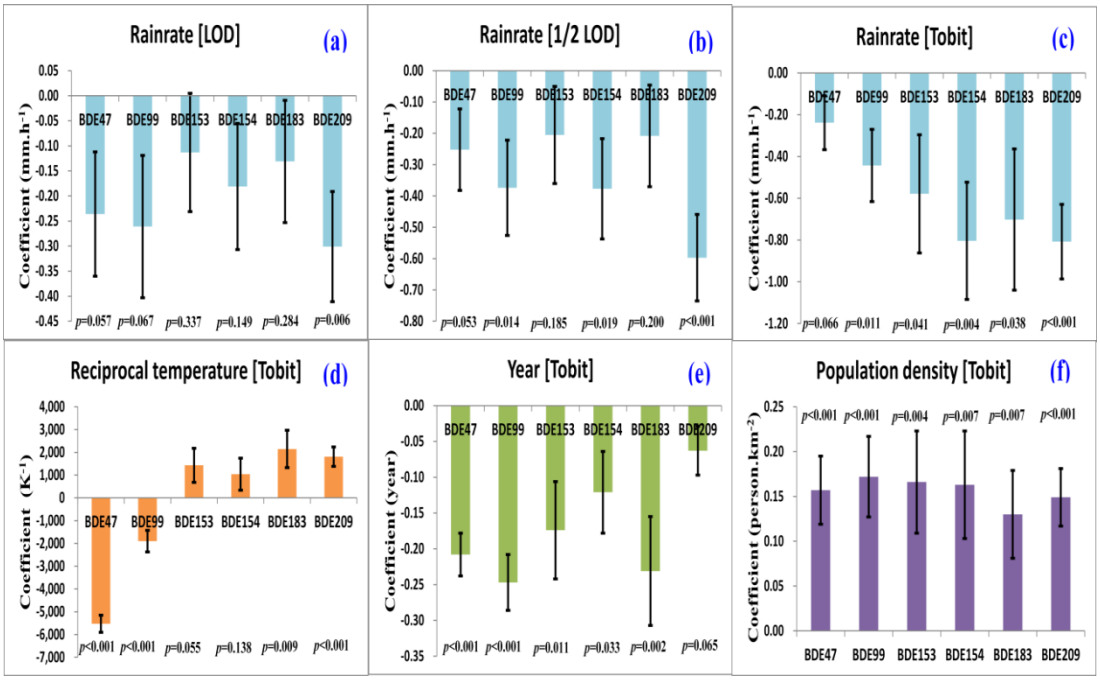

Figure 2.6 Regression coefficients on concentrations of PBDE congeners against (a) rainfall rate [LOD] (mm·h^{-1}), (b) rainfall rate [1/2 LOD] (mm·h^{-1}), (c) rainfall rate [Tobit] (mm·h^{-1}), (d) reciprocal temperature [Tobit] (K^{-1}), (e) year [Tobit], and population density [Tobit] (person·km^{-2}) across Japan.

Greater wash-out of particles (heavy PBDE congeners: BDE-153, -154, -183 and -209) than the gas phase (light PBDE congeners: BDE-47 and -99) during the rain event in Japan were in agreement with previous studies [60,61]. Thus, Tobit model displayed the better results for rainfall rate than linear model with LOD and 1/2 LOD substitutions. For yearly trends, coefficients from the Tobit model displayed a decrease for BDE-153 and -183 that coincides with the voluntary phase-out of penta- and octa-BDEs in new Japanese products in 1990 and 1999 (Table 2.4, Figure 2.6 (e)). In an opposite result, coefficients from both LOD and 1/2 LOD substitutions showed the increased trends of those congeners that disagree with the control measures in Japan (Table 2.4).

In addition to the accordance of the Tobit model with existing knowledge of rain scavenging effect on atmospheric PBDE congeners and with use patterns of PBDEs (as in the above discussion), the informal test of model specifications of the Tobit and probit models support the conclusion for the Tobit model with appropriate estimates. Wooldridge [62] stated that one way to informally evaluate whether the Tobit model is appropriate is to estimate the sign or magnitude of the ratio of coefficient estimates and standard deviation ($\gamma_i = \beta_j/\sigma$) between the Tobit model and probit model (details in Appendix). If the Tobit model holds, the ratios of β_j/σ from Tobit estimates and probit estimates have the same sign and magnitude. As a result, Table 2.5 consistently shows the same signs and the similar ratios of β/σ for both probit and Tobit

models for the explanatory variables (Y, $1/T_{outdoor}$, Ra, lnPD) that are significant (p<0.05) in both models.

Table 2.5 Tobit regression and Probit regression models on the explanatory variable

Congener	Predictor	Tobit model		Probit model	
		β_j/σ	p-value	β_j/σ	p-value
BDE-47	Y	-0.252	<0.001,***	-0.230	0.014,*
	$1/T_{outdoor}$	-6689	<0.001,***	-7356	<0.001,***
	Ra	-0.288	0.066	0.077	0.837
	lnPD	0.190	<0.001,***	0.237	0.001,**
BDE-99	Y	-0.250	<0.001,***	-0.097	0.122
	$1/T_{outdoor}$	-1920	<0.001,***	-3427	<0.001,***
	Ra	-0.448	0.011,*	-0.653	0.011,*
	lnPD	0.174	<0.001,***	0.220	<0.001,***
BDE-153	Y	-0.158	0.011,*	-0.128	0.104
	$1/T_{outdoor}$	1301	0.055	1159	0.198
	Ra	-0.526	0.041,*	-1.156	0.011,*
	lnPD	0.151	0.004,**	0.123	0.057
BDE-154	Y	-0.106	0.033,*	-0.183	0.006,**
	$1/T_{outdoor}$	915	0.138	1743	0.025,*
	Ra	-0.708	0.004,**	-0.399	0.172
	lnPD	0.143	0.007,**	0.142	0.025,*
BDE-183	Y	-0.208	0.002,**	-0.166	0.039,*
	$1/T_{outdoor}$	1931	0.009,**	845	0.366
	Ra	-0.632	0.038,*	-0.416	0.296
	lnPD	0.117	0.007,**	0.081	0.139
BDE-209	Y	-0.085	0.065	-0.023	0.710
	$1/T_{outdoor}$	2445	<0.001,***	3370	<0.001,***
	Ra	-1.090	<0.001,***	-0.937	0.002,**
	lnPD	0.201	<0.001,***	0.213	<0.001,***

For example, the β/σ ratios of Tobit and probit models for the "Year" predictor of BDE-47 are -0.252 and -0.230, respectively; or those ratios for the rainfall rate of BDE-154 are -0.106 and -0.183. Therefore, the Tobit model is appropriate for PBDE regression analysis in JMOE data with many nd values.

In the next section, we discuss how results of the Tobit model indicate the influence of environmental factors and human activities on atmospheric PBDEs.

2.3.3 Factors influencing atmospheric PBDEs

2.3.3.1 Temperature

The results of both linear model and Tobit model significantly presented negative slopes against $1/T_{outdoor}$ for gas plus particle phase concentrations of BDE-47 and -99 (with gas phase dominance), whereas positive slopes were produced for concentrations of BDE-183, and -209 (with particle phase dominance) (Table 2.4 and Figure 2.6 (d)). Previous studies have reported the negative relationship between the gas phase of light PBDE congeners (BDE-47 and -99) and reciprocal temperature [10,20,21,54]. However, the relationship between gas plus particle phases of PBDEs and reciprocal temperature has not been confirmed yet. Figure 2.6 (d) clearly shows that the regression coefficient against $1/T_{outdoor}$ for BDE-47 was higher than for BDE-99, probably due to a higher gas-phase fraction for BDE-47. On the other hand, although BDE-183, and -209 significantly present a positive slope, the regression coefficients were low. The gas-particle partitioning of PBDEs changes with temperature, with a higher gas fraction in summer and higher particle fraction in winter [31]. Along with gas-particle partitioning, hypotheses that could account for the seasonality of PBDE concentrations are as follows: (i) the emission behavior of PBDE congeners in indoor sources (e.g., constant emission related to the abrasion process of BDE-183 and -209, higher emissions by volatilization of BDE-47 and -99 in higher indoor temperature), and (ii) the seasonality of boundary layer height, leading to differences in outdoor environmental-loss processes. The combination of (i) and (ii) could represent major factors explaining seasonality of PBDE concentrations. We will confirm the quantitative calculation of these hypotheses in future work.

2.3.3.2 Rainfall rate

All PBDE congener concentrations (except BDE-47) were negatively related to rainfall rate (Table 2.4 and Figure 2.6 (c)). These confirm that the concentration of semivolatile organic compounds (SVOCs) in air may decrease significantly or even be reduced to zero during a rain event for substances that are washed-out very effectively [63]. Venier and Hites [61] found wet deposition as the main deposition process for PBDEs in the Great Lakes. In our study, greater effects of rainfall on PBDE removal occurred for heavy congeners with particle phase dominance (BDE-153, -154, -183, and -209) than for light congeners with gas phase dominance (BDE-99) (Table 2.4 and Figure 2.6 (c)). These observations confirm greater wash-out of particles than of the gas phase of PBDEs. Our results agreed well with those of Raff and Hites [60] who stated that there was a larger effect from rainfall on heavier PBDE congeners than on lighter ones. Wet and dry deposition of SVOCs that are controlled by their vapor-particle partitioning have been well documented by Bidleman [64]. Within the suite of PCB, PBDE congeners and PAH compounds, those that are less volatile and have low solubility and higher

particle fractions show greater wet and dry fluxes [64−66]. In comparison, PBDEs were more effectively removed from the atmosphere by precipitation than were PCBs [66].

2.3.3.3 Decreasing trend

BDE-209 was slightly decreased (−6%/a; $p = 0.065$); whereas BDE-47, -99, -153, -154, and -183 declined −21, −25, −17, −12, and −23%/a, respectively ($p < 0.05$), through the period 2009−2012 (Table 2.4 and Figure 2.6 (e)). The relatively steady levels of BDE-209 are likely the results of gradually decreasing numbers of new products containing BDE-209 coming into the Japanese market. The greater declines of some forms (BDE-47, -99, and -183) were likely due to the results of the stopping new products containing penta-BDEs and octa-BDEs in 1990 and 1999, and gradually decreasing of in-use products containing these flame retardants in Japan. The gradual decrease of PBDE containing products is supported by the information on the average lifespan of consumer products in Japan which is around 10−15 years [2]. In addition, the estimation of PBDE stocks in use in Japan showed the decreasing speed of penta-, octa-, and deca-BDEs following the pattern: penta > octa > deca, which is consistent with our interpretation of the changes in PBDE levels in ambient air (details in Chapter 3). Thus, atmospheric concentrations of PBDEs appear to reflect the control measures that have been implemented in Japan. The agreement between control measures and the following trend in atmospheric PBDEs has also been reported in other regions. In China, the phase-out of penta- and octa-BDEs generated a decrease in BDE-47 and -99 in atmospheric levels, with an increasing trend of BDE-209 since deca-BDE is not only still in use, but is being produced in the large volumes [32]. Long-term monitoring of atmospheric levels in Chicago and Cleveland in the Great Lakes area [9,21], United Kingdom [5], and Sweden and Finland [8] have shown declining trends of BDE-47. These significantly decreasing trends of BDE-47 could be mainly attributed to the ban of the penta- and octa-BDEs since 2004 in the EU, by the end of 2004 in North America, and since 2009 in the world [8]. Concentrations of BDE-209 were in a steady state at most Great Lakes sites from 2005−2012 [9,67]. As BDE-209 was recently removed from the United States market at the end of 2013, it may be too early to see the full effect of this market shift [67].

2.3.3.4 Population density

A positive correlation was observed between all congener concentrations and human population density within a grid cell (1 × 1 km). A 10% increase in human population density resulted in approximately 1.5% increase in each congener concentration (Table 2.4 and Figure 2.6 (f)). Generally, population density can explain spatial variation of atmospheric PBDEs. It is apparent that large industrial or urban centers, such as the Tokyo metropolitan area (site 8, *PD*: 22102, geomean $\sum_6 PBDEs$: 38.65 pg m^{-3}) and Osaka city (site 21, *PD*: 12531, geomean

$\sum_6 PBDEs$: 26.27 pg m^{-3}), release larger amounts of PBDEs to the atmosphere, possibly due to higher population density and the density of PBDE-treated products. Kunigami village (site 38, *PD*: 0, geomean $\sum_6 PBDEs$: 3.49 pg m^{-3}) and Okinoshima town (site 25, *PD*: 51, geomean $\sum_6 PBDEs$: 3.76 pg m^{-3}) are both located in rural areas where the population density (in 1 × 1 km) and the density of PBDE-treated products are very low, so that PBDE concentrations at those sites are also very low. However, some sites do not reflect the emission sources of PBDE-related population density (showing an opposite trend between PBDE concentration and population density). The average total PBDE concentration at Miyazaki city (site 36, *PD*: 4948, geomean $\sum_6 PBDEs$: 4.63 pg m^{-3}) was lower than one would expect from the local population density. The opposite trend was shown for Kagoshima city (site 37, *PD*: 155, geomean $\sum_6 PBDEs$: 14.69 pg m^{-3}): the average total PBDE concentration at this site was higher than one would expect from the population density. These sites might be affected by the specific characteristics of monitoring sites, such as building volume, distance from central business district, dwelling density, e-waste recycling, and so on [33].

2.3.3.5 Atmospheric boundary layer height (ABL)

2.3.3.5.1 Day/night and seasonal pattern of ABL

As the sampling time for the ABL data (corresponding to the PBDE sampling time) was only during early autumn and winter, at specific intervals (three or seven days per sample), the estimated ABLs would probably not show all the relevant information on the day/night, seasonal, and interannual timescales. Consequently, at first, over a period of four years, we analyzed the monthly ABLs for various representative sampling sites on land and sea to determine the trends and to confirm our estimation methods on ABL by comparison with the previous studies.

The data relevant to day/night of the urban air (Tokyo metropolitan and Osaka city) showed a distinct ABL pattern, namely, this value was much higher during the daytime, as presented in Figure 2.7 (a) and (b). On the other hand, no distinct pattern was observed in the marine ABL (the sea around the Chichijima and Okinawa islands), as presented in Figure 2.7 (c) and (d).

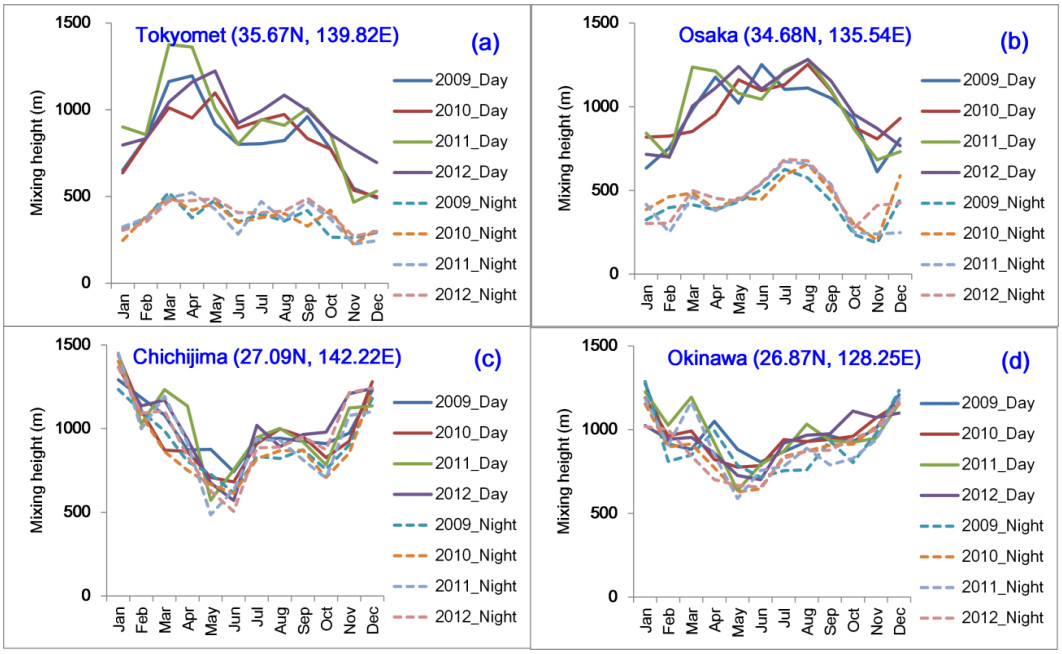

Figure 2.7 Monthly day-time and night-time of ABLs from various locations, including (a) Tokyo metropolitan, (b) Osaka city, (c) Chichijima sea, and (d) Okinawa sea, during 2009−2012.

As shown in Figure 2.7, seasonal changes in the night-time ABL (nocturnal boundary layer) are weaker than the day-time ABL (convective mixed layer), particularly for urban sites. We therefore pay attention to the convective daytime ABL for discussing the seasonal pattern. As a result, the ABL height show the differing seasonal trends for the land and marine sites. As regards the urban sites in Tokyo and Osaka, the monthly mean of the ABLs during the warm season (spring and late summer) was higher than that during the cold season (winter) (Figure 2.7 (a) and (b), Figure 2.8 (a) and (b)). In contrast, the ABLs for the marine sites (Chichijima and Okinawa) were estimated as higher during the cold season (winter) in comparison with the warm season (summer and autumn) (Figure 2.7 (c) and (d), Figure 2.8 (c) and (d)). Furthermore, Figure 2.8 indicates a consistent seasonal pattern for ABLs during 2009−2012 for both land and sea sites.

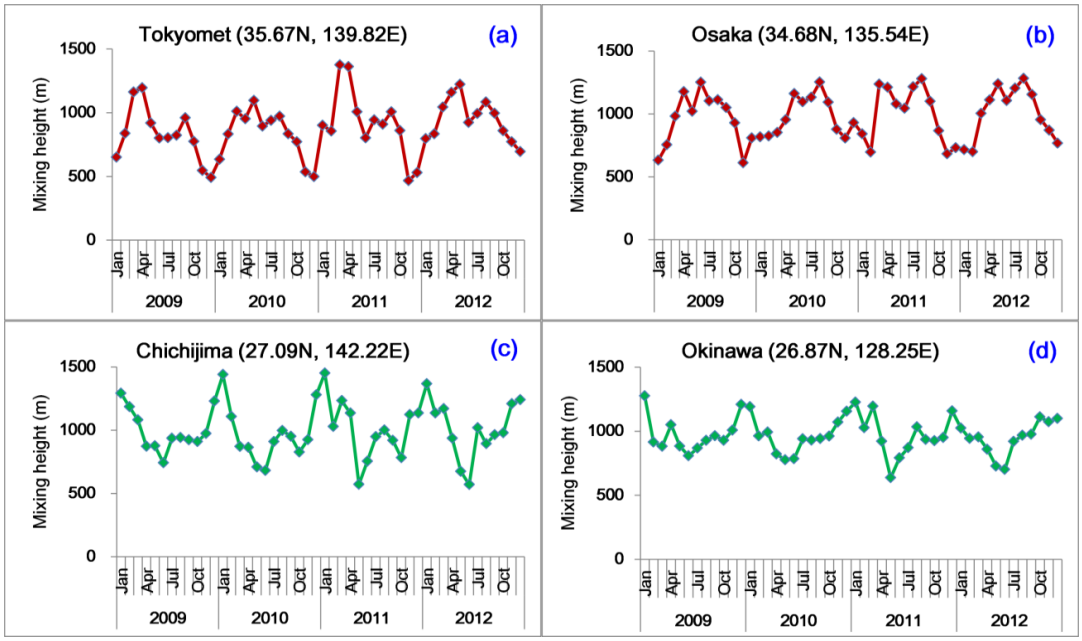

Figure 2.8 Monthly day-time (convective) ABLs from various locations, including (a) Tokyo metropolitan, (b) Osaka city, (c) Chichijima sea, and (d) Okinawa sea, during 2009−2012.

In a previous study, by using micro pulse lidar, Chen et al. [68] have measured two ABL peaks at the urban area of Tsukuba, which occurred in the early spring and autumn during the period 1999−2000. In addition, the seasonal pattern at a suburban site near Paris and at urban Hong Kong indicated that the ABL was higher during the warm period (autumn, spring, and summer) compared with the cold period (winter) [35,37]. In contrast, with the marine sites, the ABL was high in winter and low in summer over Okinawa Island and the East China Sea, observed with radiosonde and lidar data [36]. The observed ABL data obtained from the previous studies confirm our estimates on the ABL. Subsequently, we present the site-specific and time-dependent ABL relevant to PBDE sampling.

2.3.3.5.2 Site-specific and time-dependent ABL relevant to PBDE sampling

The ABL distribution plot for all the land (38) and sea (12) sites is presented in Figure 2.9 (a). Figure 2.9 (a) indicates that the 5% and 95% percentiles of ABL for the warm period were at 346 and 1547 m (arithmetic mean 748 m), whereas, for the cold period, they were at 213 and 1451 m (arithmetic mean 738 m).

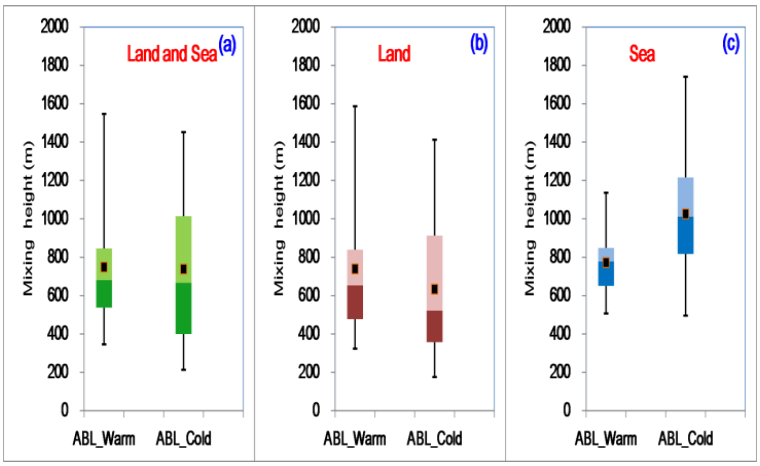

Figure 2.9 Distribution of atmospheric boundary layer height (ABL) for (a) both land and sea sites (50), (b) land sites (38), and (c) sea sites (12) relevant to PBDE sampling

The global planetary boundary layer was estimated by von Engeln and Teixeira [39] by using the reanalysis data of the European Centre for Medium Range Weather Forecasts (ECMWF). This research has shown that over Japan, between the 27th and 42nd parallels north, the boundary layer height ranged between 700 and 1400 m. This result is in agreement with our estimated ABL, using the JRA-55 database. Figure 2.9 (a) indicates that the ABL values during the warm season were only slightly higher than were those during the cold season. The reason for the seasonal variation being smaller is the differing ABL patterns on land and sea, as discussed earlier. Accordingly, as indicated in Figure 2.9 (b), clearly higher ABL values were found at 38 sites in urban and rural areas (land) during the warm season in comparison with the cold season. On the other hand, different results were produced for 12 sites at a nearby small island (sea), as shown in Figure 2.9 (c).

2.3.3.5.3 Effects of ABL height on the air concentration of PBDEs

As mentioned earlier in section 2.2.3.2, this is a follow-up study to factors influencing atmospheric PBDEs (former predictors: temperature, rainfall rate, population density, and year) with the addition the effect of ABL. Using Tobit multiple regression analysis on 298 samples, we found a consistent inverse relationship between the ABL and the air concentrations of BDE-47, -99, and -183 (p=0.009 for BDE-47, and p=0.002 for BDE-99 and -183). However, interestingly, no significant relationship (p=0.258) was found between the ABL and the air concentrations of BDE-209 (Figure 2.10, Table 2.6). These results mean that higher ABL values produce concentrations of BDE-47, -99, and -183 that are more diluted; however, this does not apply to BDE-209.

Table 2.6 Multiple regression results (with ABL) of censored (Tobit model) data on the atmospheric PBDEs in the JMOE data, with n=298

Congeners	Predictors	Unit	Coefficient	Standard Error	*p*-value	95% Confidence Interval	
BDE-47	$1/T_{outdoor}$	K^{-1}	-5290	388	<0.001,***	-6050	-4530
(6% censoring	ln*Ra*	$mm \cdot h^{-1}$	-0.050	0.023	0.025,*	-0.095	-0.006
intensity)	ln*ABL*	m	-0.210	0.080	0.009,**	-0.367	-0.052
	ln*PD*	$person \cdot km^{-2}$	0.159	0.039	<0.001,***	0.082	0.236
	Y	year	-0.204	0.032	<0.001,***	-0.267	-0.141
BDE-99	$1/T_{outdoor}$	K^{-1}	-1660	482	0.001,**	-2605	-715
(17%	ln*Ra*	$mm \cdot h^{-1}$	-0.088	0.028	0.002,**	-0.143	-0.032
censoring	ln*ABL*	m	-0.311	0.098	0.002,**	-0.503	-0.119
intensity)	ln*PD*	$person \cdot km^{-2}$	0.172	0.048	<0.001,***	0.078	0.266
	Y	year	-0.243	0.041	<0.001,***	-0.322	-0.163
BDE-183	$1/T_{outdoor}$	K^{-1}	2609	810	0.001,**	1020	4197
(63%	ln*Ra*	$mm \cdot h^{-1}$	-0.085	0.048	0.078,	-0.179	0.009
censoring	ln*ABL*	m	-0.434	0.137	0.002,**	-0.703	-0.164
intensity)	ln*PD*	$person \cdot km^{-2}$	0.118	0.048	0.015,*	0.023	0.213
	Y	year	-0.230	0.078	0.003,**	-0.383	-0.077
BDE-209	$1/T_{outdoor}$	K^{-1}	1904	408	<0.001,***	1105	2703
(34%	ln*Ra*	$mm \cdot h^{-1}$	-0.118	0.025	<0.001,***	-0.167	-0.069
censoring	ln*ABL*	m	-0.088	0.078	0.258	-0.241	0.065
intensity)	ln*PD*	$person \cdot km^{-2}$	0.141	0.031	<0.001,***	0.080	0.202
	Y	year	-0.071	0.034	0.035,*	-0.137	-0.005

Notes: *p*-value is significance level, *** represents $p<0.001$, ** represents $p<0.01$, * represents $p<0.05$, $1/T_{outdoor}$ is the reciprocal outdoor temperature (K^{-1}), ln*Ra* is the natural logarithm of rainfall rate ($mm \cdot h^{-1}$), ln*ABL* is the natural logarithm of the atmospheric boundary layer height (m), ln*PD* is the natural logarithm of population density ($person \cdot km^{-2}$), *Y* is the monitoring year, and n is the number of data points.

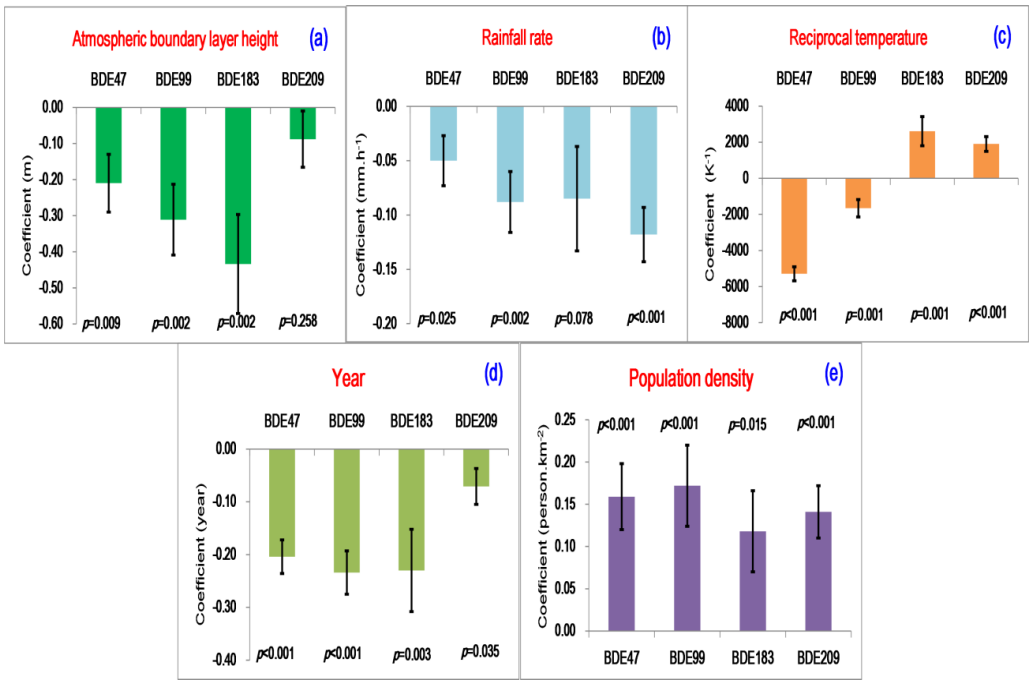

Figure 2.10 Regression coefficients of the concentrations of PBDE congeners against (a) the atmospheric boundary layer height (m), (b) rainfall rate ($mm \cdot h^{-1}$), (c) reciprocal temperature (K^{-1}), (d) year, and (e) population density ($person \cdot km^{-2}$) across Japan.

Within the suite of similar PBDE congeners (BDE-47, -99, and -183), for a long-term study (three consecutive years) in Zurich city, Diefenbacher et al. [52] indicated that the PCB concentrations (PCB-28, -52, -101, -138, -153, and -180) were strongly correlated with the mixing height (ABL) ($p<0.001$). In a short-term study (three or seven consecutive days), Bogdal et al. [30] observed a repeating day-night cycle of atmospheric PBDE concentrations, which was mainly caused by boundary layer dynamics. The day-night cycle of the ABL produced an enrichment of PBDEs in air during the night and a dilution of PBDEs during the day at summer time in Zurich city. Here, we regressed the relationship between the natural logarithm of the modeled ABL (day- and night-time equivalent to 1500 m and 100 m, respectively) and the measured PBDE congeners (BDE-47, -99, and -209), using the data reported by Bogdal et al. [30]. The coefficient of determination (R-squared) was high at 0.61 and 0.66 for BDE-47 and -99, respectively, with the same significance level $p<0.01$. In contrast, the R-squared was low at 0.29 for BDE-209, with the significance level being $p=0.04$. This finding is in agreement with the weak correlation between BDE-209 and ABL found in our study.

2.3.3.5.4 Implication of combining ABL, particle size distribution, and indoor emission mechanism on explaning the atmospheric transport and deposition of PBDEs

Bentzen et al. [69] have documented the vertical mixing (or boundary layer height) in the

atmosphere, with the application of compartmental box models. These authors have indicated that the description of the vertical mixing processes was appropriate for modeling the movement of pollutants in the gas phase in the atmosphere, as well as the pollutants attached to small aerosols that were mixed by turbulent eddies, similar to gasses. Accordingly, particles smaller than 2 μm remain in the ambient air for a longer time and are not as efficiently removed by wet or dry deposition [64,70]. On the other hand, pollutants attached to larger aerosols tend to settle under the influence of gravity and can be transported vertically downward through a stable boundary layer [69]. As a result, the particle wash-out by rain scavenging and particle deposition flux was found to be higher for BDE-209 compared with BDE-47 and -99 [71,72].

Various researchers have conducted studies on the size distribution of airborne particle-bound PBDEs [24,26,27,72,73]. Okonski et al. [26] have indicated that most (81%, 90%, and 91%, respectively) of the BDE-47, -99, and -183 was found in the fine particles (0.49−3.0 μm), whereas only 65% of the BDE-209 was found in these particles. On the other hand, the distribution of BDE-209 was higher (35%) in the larger particles (3−10 μm) compared with the distribution of the BDE-47, -99, and -183 (19%, 10%, and 9%, respectively). Another study has found that BDE-209 was highly correlated (p<0.01) with large particles (3−10 μm in diameters) [73].

Zhang et al. [72], particularly, have conducted a study on the particle size distribution of PBDEs at different heights in the urban area of Guangzhou during August and December in 2010. These authors have found that the distribution of particulate-bound PBDEs (BDE-47, -99, -183, -207, and -209) was bimodal, with a major peak at 0.56−1.0 μm and a minor peak at 3.2−5.6 μm, relevant to heights of 100 and 150 m. However, on the surface, 1.5 m above the ground, only the particle size distribution of airborne BDE-209 significantly peaked at a major fraction of 5.6−10 μm and a minor fraction of 0.56−1.0 μm. Consequently, a much higher fraction of BDE-209 was distributed in the large particles in the near-ground air, compared with those at heights of 100 and 150 m. These significant differences suggest that the BDE-209 bound to large particles might not be conveyed at high altitudes (e.g., 100 or 150 m). On the other hand, BDE-47, -99, and -183 in the fine particles in both the near-ground and the upper air undergo less dry deposition and can be transported to higher altitudes.

Furthermore, indoor dust and indoor air are important emission sources of BDE-209, as BDE-209 is emitted from treated products used indoors and subsequently moved outdoors. In Japan, deca-BDE (mainly BDE-209) is still in use and the in-use stocks of deca-BDE containing products provide an ongoing source of emission to the environment. Abrasion or weathering are the main transfer mechanisms of BDE-209 from the treated products into the indoor dust and indoor air [45,46]. The particles generated from abrasion/weathering generally have an aerodynamic diameter larger than 2 μm [74]. Consequently, BDE-209 is mainly found in indoor

dust, with a diameter of 75−150 μm [75], and in the indoor air with $PM_{2.5}$, PM_{10}, and TSP [27].

The findings on the differing behaviors of the PBDE congeners, as discussed above, verify the inverse relationship between the mixing height and the air concentrations of BDE-47, -99, and -183 (mainly associated with the gas phase and fine particles). The weak relationship between the mixing height and the BDE-209 concentration (high fraction in coarse particles) is confirmed by our study. However, the reasons for differences in regression coefficients among the BDE-183 (-0.434), BDE-99 (-0.311), and BDE-47 (-0.210) are still unclear.

2.4 Conclusions

With a large number of PBDE data across Japan, we successfully elucidated the factors influencing atmospheric PBDEs and demonstrated the impact of the Tobit model on censored data. The Tobit model is recommended, particularly when the censoring density is large. In contrast, simple substitution methods are not recommended except when the censoring intensity is low. The Tobit regression analysis revealed concentrations of all the PBDE congeners to be influenced by a combination of year, population density, temperature, rainfall rate, and ABL. We found that all PBDE-congener concentrations that originate from different locations in Japan have exhibited a decrease during 2009−2012. The human population density (as an indicator of emission source presenting the spatial variation of atmospheric PBDEs) showed a positive correlation with all PBDE congener concentrations, whereas PBDEs showed a negative correlation with rainfall rate. Seasonal patterns were opposite for light congeners (BDE-47 and -99), which increased with temperature, and heavy congeners (BDE-183, and -209), which decreased with temperature. The ABL has a strong influence on BDE-47, -99, and -183, which are associated with the gas phase and fine particles. In contrast, BDE-209, which is associated with larger particles, is less affected by vertical mixing, as the influence of settling gravity in the near-ground air is a more important factor. This suggests that BDE-209 bound particles generated from abrasion process in indoor dust and air, and their settling characteristics in outdoor air provide insightful understanding on the atmospheric transport and deposition of BDE-209.

In addition, the emission mechanism from indoor into outdoor air is an important pathway to understanding the fate and behavior of atmospheric PBDEs. As regards BDE-47 and -99, associated with high volatility and the predominance of the gas fraction, the transfer mechanism from treated products into indoor air is mainly the volatilization process. On the other hand, BDE-209 is a non-volatile compound unable to volatilize and re-condense on larger aerosols; therefore, this substance could have entered an environment already associated with larger particles. This supposition is consistent with the alternate emission pathways for PBDEs, either from a physical process (abrasion/weathering) or from direct partitioning from flame-retarded materials to particulate matter.

References

1. Japan Ministry of Environment (JMOE) (2014) PBDE demand in Japan. http://www.env.go.jp/chemi/dioxin/chosa/result_h26.pdf (in Japanese, accessed Sep.27, 2015)

2. Murakami S, Oguchi M, Tasaki T, Daigo I, Hashimoto S (2010) Lifespan of commodities, part I. Journal of Industrial Ecology 14:598–612

3. Sakai S, Hirai Y, Aizawa H, Ota S, Muroishi Y (2006) Emission inventory of deca-brominated diphenyl ether (DBDE) in Japan. J Mater Cycles Waste Manag 8: 56–62

4. Arinaitwe K, Muir DCG, Kiremire BT, Felin P, Li H, Teixeira C (2014) Polybrominated diphenyl ethers and alternative flame retardants in air and precipitation samples from the Northern Lake Victoria region, East Africa. Environ Sci Technol 48:1458–1466

5. Birgul A, Katsoyiannis A, Gioia R, Crosse J, Earnshaw M, Ratola N, Jones KC, Sweetman AJ (2012). Atmospheric polybrominated diphenyl ethers (PBDEs) in the United Kingdom. Environ Pollut 169:105–111

6. Gevao B, Ghadban AN, Porcelli M, Ali L, Rashdan A, Al-Bahloul M, Matrouk K, Zafar J (2013) Seasonal variations in the atmospheric concentrations of polybrominated diphenyl ethers in Kuwait. Sci Total Environ 454–455:534–541

7. Hayakawa K, Takatsuki H, Watanabe I, Sakai S (2004) Polybrominated diphenyl ethers (PBDEs), polybrominated dibenzo-p-dioxins/dibenzofurans (PBDD/Fs) and monobromo-polychlorinated dibenzo-p-dioxins/dibenzofurans (MoBPXDD/Fs) in the atmosphere and bulk deposition in Kyoto, Japan. Chemosphere 57:343–356

8. Kong D, MacLeod M, Hung H, Cousins IT (2014). Statistical analysis of long-term monitoring data for persistent organic pollutants in the atmosphere at 20 monitoring stations broadly indicates declining concentrations. Environ Sci Technol 48:12492–12499

9. Ma Y, Salamova A, Venier M, Hites RA (2013) Has the phased-out of PBDEs affected their atmospheric levels? Trends of PBDEs and their replacements in the Great Lakes atmosphere. Environ Sci Technol 47:11457–11464

10. Melymuk L, Robson M, Helm PA, Diamond ML (2012) PCBs, PBDEs, and PAHs in Toronto air: spatial and seasonal trends and implications for contaminant transport. Sci Total Environ 429:272–280

11. Japan Ministry of Environment (JMOE) (2013) Results of the environmental monitoring. http://www.env.go.jp/chemi/kurohon/2013/sokutei/pdf/03_04_14.pdf (in Japanese, accessed Feb.18, 2015)

12. UNEP (2015) Global monitoring plan under the Stockholm Convention: the 2nd POPs monitoring report Asia-Pacific region

13. Tobin BYJ (1958) Estimation of relationships for limited dependent variables. Econometrica 26:24–36

14. Amemiya T (1984) Tobit models: a survey. J Econom 24:3–61

15. He W, Qin N, He QS, Kong XZ, Liu WX, Wang QM, Yang C, Jiang YJ, Yang B, Bai ZL, Wu WJ, Xu FL (2014) Atmospheric PBDEs at rural and urban sites in central China from 2010 to 2013: residual levels, potential sources and human exposure. Environ Pollut 192:232–243

16. Hites RA (2015) A statistical approach for left-censored data: distributions of atmospheric polychlorinated biphenyl concentrations near the Great Lakes as a case study. Environ Sci Technol Lett 2:250–254

17. Lubin JH, Colt JS, Camann D, Davis S, Cerhan JR, Severson RK, Bernstein L, Hartge P (2004) Epidemiologic Evaluation of Measurement Data in the Presence of Detection Limits. Environ Health Perspect 112:1691–1696

18. Helsel DR (2012) Statistics for censored environmental data using Minitab and R, 2nd edition. John Wiley & Sons, Hoboken, New Jersey.

19. Schnedler W (2005) Likelihood estimation for censored random vectors. Econometric Reviews 24:195–217

20. Gouin T, Harner T, Daly G, Wania F, Mackay D, Jones KC (2005) Variability of concentrations of polybrominated diphenyl ethers and polychlorinated biphenyls in air: implications for monitoring, modeling and control. Atmos Environ 39:151–166

21. Venier M, Hites RA (2008) Flame retardants in the atmosphere near the Great Lakes. Environ Sci Technol 42:4745–4751

22. MacLeod M, Scheringer M, Podey H, Jones KC, Hungerbühler K (2007) The origin and significance of short-term variability of semivolatile contaminants in air. Environ Sci Technol 41:3249−3253

23. Moeckel C, MacLeod M, Hungerbühler K, Jones K C (2008) Measurement and modeling of diel variability of polybrominated diphenyl ethers and chlordanes in air. Environ Sci Technol 42:3219−3225

24. Shi S, Huang Y, Wan K, Dong L, Yang Y (2013) Levels and seasonal variations of polybrominated diphenyl ethers in the urban atmosphere of Beijing. China Bull Environ Contam Toxicol 90:296–301

25. Yang M, Qi H, Jia HL, Ren NQ, Ding YS, Ma WL, Liu LY, Hung H, Sverko E, Li YF (2013) Polybrominated diphenyl ethers in air across China: levels, compositions, and gas-particle partitioning. Environ Sci Technol 47:8978–8984

26. Okonski K, Degrendele C, Melymuk L, Landlová L, Kukučka P, Vojta Š, Kohoutek J, Čupr P, Klánová J (2014) Particle size distribution of halogenated flame retardants and implications for atmospheric deposition and transport. Environ Sci Technol 48:14426–14434

27. Li Y, Chen L, Ngoc DM, Duan YP, Lu ZB, Wen ZH, Meng XZ (2015) Polybrominated diphenyl ethers (PBDEs) in PM2.5, PM10, TSP, and gas phase in office environment in Shanghai, China: Occurrence and human exposure. PLoS One 10:1–15

28. Drage DS, Newton S, de Wit CA, Harrad S (2016) Concentrations of legacy and emerging flame retardants in air and soil on a transect in the UK West Midlands. Chemosphere 148:195–203

29. Juda-Rezler K, Reizer M, Oudinet JP (2011) Determination and analysis of PM10 source apportionment during episodes of air pollution in Central Eastern European urban areas: The case of wintertime 2006. Atmos Environ 45:6557−6566

30. Bogdal C, Wang Z, Buser AM, Scheringer M, Gerecke AC, Schmid P, Müller CE, MacLeod M, Hungerbühler K (2014) Emissions of polybrominated diphenyl ethers

(PBDEs) in Zurich, Switzerland, determined by a combination of measurements and modeling. Chemosphere 116:15–23

31. Harner T, Shoeib M (2002) Measurements of octanol - air partition coefficients (K_{OA}) for polybrominated diphenyl ethers (PBDEs): predicting partitioning in the environment. J Chem Eng Data 47:228–232

32. Li WL, Qi H, Ma WL, Liu LY, Zhang Z, Mohammed MO, Song WW, Zhang Z, Li YF (2015) Brominated flame retardants in Chinese air before and after the phase out of polybrominated diphenyl ethers. Atmos Environ 117:156–161

33. Melymuk L, Robson M, Helm PA, Diamond ML (2013) Application of land use regression to identify sources and assess spatial variation in urban SVOC concentrations. Environ Sci Technol 47:1887–1895

34. Coen MC, Praz C, Haefele A, Ruffieux D, Kaufmann P, Calpini B (2014) Determination and climatology of the planetary boundary layer height above the Swiss plateau by in situ and remote sensing measurements as well as by the COSMO-2 model. Atmos Chem Phys 14:13205–13221

35. Pal S, Haeffelin M (2015) Forcing mechanisms governing diurnal, seasonal, and interannual variability in the boundary layer depths: Five years of continuous lidar observations over a suburban site near Paris. J Geophys Res Atmos 120:11936–11956

36. Kuribayashi M, Ohara T, Shimizu A (2011) Temporal variation and vertical structure of the marine atmospheric mixed layer over the East China Sea from Mie-scattering lidar data. SOLA 7:189–192

37. Yang D, Li C, Lau AKH, Li Y (2013) Long-term measurement of daytime atmospheric mixing layer height over Hong Kong. J Geophys Res Atmos 118: 2422–2433

38. Chan KM, Wood R (2013) The seasonal cycle of planetary boundary layer depth determined using COSMIC radio occultation data. J Geophys Res Atmos 118: 12422–12434

39. von Engeln A, Teixeira J (2013) A planetary boundary layer height climatology derived from ECMWF reanalysis data. J Climate 26:6575−6590

40. Kobayashi S, Ota Y, Harada Y (2015) The JRA-55 reanalysis: General specifications and basis characteristics. J Meteorol Soc Jpn 93:5−48

41. Björklund JA, Thuresson K, Cousins AP, Sellström U, Emenius G, de Wit CA (2012) Indoor Air Is a Significant Source of Tri-decabrominated Diphenyl Ethers to Outdoor Air via Ventilation Systems. Environ Sci Technol 46:5876–5884

42. Zhang X, Diamond ML, Ibarra C, Harrad S (2009) Multimedia modeling of polybrominated diphenyl ether emissions and fate indoors. Environ Sci Technol 43: 2845−2850

43. Kemmlein S, Hahn O, Jann O (2003) Emissions of organophosphate and brominated flame retardants from selected consumer products and building materials. Atmos Environ 37:5485–5493

44. Wilford BH, Thomas GO, Alcock RE, Jones KC, Anderson DR (2003) Polyurethane foam as a source of PBDEs to the environment. Organohalogen Compd 61:219–222

45. Webster TF, Harrad S, Millette JR, Holbrook RD, Davis JM, Stapleton HM, Allen J G, McClean MD, Ibarra C, Abdallah MAE, et al (2009) Identifying transfer mechanisms and sources of decabromodiphenyl ether (BDE 209) in indoor environments using environmental forensic microscopy. Environ Sci Technol 43: 3067−3072

46. Rauert C, Harrad S (2015) Mass transfer of PBDEs from plastic TV casing to indoor dust via three migration pathways–A test chamber investigation. Sci Total Environ 536:568–574

47. Japan Meteorological Agency (JMA) (2015) Meteorological data in Japan. http://www.jma.go.jp/jma/indexe.html. (accessed Feb.18, 2015)

48. e-Stat (2015) Portal Site of Office Statistic of Japan. http://e-stat.go.jp/SG2/eStatGIS/page/download.html. (accessed Feb.18, 2015)

49. Dien NT, Hirai Y, Miyazaki T, Sakai S (2016) Factors influencing atmospheric concentrations of polybrominated diphenyl ethers in Japan. Chemosphere 144: 2073–2080

50. Wallace JM, Hobbs PV (2006) Atmospheric Science – an Introductory Survey. Elseviers Inc.: Washington.

51. Vogelezang DHP, Holtslag AAM (1996) Evaluation and model impacts of alternative boundary-layer height formulations. Boundary Layer Meteorol 81:245–269

52. Diefenbacher PS, Bogdal C, Gerecke AC, Glüge J, Schmid P, Scheringer M, Hungerbühler K (2015) Emissions of polychlorinated biphenyls in Switzerland: A Combination of Long-Term Measurements and Modeling. Environ Sci Technol 49 (4):2199−2206

53. Limpert E, Stahel WA, Abbt M (2001) Log-normal distributions across the sciences: Keys and clues. BioScience 51:341–352

54. Hoh E, Hites RA (2005) Brominated flame retardants in the atmosphere of the East-Central United States. Environ Sci Technol 39:7794–7802

55. Gouin T, Thomas GO, Chaemfa C, Harner T, Mackay D, Jones KC (2006) Concentrations of decabromodiphenyl ether in air from Southern Ontario: implications for particle-bound transport. Chemosphere 64:256–261

56. Shoeib M, Ahrens L, Jantunen L, Harner T (2014) Concentrations in air of organobromine, organochlorine and organophosphate flame retardants in Toronto, Canada. Atmos Environ 99:140–147

57. Cetin B, Odabasi M (2008) Atmospheric concentrations and phase partitioning of polybrominated diphenyl ethers (PBDEs) in Izmir, Turkey. Chemosphere 71:1067–1078

58. Castro-Jiménez J, Mariani G, Vives I, Skejo H, Umlauf G, Zaldívar JM, Dueri S, Messiaen G, Laugier T (2011) Atmospheric concentrations, occurrence and deposition of persistent organic pollutants (POPs) in a Mediterranean coastal site (Etang de Thau, France). Environ Pollut 159:1948–1956

59. Zeghnoun A, Pascal M, Fréry N, Sarter H, Falq G, Focant JF, Eppe G (2007) Dealing with the non-detected and non-quantified data: the example of the serum dioxin data in the French dioxin and incinerators study. Organohalogen Compounds 69

60. Raff JD, Hites RA (2007) Deposition versus photochemical removal of PBDEs from Lake Superior air. Environ Sci Technol 41:6725–6731

61. Venier M, Hites RA (2008) Atmospheric deposition of PBDEs to the Great Lakes featuring a Monte Carlo analysis of errors. Environ Sci Technol 42:9058–9064

62. Wooldridge JM (2009) Introductory Econometrics: A Modern Approach, 4th Edition. Mason, OH: South-Western Cengage Learning

63. Cousins IT, Beck AJ, Jones KC (1999) A review of the processes involved in the exchange of semi-volatile organic compounds (SVOC) across the air–soil interface. Sci Total Environ 228:5–24

64. Bidleman T (1988) Atmospheric processes − Wet and dry deposition of organic compounds are controlled by their vapor-particle partitioning. Environ Sci Technol 22:361−367

65. Hoff RM, Strachan WMJ, Sweet CW, Chan CH, Shackleton M, Bidleman TF, Brice KA, Burniston DA, Cussion S, Gatz DF, Harlin K, Schroeder WH (1996) Atmospheric deposition of toxic chemicals to the Great Lakes: a review of data through 1994. Atmos Environ 30:3505–3527

66. ter Schure AFH, Larsson P, Agrell C, Boon JP (2004) Atmospheric transport of polybrominated diphenyl ethers and polychlorinated biphenyls to the Baltic Sea. Environ Sci Technol 38:1282–1287

67. Venier M, Salamova A, Hites RA (2015) Halogenated flame retardants in the Great Lakes Environment. Acc Chem Res 48:1853–1861

68. Chen W, Kuze H, Uchiyama A, Suzuki Y, Takeuchi N (2001) One-year observation of urban mixed layer characteristics at Tsukuba, Japan, using a micro pulse lidar. Atmos Environ 35:4273–4280

69. Bentzen E, Macleod M, Hickie B, Gasic B, Hungerbuhler K, Mackay D (2011) Mixing in the atmosphere and surface waters with application to compartmental box models. In Handbook of Chemical Mass Transport in the Environment: Thibodeaux LJ, Mackay D, Eds. Taylor and Francis Group, Boca Raton:565−588

70. Kurokawa Y, Takahiko M, Matayoshi N, Satoshi T, Kazumi F (1998) Distribution of polychlorinated-p-dioxins and dibenzofurans in various sizes of airborne particles. Chemosphere 37:2161−2171

71. Li J, Zhang G, Xu Y, Liu X, Li XD (2010) Dry and wet particle deposition of polybrominated diphenyl ethers (PBDEs) in Guangzhou and Hong Kong, South China. J Environ Monit 12:1730−1736

72. Zhang BZ, Zhang K, Li SM, Wong CS, Zeng EY (2012) Size dependent dry deposition of airborne polybrominated diphenyl ethers in urban Guangzhou, China. Environ Sci Technol 46:7207−7214

73. Wilford BH, Thomas GO, Jones KC, Davison B, Hurst DK (2008) Decabromodiphenyl ether (deca-BDE) commercial mixture components, and other PBDEs, in airborne particles at a UK site. Environ Int 34:412−419

74. Hazrati S, Harrad S (2006) Causes of variability in concentrations of polychlorinated biphenyls and polybrominated diphenyl ethers in indoor air. Environ Sci Technol 40:7584−7589

75. Wei H, Turyk M, Cali S, Dorevitch S, Erdal S, Li A (2009) Particle size fractionation and human exposure of polybrominated diphenyl ethers in indoor dust from Chicago. J Environ Sci Heal A 44:1353–1361

Chapter 3 Policy and technological control measures of PBDEs

3.1 Introduction

3.1.1 Stockholm Convention and Japan regulation on PBDEs

Polybrominated diphenyl ethers (PBDEs) are some of the most widely used brominated flame-retardants (BFRs), and include three major PBDE technical mixtures, namely, penta-BDE, octa-BDE, and deca-BDE. The indicated widespread and persistent occurrence of PBDEs in the indoor and outdoor environments poses a potential risk to animals and humans [1]. Because of their apparent toxicity, penta- and octa-BDEs were phased out worldwide and were listed as persistent organic pollutants (POPs) under the 2009 Stockholm Convention [2]. In 2012, the European Chemicals Agency (ECHA) identified deca-BDE as a substance of extremely high concern [3]. The Agency has specified deca-BDE as being extremely bioaccumulative, and has stipulated the substance as persistent, bioaccumulative, and toxic (PBT). In 2013, Norway tabled a proposal to list deca-BDE as a POP under the Convention [4]. Recently, the Persistent Organic Pollutants Review Committee (POPRC) has recommended that the Stockholm Convention consider listing and specifying the control measures relevant to deca-BDE in its Annex A (with the specific exemption of various critical legacy spare parts used in the automotive and aerospace industries that still need to be defined) [5].

3.1.2 Domestic demand for PBDEs in Japan

In Japan, limiting the domestic demand for commercial penta-, octa-, and deca-PBDEs had started decades earlier with penta- and octa-BDEs being phased out in 1990 and 1999, respectively. Although deca-BDE is still in use in Japan, the domestic demand has been declining gradually from 10,000 ton in 1990 to only 900 ton in 2013) [6].

3.1.3 In-use PBDE stock and their atmospheric emission

Even though POP-PBDEs (penta- and octa-BDEs) and deca-BDE were phased out and restricted, as mentioned above, the main challenge to eliminating the substances is identifying the existing in-use stocks of PBDE-containing products and disposing of PBDE-containing waste [7,8]. As penta- and octa-BDEs were phased out in 1990 and 1999, respectively, in Japan, few remaining in-use products are expected still to contain these POP-PBDEs. Although the volume of deca-BDE being used is gradually declining, the deca-BDE contained in the in-use products will continue to be a source of exposure to PBDEs for humans and the environment. In Japan, the largest stock of deca-BDE is contained in the consumer products currently in use, and the emissions from such products were estimated the largest source of the deca-BDE in the air [9,10]. Therefore, it is important to consider the emissions during the service life of the deca-BDE-containing products. Furthermore, in a modelling study, Csiszar et al. [11] have

concluded that the secondary emissions (chemical volatilization from water or soil) of PBDEs were minimal compared with the emissions from the continued use of the substances. In effect, the estimated atmospheric emissions of deca-BDE were higher than were the hydrospheric and soil emissions of the substance [12]. The decline in the stock of PBDEs provides an insight into the effectiveness of efforts to reduce the levels of PBDEs in the environment [8]. Therefore, estimating the amounts of PBDE contained in products at present and in the near future is important to improving the understanding of the emission sources of the substances. Such understanding is clearly a significant factor in the drafting of policy measures to reduce PBDE emissions.

3.1.4 The aim of study

The aim of this study is to estimate (i) the amount and the time trend of PBDE stocks and (ii) their atmospheric emissions in Japan. We used a population balance model to estimate the stocks of penta-, octa-, and deca-BDEs in Japan from 1985 to 2013, and to predict the amounts until 2040, based on two cases of regulating deca-BDE. The results are discussed by comparing them with the annual trend of atmospheric PBDE concentrations in Japan from 2009 to 2012.

3.2 Methodology

3.2.1 Population balance model

The in-use stocks of penta-, octa-, and deca-BDEs were estimated by using a population balance model. This model combines the statistics on the annual demand for PBDEs [6] with a survival function for the lifetime of the products containing PBDEs (Eq 1), and estimates the in-use stock of PBDEs (Eq 2).

$$F(d) = \exp\left\{-\left(\frac{d}{\eta}\right)^{m}\right\} \qquad \textbf{Eq 1}$$

where m is the shape parameter of the Weibull distribution, η is the scale parameter of the Weibull distribution, and $F(d)$ is the survival rate of PBDE-containing products, with d the age (d years after production).

$$S(i,y) = \sum_{t=1985}^{y} D(i,t) \cdot F(y-t) \qquad \textbf{Eq 2}$$

where $S(i, y)$ is the in-use stock of i (penta-BDE, octa-BDE, or deca-BDE) in year y, and $D(i, t)$ is the domestic demand of i in year t.

For the survival function, we assumed a Weibull distribution often used to represent the lifetime of products [13,14]. The information on the shape and scale parameters for PBDE-containing products was selected to reflect the major PBDE usages. Table 3.1 shows the ranges of two parameters for various flame retarded products, such as textiles (e.g., curtains, carpets), electrical appliances (e.g., TVs, computers), vehicles (e.g., the interior of automobiles),

and construction materials (e.g., plastic insulation, composite panels) [14−16].

Table 3.1 Literature review on shape and scale parameters for survival function

Items	Shape parameters	References	Average lifespans (years)	References
TVs	3.5	[15]	10	[16]
Slabstock polyurethane foam (PUF)	2.4	[15]	10−15	[16]
Electrical appliances	2.4	[14]	10.3	[16]
Vehicles	−	−	12	[16]
Furniture	−	−	10.2	[16]
Plastic pallet	−	−	15	[16]
Construction materials	−	−	20	[16]

(−) indicates no information

3.2.2 Scenario setting

Based on the general information on the shape and scale parameters (Table 3.1) for PBDE-containing products, we performed a scenario analysis using these two parameters (Table 3.2).

Table 3.2 Scenarios for shape and scale parameters of the Weibull distribution for the survival function

Scenario	#1	#2	#3	#4	#5	#6	#7	#8	#9	#10	#11	#12
Shape m	2	3	4	5	2	3	4	5	2	3	4	5
Scale (year) η	10				15				20			

As there are four instances of the shape parameter m (i.e., 2, 3, 4, and 5) and three instances of the scale parameter η (i.e., 10, 15, and 20 years), there are 12 scenarios. In this study, we considered only the first use (excluding reuse and/or storage) of PBDE-containing products. In addition, the same shape and scale parameters for penta-, octa-, and deca-BDE-containing products were assumed for each scenario.

3.2.3 The statistical data on domestic demand for PBDEs (1986−2013)

The statistical data on the annual domestic demand for commercial penta-, octa-, and deca-BDEs were published by the Japan Ministry of Environment [6]. The changes in the domestic demand for penta-, octa-, and deca-BDEs are indicated in Figure 3.1.

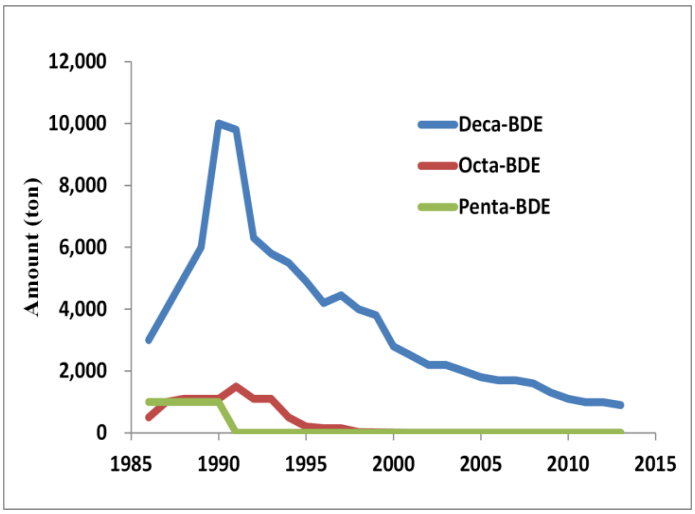

Figure 3.1 Annual statistics of domestic demand for PBDEs in Japan (JMOE, 2014)

The figure shows that the use of penta- and octa-BDEs ended in 1990 and 1999, respectively, and indicates the gradual decrease in the use of deca-BDE after 1990. The consumption of penta-BDE had amounted to 1,000 ton.year^{-1} during 1986−1990. The consumption of octa-BDE had peaked at 1,500 ton in 1991 and had subsequently slightly decreased until the phase-out after 1999. The consumption of deca-BDE had increased from 1986 (3,000 ton) and had peaked in 1990 (10,000 ton) with a gradual decrease to 900 ton in 2013. In Europe, the industrial consumption of deca-BDE had peaked during the 1990s at 9,100 ton.year^{-1} and had decreased slightly during the 2000s to between 6,900 and 8,600 ton.year^{-1} [12,17,18]. No detail information was available on the domestic demand for PBDEs in the U.S. and Canada. However, Abbasi et al. [8] have indicated that penta- and octa-BDEs were phased out in 2004, and the production of deca-BDE was expected to stop after 2013. We aimed to determine whether the phase-out of penta-, and octa-BDEs and the gradual decline in deca-BDE have affected the atmospheric levels of these substances in Japan. We therefore analyzed the time trend of the atmospheric PBDE data, monitored by JMOE (2009−2012), to determine the association between the consumption of PBDEs and the PBDE concentration in the air.

3.2.4 Statistical analysis of PBDE concentrations in ambient air (2009−2012)

In our analysis, we employed the atmospheric PBDE monitoring data from the Japanese Ministry of Environment (JMOE) for the period 2009−2012 [19,20]. The statistical method for atmospheric PBDE concentrations has been described in Dien et al., [21]. The arithmetic mean and the range of atmospheric levels for penta-, octa-, and deca-BDEs were 0.39 (0.02−36), 0.19 (0.05−11), and 12.2 (2−290) pg.m^{-3}, respectively, at 38 sites across Japan during 2009−2012. The non-detected values were replaced by half the limit of detection (LOD).

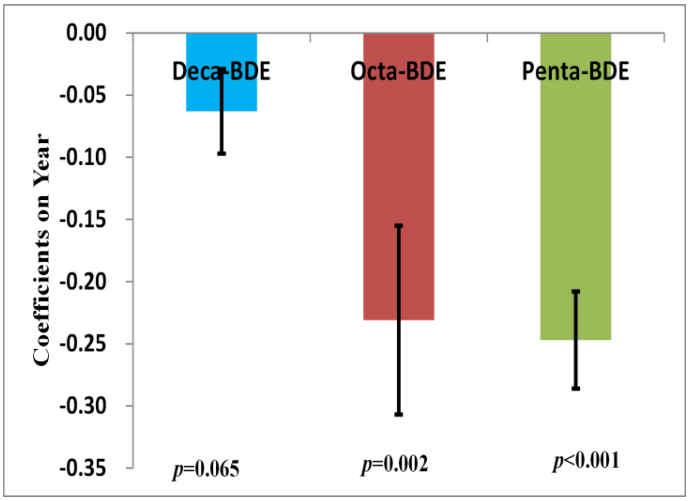

Figure 3.2 Decreasing trend of PBDEs in the air in Japan from 2009 to 2012

Our previous regression analysis [21], using the Tobit model, has determined that BDE-209 (deca-BDE) had decreased slightly (−6%/y; p=0.065), whereas BDE-99 (penta-BDEs), and BDE-183 (octa-BDE) had declined by −25, and −23%/y, respectively, (p<0.05) in Japan from 2009 to 2012 (Figure 3.2). These results confirm a similar declining trend between PBDE consumption and the PBDE concentration in the air.

3.2.5 Prediction of in-use deca-BDE stocks until 2040, based on two cases of future regulation

We first estimated the domestic demand of deca-BDE in order to predict the future of the deca-BDE stocks in use. Two future regulation cases were considered, namely, (1) deca-BDE is used as is, and (2) deca-BDE is discontinued after 2020. We constructed a forecasting model for the first case, based on the statistical domestic demand for PBDEs in Japan for 1990−2013, in order to predict the demand from 2014 to 2040 by using the exponential decay function in Eq 3

$$D(t) = D_0 \cdot \exp(-at) \qquad \textbf{Eq 3}$$

where $D(t)$ is the domestic demand of deca-BDE in year t, D_0 is the domestic demand for deca-BDE in the starting year, and a is the rate of decay ($a < 0$).

For the second case, a similar prediction was made for the period 2014 to 2020, and a 0 amount was placed for the period 2021 to 2040. Subsequently, the population balance model mentioned above was applied to predict the future of the deca-BDE stocks in use.

3.3 Results and discussion

We estimated the survival rate of PBDE-containing products, the amount of PBDE stocks in use, and the relative declining rate of PBDE stocks in use. Interestingly, the settings for all 12 scenarios produced consistent results, as shown in Figures 3.3−3.5.

3.3.1 Survival rates of PBDE-containing products

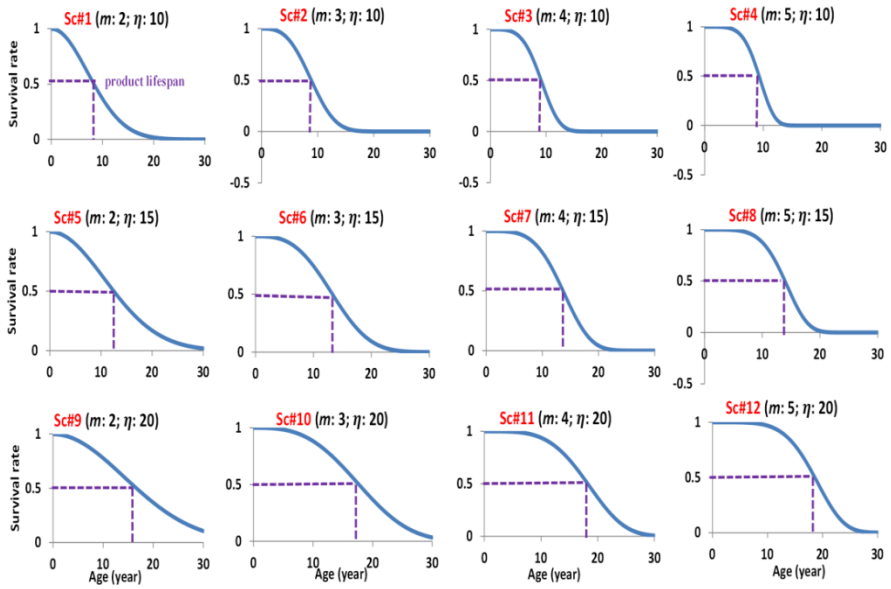

Figure 3.3 Survival rates of PBDE-containing products for Scenarios #1−12
Sc is scenario, *m* is the shape parameter, and η is the scale parameter of the Weibull distribution

Differently shaped curves of the survival rates are presented in Figure 3.3 for a wide range of product lifespans (8−19 years, with calculated values at *F(d)*=0.5 for each scenario). These estimated lifespans are in agreement with the average lifespan of consumer products in Japan, which is approximately 10−15 years, as determined by Murakami et al. [13].

3.3.2 Time trend and amount of PBDE stocks in use (1986−2013)

Figure 3.4 presents the changes in the amounts of PBDE stocks in use, with the higher amounts being in the higher scale parameters for the 12 scenarios. For example, the highest PBDE stocks were estimated with scale parameters of 20 (scenarios 9−12). However, the amount trend for the three PBDE types consistently showed the following amount pattern: deca-BDE > octa-BDE > penta-BDE.

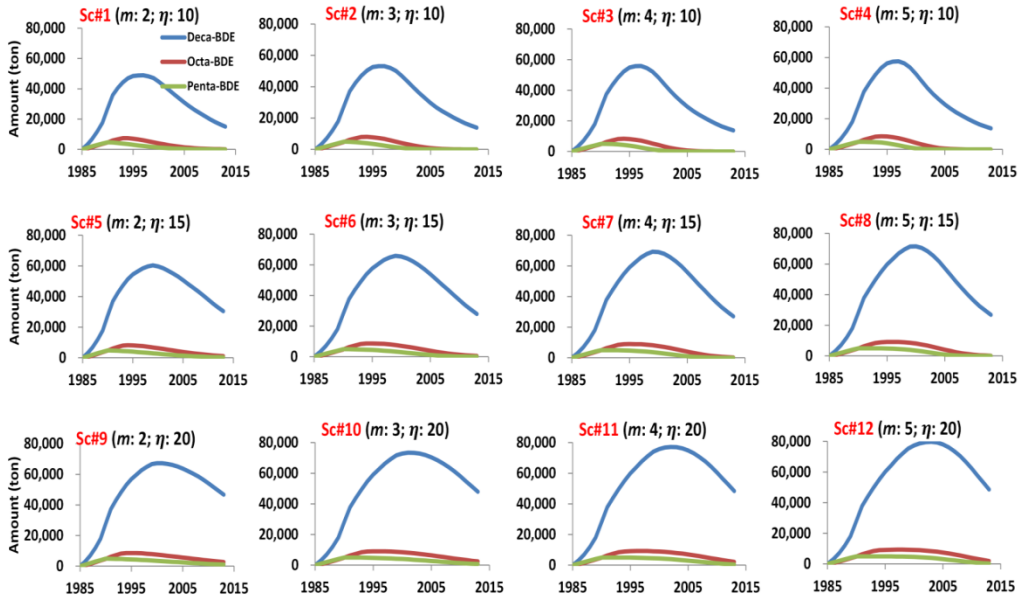

Figure 3.4 Time trend and amount of PBDE stocks in use for Scenarios #1−12
Sc is scenario, *m* is the shape parameter, and η is the scale parameter of the Weibull distribution

Figure 3.4 shows that the in-use penta- and octa-BDEs stocks had peaked at respectively 4,700 (4,500−5,000) ton and 8,700 (7,500−9,200) ton in the early 1990s, whereas the in-use deca-BDE stocks had peaked at 65,000 (35,000−80,000) ton in the early 2000s. In a similar comparison, Earnshaw et al. [12] have indicated that the in-use stocks of deca-BDE in Europe had peaked at 80,000 (60,000−110,000) ton in the early 2000s. On the other hand, Abbasi et al. [8] have estimated that the peak in-use phase of penta- and octa-BDEs stocks in the U.S. and Canada had occured in 2004, whereas that of deca-BDE had occurred in 2008. Probably, the different dates and amounts of peak stocks could be ascribed to factors such as the rate of consumption, usage patterns, and the regulation of PBDEs in the different regions.

In 2013, the estimated in-use stocks of deca-BDE in Japan were in the range 13,700−48,600 ton, whereas those of penta- and octa-BDEs ranged between 0−1,060 and between 1.3−2,750 ton, respectively Figure 3.4. These results suggest that the in-use stocks of deca-BDE would persist in society, whereas the penta- and octa-BDEs stocks could be depleted in the near future. The predicted amounts of in-use stocks of PBDEs until 2040 will be presented in the next section.

3.3.3 Decreasing speed of in-use PBDE stocks

Similarly, in Figure 3.5, the changes in the speed at which the in-use PBDE stocks were decreasing are represented by shape and scale changes. However, the decreasing trend for the PBDE types was consistent.

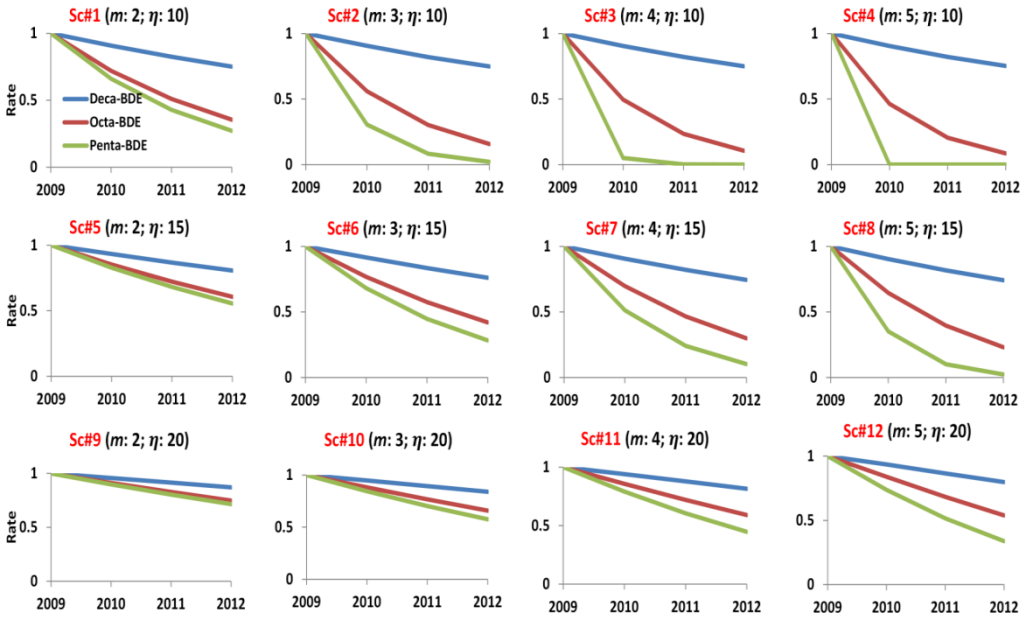

Figure 3.5 Decreasing speed of in-use PBDE stocks for Scenarios #1−12 (FY2009 = 1.0)
Sc is scenario, *m* is the shape parameter, and η is the scale parameter of the Weibull distribution

Figure 3.5 shows that for a wide range of the shape and scale parameters, relevant to the survival rate of the products, the decreasing speed of the penta-, octa-, and deca-BDEs stocks in use (FY2009=1.0) satisfied the following pattern penta- > octa- > deca-BDEs. This finding is consistent with the changes in the PBDE levels in ambient air, as shown in Figure 3.2.

3.3.4 Choosing the appropriate scenario

Among the scenarios, scenario 6 shows that the stocks of PBDE-containing products have declined at a rate proportional to the PBDE levels in the air. As a result, the speed of decrease of the in-use deca-, octa-, and penta-BDEs (−8%, −19%, and −24%/year, respectively) corresponded with the decreasing trend of these compounds in the air (−6%, −23%, and −25%/year, respectively). The relatively stable levels of deca-BDE in the air are likely the result of the gradually decreasing number of new deca-BDE containing products coming onto the Japanese market. The greater declines of penta- and octa-BDEs in the air is likely the result of stopping new products containing penta-BDEs and octa-BDEs in 1990 and 1999, respectively, and the gradual decrease in the in-use products containing these flame-retardants in Japan. Abbasi et al. [8] have found that the rate of decline of PBDE-containing products in the U.S. and Canada was proportional to the atmospheric levels of PBDEs. This association has been confirmed, as secondary emissions of PBDEs from contaminated soils and surface waters have been estimated negligible in comparison with the primary emissions [11].

In addition, it was estimated from scenario 6 that the in-use stock of deca-BDE in 2002 was 62,000 ton, which is in agreement with the estimate by Sakai et al. [9] (60,000 ton in 2002) and Tokai et al. [10] (49,300 ton in 2003, as a decreasing trend after 1999). We therefore chose scenario 6 as an appropriate estimate for all the estimations of the in-use stocks of PBDEs. From Sc#6 in Figure 3.4, the amount of in-use deca-BDE stocks was estimated at approximately 28,000 ton in 2013. However, the stocks of penta- and octa-BDEs were low (approximately 500 and 60 tons, respectively) and could be depleted in the near future. However, the considerable remaining amount of deca-BDE would likely be a source of emission to the atmosphere for several years.

3.3.5 Atmospheric emission of deca-BDE containing products

To estimate the atmospheric emission from deca-BDE containing products, the range used for the air emission factor was $3x10^{-6}$−$3x10^{-5}$ [9].

As a result, the estimated atmospheric emission of deca-BDE in Japan ranged between 84 and 841 kg.year^{-1}, relative to 28,000 ton of deca-BDE stock, in 2013 (Table 3.3). Abbasi et al. [8] have used the same air emission factor and have estimated the deca-BDE atmospheric emissions in the U.S. and Canada at 350−3,500 kg.year^{-1} in 2014, when the relevant stocks range was 4,000−120,000 ton (Table 3.3). Earnshaw et al. [12] have estimated the atmospheric emissions of deca-BDE at 5,800 kg.year^{-1}, relative to 60,000 ton deca-BDE stocks in Europe in 2010 (population 590 million), based on substance flow analysis. In addition, Bogdal et al. [22] have used a back-calculated model (based on field measurements) to estimate the deca-BDE air emission in Switzerland in 2010, of which the range was 41−180 kg.year^{-1} (mean value 78 kg.year^{-1}).

Table 3.3 indicates that the level of atmospheric deca-BDE emissions per capita in Japan is nearly the same or slightly lower than are those of other regions. In addition, Table 3 indicates the comparative atmospheric deca-BDE levels [21−24].

Table 3.3 Worldwide status of deca-BDE in stocks, atmospheric emissions, and levels

Parameters	Japan (population ~126.4 million)	U.S. and Canada (population ~318.9+35.5 million)	Switzerland (population ~8 million)	Europe (population ~590 million)
Year	2013	2014	2010	2010
Stock in use (ton)	28,000 (13,700−48,600)	(4,000−120,000)	−	60,000
Stock in use ($g.capita^{-1}$)	222 (109−385)	(200−2,000)	−	102
Atmospheric emission ($kg.y^{-1}$)	(84−841) [(1)]	(350−3,500) [(1)]	78 (41−180) [(2)]	5,800 [(3)]
Atmospheric emission ($\mu g.capita^{-1}.d^{-1}$)	(1.8−18.2)	(2.7−27.1)	26.5 (14−60.5)	27
Atmospheric level ($pg.m^{-3}$)	12.2 (2−290) [(4)]	(56−77) [(5)]	34.6 (3.5−314)	8.0 (0.1−177) [(6)]
References	This study	Abbasi et al., 2015	Bogdal et al., 2014	Earnshaw et al., 2013

[(1)] Using the atmospheric emission factor of deca-BDE: $3x10^{-06}$−$3x10^{-05}$ (Sakai et al., 2006); [(2)] Back calculated from air measurement; [(3)] Emission based on substance flow analysis (SFA); [(4)] Dien et al., 2016; [(5)] Ma et al., 2013; [(6)] Earnshaw et al., 2015. The values not in parentheses are mean values, the values in parentheses indicate a range, and (−) represents no information

3.3.6 Prediction of in-use deca-BDE stocks until 2040

Figure A3.1 (in Appendix) indicates that the forecasting data fitted well with the statistical data.

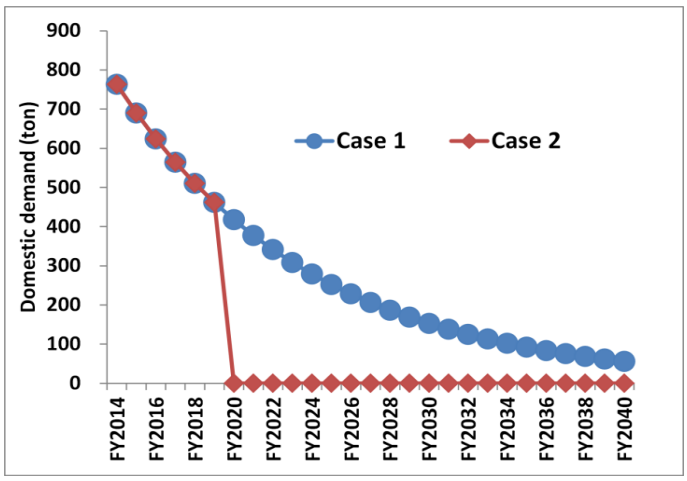

Figure 3.6 Forecasting domestic demand of deca-BDE in Japan from 2014 to 2040 with Case 1 where deca-BDE is used as is and Case 2 where deca-BDE is discontinued after 2020

As a demonstration of the forecasting data, Figure 3.6 indicates that the estimated domestic demand for deca-BDE will be approximately 417 ton in 2020 (for both case 1 and case 2) and 56 ton in 2040 (for case 1). Figure A3.2 (a) and (b) (in Appendix) show the estimates of the in-use stocks of penta-, octa-, and deca-BDEs in Japan from 1986 to 2040. Penta- and octa-BDEs were estimated at 20 ton and less than 1 ton in 2020, respectively, indicating that they would be nearly depleted in society (Figure A3.2 (a) and (b)). Abbasi et al. [8] have estimated that most of the in-use penta- and octa-BDE stocks would be phased out by 2020 in the U.S. and Canada.

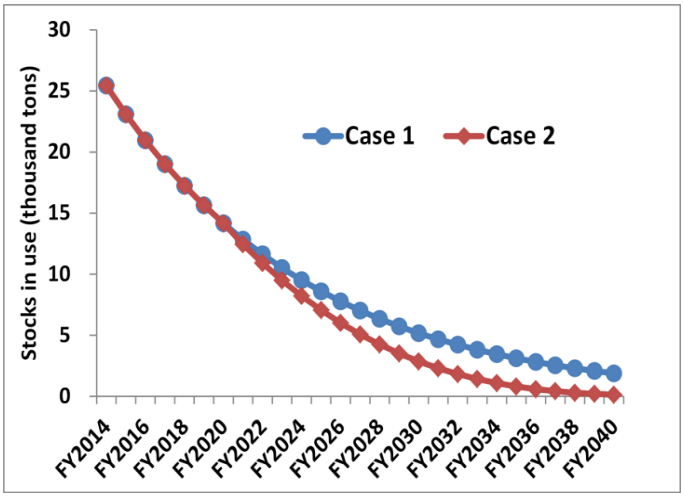

Figure 3.7 Estimating in-use deca-BDE stocks in Japan from 2014 to 2040 with Case 1 where deca-BDE is used as is and Case 2 where deca-BDE is discontinued after 2020

As regards the deca-BDE relevant to case 1, the amount and time trend of the in-use deca-BDE stocks in Japan indicate a considerable amount of this substance would remain until 2030 (5,200 ton) and 2040 (1,900 ton) if deca-BDE were still applied in new products (Figure 3.7). On the other hand, assuming deca-BDE was discontinued after 2020, the in-use deca-BDE stock would be reduced by half in 2030 and by 1/14 in 2040 compared with case 1 (Figure 3.7). Consequently, although the domestic demand for deca-BDE was assumed to be zero after 2020, the stocks in use would remain until at least 2030 (2,900 ton), but would decline significantly in 2040 (130 ton). Abbasi et al. [8] have assumed that deca-BDE was not used in new products after 2013 in the U.S. and Canada. However, these authors have estimated that approximately 70,000 ton of deca-BDE would remain in the use phase by 2020.

Figure A3.3 (in Appendix) shows the estimated atmospheric emissions of deca-BDE in Japan for 2014− 2040, relevant to case 1 and case 2, by using the air emission factor of 1.5×10^{-5} (median value) [9]. Again, by implementing the regulation according to case 2, the atmospheric emissions of deca-BDE would be reduced significantly after 2030 compared with case 1 (Figure A3.3). Consequently, it is crucial to draft appropriate policy measures to reduce the emission of deca-BDE, even though a significant effect would only be discernable a decade later.

In this study, we considered only the first use of PBDE-containing products; therefore, the waste stream and the recycling activity were not included in our assessment. The waste phase of PBDEs and the recycling material could contribute to the accumulation of the in-use stocks and the attendant atmospheric emissions, leading to an underestimation in our values. Accordingly, it is deemed necessary to discuss the omission of these flows in this current study.

3.3.7 Effect of waste phase and material recycling on deca-BDE in-use stocks and the attendant atmospheric emissions

As was shown in the previous section, the in-use stocks of penta- and octa-BDEs in Japan are extremely small; therefore, it is assumed that these POP-PBDE containing products would not have a significant effect on the waste stream and recycling sector. On the other hand, deca-BDE is added mainly to the plastic components of home appliances (e.g., the casings and internal components of vacuum cleaners). The amount of deca-BDE contained in the domestic waste streams in Japan was estimated at 5,300 ton, compared with 60,000 ton of in-use deca-BDE stocks, in 2002 [9]. This finding indicates that less than 10% of the in-use deca-BDE stocks would enter the waste stream annually. Abbasi et al. [8] have presented a similar result, namely, less than 10% of deca-BDE flowing into the waste phase in the U.S. and Canada. In Japan, the disposal of PBDE containing products are usually incinerated and/or landfilled. However, incinerated and/or landfilled would not likely be the main source of deca-BDE emissions to the atmosphere in Japan. In general, landfill could be a source of PBDEs to the air, although evidence on the importance of this emission source is inconclusive [25]. Furthermore,

UNEP. [7] has stated that PBDE emissions were small and therefore of relatively minor environmental significance in industrial countries with state-of-the-art landfills. However, landfilling PBDE-containing wastes is the least preferred option in goal-oriented waste management, and, generally, should be avoided [7].

In Japan, legislation specifies that four types of domestic home appliances should be recycled, including air conditioners, television sets, refrigerators, and washing machines. The recycling processes of home appliances usually include the dismantling and crushing of deca-BDE containing plastic components. Most of the deca-BDE containing crushed plastics are incinerated and/or landfilled. Only a small amount of deca-BDE containing-crushed plastics (100 ton.year^{-1}) was recycled into new products, or was exported [9]. Consequently, the flow of recycled deca-BDE containing products is rather small in Japan. In view of environmental emissions, the life cycle assessment of the back covers of television cabinets containing brominated flame-retardants has revealed that material recycling was a significant contributor to deca-BDE exposure [26]. Accordingly, the material recycling of plastics containing deca-BDE could prolong the resident time of this substance in society and could increase the attendant emission potential. Therefore, the persistence and recirculation of deca-BDE should be prevented. To achieve this aim, the recycling of deca-BDE containing materials should follow the appropriate separation technology recommended by the best available techniques (BAT) and best environmental practices (BEP) under the Stockholm Convention. Or else, the recycling of materials containing deca-BDE should be phased out where feasible [7].

As discussed above, although the waste phase and material recycling flow of deca-BDE containing–products do not likely affect the deca-BDE stocks in use, environmental emissions could potentially occur if waste management were inappropriate. Therefore, material recycling will be incorporated in our future estimation of the stocks and flows of PBDEs in products from use to waste in Japan.

3.4 Conclusion

The estimated decreasing rates of penta-, octa-, and deca-BDEs contained in products in use, based on the domestic demand for PBDEs in Japan and the product lifespan, are consistent with the declining rates of the measured concentrations in ambient air. This agreement suggests that the control measures for commercial PBDEs in Japan have been effective to date. However, if commercial deca-BDE were used as is, the current (2013) and future (until 2040) stocks of in-use deca-BDE containing products would be an ongoing source of deca-BDE emissions to the environment. On the other hand, if commercial deca-BDE were discontinued after 2020, it is estimated that most of the deca-BDE would be phased out by 2040. Therefore, drafting appropriate policy measures to reduce the emissions of deca-BDE nationally is important, even though significant effects would only be apparent after approximately a decade. In addition, to

prevent the persistence and recirculation of deca-BDE, and the attendant emission potential, the recycling of PBDE-containing materials should conform to the appropriate PBDE separation and removal measures.

References

1. Besis A, Samara C (2012) Polybrominated diphenyl ethers (PBDEs) in the indoor and outdoor environments − A review on occurrence and human exposure. Environ Pollut 169:217–229

2. UNEP (2009) Stockholm Convention on Persistent Organic Pollutants (POPs): the new POPs under the Stockholm Convention. http://chm.pops.int/TheConvention/ThePOPs/TheNewPOPs/tabid/2511/Default.aspx . Accessed 18 February 2015

3. European Chemicals Agency (ECHA) (2012) Agreement of the member state committee on the identification of bis (pentabromophenyl) ether [decabromodiphenyl ether] as a substance of very high concern (adopted on 29 November 2012)

4. UNEP (2013) Proposal to list decabromodiphenyl ether (commercial mixture) in Annexes A, B and/or C to the Stockholm Convention on Persistent Organic Pollutants. UNEP/POPS/PORC.9/2

5. UNEP (2015) Report of the Persistent Organic Pollutants Review Committee (POPRC) on the work of its eleventh meeting. Rome, Italy. 19–23 October 2015

6. Japan Ministry of Environment (JMOE) (2014) PBDE demand in Japan. http://www.env.go.jp/chemi/dioxin/chosa/result_h26.pdf (in Japanese). Accessed 26 September 2014

7. UNEP (2015) Guidance on best available techniques and best environmental practices for the recycling and disposal of articles containing PBDEs listed under the Stockholm Convention on Persistent Organic Pollutants

8. Abbasi G, Buser AM, Soehl A, Murray MW, Diamond ML (2015) Stocks and flows of PBDEs in products from use to waste in the U.S and Canada from 1970 to 2020. Environ Sci Technol 49:1521−1528

9. Sakai S, Hirai Y, Aizawa H, Ota S, Muroishi Y (2006) Emission inventory of deca-brominated diphenyl ether in Japan. J Mater Cycles Waste Manag 8:56–62

10. Tokai A, Iwata M, Nakanishi J (2008) Risk Assessment Document Series 23, Decabromodiphenylether. Maruzen Co. (in Japanese)

11. Csiszar SA, Diamond ML, Daggupaty SM (2014) The magnitude and spatial range of

current-use urban PCB and PBDE emissions estimated using a coupled multimedia and air transport model. Environ Sci Technol 48:1075−1083

12. Earnshaw MR, Jones KC, Sweetman AJ (2013) Estimating European historical production, consumption and atmospheric emissions of decabromodiphenyl ether. Sci Total Envi 447:133–142

13. Murakami S, Oguchi M, Tasaki T, Daigo I, Hashimoto S (2010) Lifespan of commodities, Part I. J Ind Ecol 14:598–612

14. Oguchi M, Murakami S, Tasaki T, Daigo I, Hashimoto S (2008) Product flow analysis of various consumer durables in Japan. Resour Conserv and Recy 58:463–480

15. Tasaki T, Takasuga T, Osako M, Sakai S (2004) Substance flow analysis of brominated flame retardants and related compounds in waste TV sets in Japan. Waste Manage 24: 571–580

16. National Institute for Environmental Studies (NIES), Japan (2016) Lifespan database for Vehicles, Equipment, and Structures (LiVES). http://www.nies.go.jp/lifespan/isic_search_e.php. Accessed 18 February 2016

17. BSEF (2010) Brominated flame retardant: Decabromodiphenyl ether fact sheet

18. VECAP (2010) Striving for excellence -annual progress report 2010. Brussels, Belgium: European Flame Retardants Association. http://www.vecap.info/uploads/VECAP_2011_light.pdf. Accessed 18 February 2015

19. Japan Ministry of Environment (JMOE) (2013) Results of the environmental monitoring. http://www.env.go.jp/chemi/kurohon/2013/sokutei/pdf/03_04_14.pdf (in Japanese). Accessed 20 June 2015

20. UNEP (2015) Global monitoring plan under the Stockholm Convention: The 2nd POPs monitoring report Asia-Pacific region

21. Dien NT, Hirai Y, Miyazaki T, Sakai S (2016) Factors influencing atmospheric concentrations of polybrominated diphenyl ethers in Japan. Chemosphere 144:2073–2080

22. Bogdal C, Wang Z, Buser AM, Scheringer M, Gerecke AC, Schmid P, Müller CE, MacLeod M, Hungerbühler K (2014) Emissions of polybrominated diphenyl ethers (PBDEs) in Zurich, Switzerland, determined by a combination of measurements and

modeling. Chemosphere 116:15–23

23. Ma Y, Salamova A, Venier M, Hites RA (2013) Has the phase-out of PBDEs affected their atmospheric levels? Trends of PBDEs and their replacements in the Great Lakes atmosphere. Environ Sci Technol 47:11457–11464

24. Earnshaw MR, Jones KC, Sweetman AJ (2015) A first European scale multimedia fate modelling of BDE-209 from 1970 to 2020. Envi Int 74: 71–81

25. Weinberg I, Dreyer A, Ebinghaus R (2011) Landfills as sources of polyfluorinated n compounds, polybrominated diphenyl ethers and musk fragrances to ambient air. Atmos Environ 45: 935−941

26. Hirai Y, Sato S, Sakai S (2007) Life cycle assessments on recycling of TV cabinet back covers containing brominated flame retardants. Organohalogen Compd 69:920–92

Chapter 4 Technological control measures for Pentachlorophenol (PCP)

4.1 Introduction

4.1.1 The use of PCP

Pentachlorophenol (PCP) was widely used in agricultural and industrial applications as wood preservative, herbicide, pesticide, fungicide and broad-spectrum biocide over the world [1]. Its use has declined due to its high toxicity and slow biodegradation.

4.1.2 PCP contaminated soil

In the USA, several PCP-contaminated sites have been classified as superfund sites [2–4]. Also, the An-Shun site (Southern Taiwan) has been known for its extremely high concentration of PCP (0.312 – 110 μg/g) and polychlorinated dibenzo-p-dioxins and dibenzofurans, in brief, dioxins or PCDD/Fs (36 ng I-TEQ/g) in soil. These high concentrations in the soil around the site of an old factory are related to the former industrial production of chlorophenols (CPs) [5]. There is, therefore, considerable interest in the remediation of this site.

4.1.3 Treatment PCP by nanomaterials

During the last decade, the use of bimetallic particles has been investigated as a means of overcoming the limitations associated with the unmodified ZVI used to degrade halogenated organic compounds (HOCs) [6–12]. Researchers have found that nano-scale Pd/Fe bimetallic particles exhibited higher activity for the transformation of HOCs than primary Fe alone due to their high activity in reduction and catalysis [13–15]. Pd, a precious metal, exhibited excellent catalysis capability in reductive dechlorination of HOCs [13,14]. The enhancement is a consequence of catalytic hydrogenation that results from palladium's ability to intercalate large amounts of hydrogen [16]. The application of Pd/Fe has been well studied in groundwater remediation of chlorinated solvents, such as trichloroethylene [17,18]. Efficient degradation of chlorophenols (CPs) [14,15], hexachlorobenzene [19], and PCP [20,21] by Pd/Fe bimetallic nanoparticles has been demonstrated in the aqueous system. The reactivity of metallic/bimetallic particles and materials decreases over time due to inactivation of the catalyst [22,23]. Under environmental conditions especially sulfides and carbonates are common deposits of oxidized iron. Reactivation of (bi-)metallic materials is possible through acidic rinsing, yet in-situ regeneration of reactive zones is not always technically and practically feasible [24]. One of the strategies explored is to prolong the reactive timespan of the catalyst by applying an acidic polymer-containing coating on the particle surface. Bimetallic particles can be more effectively coated with an acidic layer by adding a polymer. Acidification also activates the catalyst by accelerating hydrogen production and by removing metal oxides coating the particle's surface [21]. For this reason, a novel catalytic biocomposite (BioCAT) has been developed, by coating

biologically encapsulated nanoparticles agents onto the ZVI particle's surface. BioCAT powder contains *hot-spots* of trace amounts of catalytic metals coated onto ZVI particles through a proprietary green production technology. These hot spots *in-situ* generate reactive hydrogen and catalyze reductive dechlorination making the product extremely reactive. BioCAT's co-catalyst is locally alloyed onto microscopic iron cores, by a patented process using a mechanical and thermal field. This innovative dry process is to be compared to the conventional wet synthesis of bimetallic catalysts, in which palladium is precipitated onto ZVI in ethanol [13,17,25], creating a palladium shell surrounding the iron [26] rather than local nanometer size hot spots situated onto the iron surface. Palladium particles maintain their nano-dimensions also after reacting with iron. When using BioCAT catalysis, this incorporation contributes to an increase in surface area and in the number of reactive bimetallic sites on the ZVI surface.

Previous studies focused on PCP remediation by zerovalent iron and Pd/Fe bimetal in aqueous system, and no work describing the application of combinations of catalytic Pd nanoparticles, ZVI, and stabilizing biocomponents to remediate PCP-contaminated soil at room temperature was found in peer-viewed literature. Therefore, this study focused on PCP remediation by BioCAT in a soil system.

4.1.4 The aim of this study

The objective of this work was to assess reductive dechlorination by means of BioCAT catalyst, to evaluate the efficiencies achieved at different dosages, and to propose degradation rates and pathways for remediating PCP-contaminated soils. Reductive dechlorination is based on chloride release and accumulation of lower chlorinated intermediates and non-chlorinated end-products. Additionally, pH and ORP were monitored in an effort to correlate these parameters with PCP removal.

4.2 Materials and Methods

4.2.1 Chemicals

Throughout this study PCP (AccuStandard, >95%) and all other organic reagents (hexane, dichloromethane, acetone, and methanol) used were of analytical grade. All aqueous solutions were prepared in water purified with a Milli-Q system (18.2 MΩ/cm).

4.2.2 Sandy soil samples

Sandy soil samples with average specific surface area (BET) of 3 m^2/g were collected from a construction site close to the campus of National Central University. The composition of the sandy soil was primarily sand with a low clay fraction, expected to be broadly similar to the sandy soil from the An Shun Site [27].

4.2.3 Bimetallic iron (BioCAT) slurry preparation and characterization

A reactive mixture was composed of 99 g of micron-sized zerovalent iron powder together with 1 g of spray-dried microbial biomass, containing palladium nanoparticles stabilized in *Shewanella oneidensis* and prepared according to a modified protocol described in Windt et al. [28]. This mixture was added to one of the milling cups of a Retsch PM 400 ball milling station and the powders were ball-milled for 45 minutes under nitrogen gas atmosphere, to prevent oxidation. Then, 2 g of the resulting milled and mixed powder were added to 18 g of water containing a polyacrylic acid-based thickening agent, and then adjusted with phosphoric acid to pH 5.5, the lowest pH at which the thickening agent was still stable. A thickening agent was added for two main reasons: (i) the increasing viscosity of the particle slurry prevents sedimentation and agglomeration of the particle dispersion and (ii) by adding a polymer, the bimetallic particles can be more effectively coated with an acidic layer since the acidification activates the catalyst. The liquid mixture ('slurry') was stirred gently to obtain a homogeneous dispersion. The resulting mixture is available as a commercial product, BioCAT [29].

Transmission Electron Microscopy (TEM) was used to characterize the palladium nanoparticles stabilized in *Shewanella oneidensis* microbial biomass, according to the protocol first described in Windt et al. [30]. BioCAT bimetallic particles were examined using a high-resolution Philips XL30 Environmental Scanning Electron Microscope (SEM) operating at 25 kV. The microscope was equipped with an EDAX Energy-Dispersive X-ray (EDX) detector type Super Ultrathin Window (SUTW) for quantitative analysis.

4.2.4 Preparation of PCP spiked soil

Sandy soil was pre-cleaned using n-hexane for 12 h to eliminate organic contaminants. The soil was subsequently air-dried in a fume hood for complete removal of hexane. The PCP contaminated soil was prepared by spiking a 50 mg/kg PCP-acetone solution onto the pre-treated soil. The contaminated soil samples were homogenized vigorously for 15 min and then placed for at least 1 day in the fume hood until all acetone was evaporated. The soil was then placed into a brown glass vial and sealed with a cap for 1 day without shaking to allow the PCP to adsorb onto the soil matrix [27]. To determine the PCP concentration in spiked soil, 2.0 g PCP-spiked soil was subjected to Soxhlet extraction using acetone: hexane (1:2) and analyzed by GC/MS. The contamination level was determined as 85±5.7 mg PCP /kg-spiked soil.

4.2.5 Microcosm batch test

Microcosm batch tests were performed in 25 mL closed glass serum vials with septum stopper (Bellco Glass Inc.), as described in Figure 4.1.

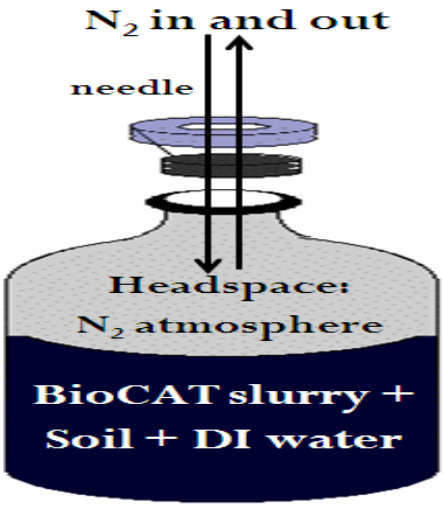

Figure 4.1 Experimental setup for conducting microcosm tests

Different dosages in terms of weight (0 = blank; 200; 400; 600 mg) of BioCAT slurry were prepared from a homogeneous mixture of 20 g BioCAT slurry as described in section 2.2. These dosages were added to serum vials each containing 2 g of dry, PCP- spiked sandy soil; then 3 mL of deoxygenated and deionized water was added to the vials, and these vials were sealed with septum stopper and aluminum cap. Each vial was flushed for 10 minutes with N_2 gas and shaken at 100 rpm for 1 hour with a horizontal shaker. All experimental tests were conducted at 25 (±1) ^{0}C. Soil slurries were collected following degradation times of up to 21 days and measured for pH and ORP. Each experiment was performed in duplicate and average values are presented. Blank samples (without BioCAT slurry) were prepared according to the same procedures. The sacrificial sampling was included in these experiments. The use of sacrificial sampling is particularly necessary in cases where the transformation products (dechlorinated products) were determined and the pH-value and the ORP were monitored at each sampling time. During the course of reaction, the ORP and pH values in the vials were monitored by a pH/ORP meter (Jenco model 6173). Deionized water used for microcosm tests was boiled for 20 - 30 minutes while stirring (closing with a loose lid), cooled to room temperature and then flushed with N_2 for at least 90 minutes.

4.2.6 Extraction and determination of PCP

At the end of each testing period, blank and treated sample vials were collected for analysis of residual PCP and byproducts, after separation of solid and aqueous phases by Whatman filter (blue band). The solid phases (2.0 g) were subjected to Soxhlet extraction for 7 hours with 150 mL of a hexane/methanol mixture (1:1 v/v). The PCP in aqueous phases was extracted by liquid-liquid extraction using n-hexane after pH adjustment to 1 with HCl (0.5 M); then the solvent was evaporated from the resulting extract and the concentrate was again diluted in

hexane. PCP was analyzed by injecting 1.0 μL of the extract into an Agilent 6890 gas chromatograph (GC) equipped with a mass spectrometry detector (MSD) and a DB-5ms column (60 m x 0.25 mm i.d x 0.25 μm film thickness). The GC injector was maintained at 280^{o}C, the detector at 260^{o}C. The oven temperature program included a holding time for 2 min at 60^{0}C, a ramp by 15^{o}C min^{-1} up to 280^{o}C, and a final hold at 280^{o}C for 3 min. With a carrier gas flow of 1.5 mL Helium/min, the retention time of PCP was 14.74 min. Identification of PCP and its byproducts was performed in both the gas phase and soil in the full scan mode from 40 to 500 amu, and compared to standard compounds in the NIST database with matches over 98%. Only dechlorination products were detected. All samples were analyzed in duplicate and average values with standard deviations were shown in the figures.

4.2.7 Chloride analysis

Chloride samples were analyzed using a Dionex DX-120 ion chromatograph. Anion separation was accomplished by an IonPac AS9_HC ion exchange column Dionex. The eluent fluid consisted of a solution of 9 mM sodium carbonate in deionized water. An isocratic flow rate of 1 mL/min was used for chloride analysis. Quantification was facilitated by means of a calibration curve developed from a series of aqueous solutions containing deionized water and known chloride concentration.

4.3 Results and discussion

4.3.1 Characteristics of commercial BioCAT

The bio-Pd component was examined by TEM, and consists of spray-dried microbial biocomponents containing zerovalent metallic palladium nanoparticles with average size of about 10 nm. The surface properties of the BioCAT product used in this study were analyzed by SEM (Figure 4.2 (a) and (b)).

From Figure 4.2 (a), it can be observed that the BioCAT particles were spherical in shape. The individual particle average diameter was measured to be 2 – 3 micron. Upon stronger magnification, at the surface of the individual spheres, small spots of nanometer-size with high density could be observed (Figure 4.2 (b)). These surface hot-spots were further analyzed through SEM-EDX, and were found to be enriched in carbon, palladium and iron (Table 4.1).

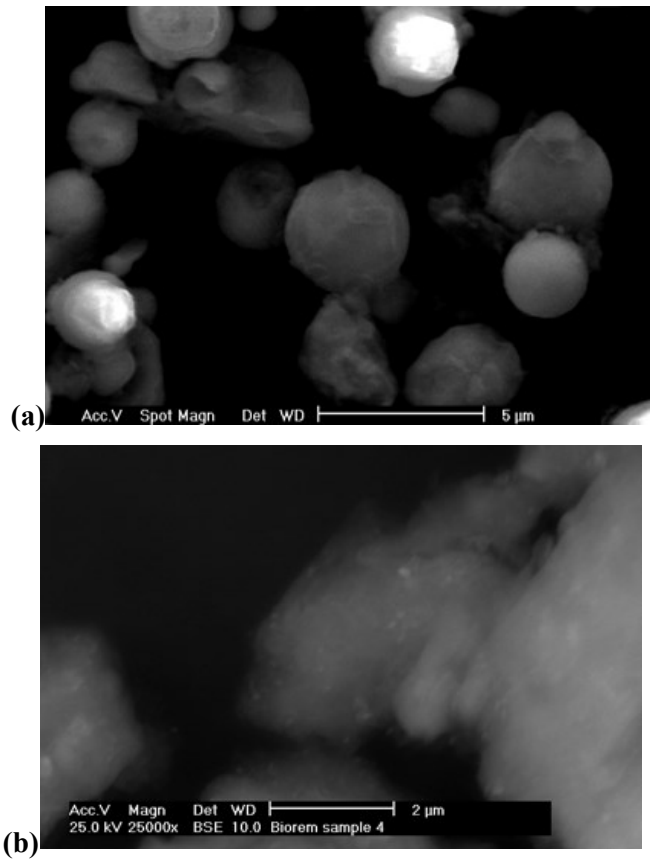

Figure 4.2 (a) Scanning Electron Microscopy picture of individual and spherical BioCAT particles, as used in this study (typical size of 2 to 3 microns) and **(b)** Upon stronger magnification (x25,000), local hot-spots of higher density can be observed at the individual particle surface.

Table 4.1 SEM-EDX analysis of the dense hot-spots located at the surface of the BioCAT bimetallic particles.

Element	Weight Percentage (% wt.)
C	18.28
Na	1.58
Si	0.57
P	0.54
Pd	2.51
Fe	76.52

The carbon in these bimetallic hotpots could originate from microbial biomass used for the biochemical production process of the bio-palladium component, as described in Windt et al. [28].

4.3.2 PCP removal with BioCAT

The total PCP removal efficiencies are calculated by determining the difference between the initial PCP amount on the one hand and the final amount in soil and liquid on the other hand as in Eq 1

$$\text{Total PCP removal (\%)} = \frac{([\text{PCP}]_{\text{initial}} - \{[\text{PCP}]_{\text{in liquid}} + [\text{PCP}]_{\text{in solid}}\}) * 100}{[\text{PCP}]_{\text{initial}}} \qquad \textbf{Eq 1}$$

The amount of BioCAT dosed and reaction time are the two major factors affecting removal efficiency. Figure 4.3 displays these PCP removal efficiencies from sandy soil as a function of time at the three selected dosages of 200 mg, 400 mg and 600 mg BioCAT slurries, respectively.

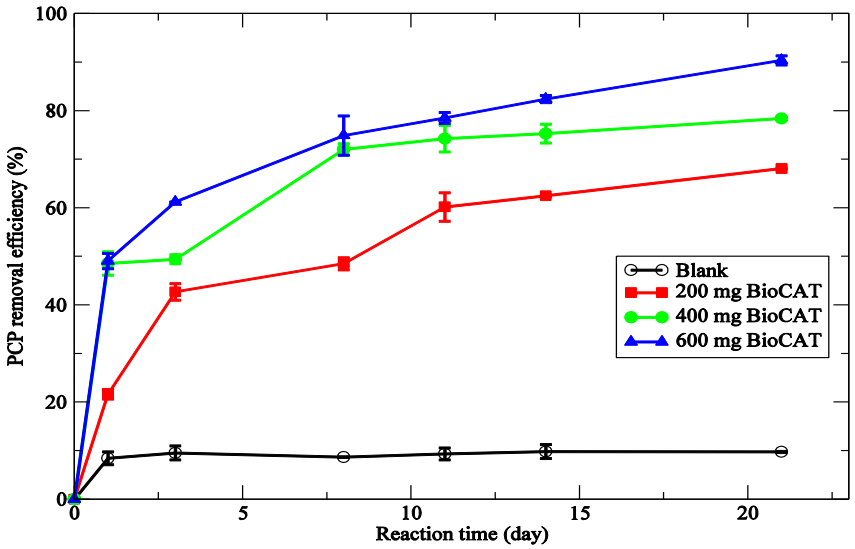

Figure 4.3 Total PCP removal efficiency (%) at three distinct levels of BioCAT dosage

After 21 days of treatment, PCP removal efficiencies of 68.1%, 78.4%, and 90.4% were reached with a BioCAT dosage of 200 mg, 400 mg and 600 mg, respectively. The efficiency increases with rising BioCAT dosage and treatment time. Higher dosage of BioCAT particles substantially speeded up the initial reaction, whereby PCP contacts with greater numbers of active surface sites of iron particles and greater area of adsorptive bio-Pd sites. The blank sample only shows a small initial loss, possibly due to the PCP remaining in the headspace with N_2 atmosphere or adsorbed on walls. All blank and treated samples were analyzed for their PCP content at specific times. Interestingly, most of the PCP in soils desorbs to the liquid phase and the desorptive behaviors are the same for both blank and samples treated with BioCAT (Figure 4.4).

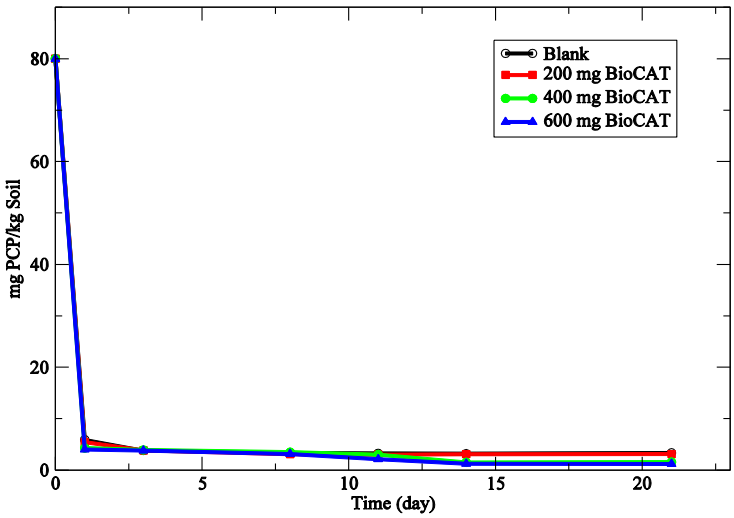

Figure 4.4 PCP remaining in the soil

This can be explained by the high interparticle porosity and the low specific surface area of sandy soil; hence, desorption occurs easily and leads to ready PCP desorption from soil. In principle, PCP is ionizable, yet it is also a hydrophobic organic contaminant (HOC) with $\log K_{ow}$ = 5.05, so that the retention of PCP is strongly related to the natural organic matter content. The sorption ability of PCP in soil increases with high humic acid content [31]. Consequently, in the presence of a higher organic matter content of the soil PCP would remain more attached to the soil, resulting in less desorption to aqueous phase. On the other hand, in this sandy soil with low organic matter, desorption of PCP from soil to the liquid phase should be fast. Therefore, the rate of PCP removal by BioCAT treatment depends on the concentration of aqueous phase and the presence of organics in soil.

A first order model has frequently been used to characterize the iron-mediated degradation of redox-amenable contaminants [32]. According to Zhang et al. [8], Liu et al. [14] , and Zhou et al. [33] dechlorination of chlorophenols and chlorobenzene by bimetallic Pd/Fe and Ni/Fe systems follow pseudo-first order kinetics. Thus, the first order model was applied to describe the elimination of PCP by BioCAT slurry and found to fit well:

$C_t = C_0 * e^{-kt}$ **Eq 2**

(where C_t is the concentration of PCP at time t, C_0 is the initial concentration, k is the first order rate constant (day^{-1}), and t is the reaction time. The first order rate constant is derived from the rate of PCP loss).

First order kinetics effectively describe the degradation of PCP by BioCAT during the full treatment period of 21 days (Figure 4.5).

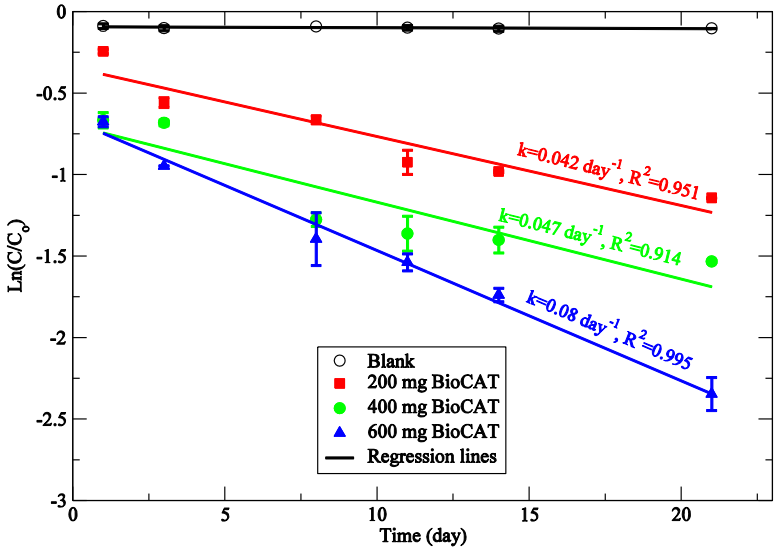

Figure 4.5 First-order rate constants and first-order kinetics linear regression correlation coefficient (R^2)-monitoring during 21 days

First order kinetics fit well at all three dosages. The average decay rate constant (k) during the full 21 days period (Figure 4.5) increases from 0.042 to 0.08 d^{-1} as the dosage rises from 200 mg to 600 mg BioCAT. However, Figures 4.3 also suggests that the PCP level rapidly reduced during the first 8 days and that then the removal rate slowed down. Thus, one could consider involving two different reaction kinetics. The alternative is deactivation, related to e.g. catalyst alteration, or to the creation of mass transfer barriers. During dechlorination, the deposition of ferrous and ferric hydroxides onto the iron surface could passivate the bimetallic surface by hindering the transport of chlorinated molecules as well as by blocking access to reactive sites on its surface [34]. In earlier PCP dechlorination investigations involving Pd/Fe [7, 35], a 40% PCP loss from aqueous solutions over 25 days was not so well described by first order kinetics, as evidenced by the steeper slope of the curve during the first three days reaction time, as compared to the more gradual loss of PCP at longer reaction times; the resulting rate constant was two orders of magnitude lower, at 6.6 (±2.8)x10^{-4}. Kim and Carraway [7] also investigated other bimetal catalysts (Ni/Fe, Cu/Fe, and Pt/Fe), which showed similar reaction rates and non-exponential PCP loss. Gunawardana et al. [36] showed that nickel coated and acid washed (Ni_c/Fe) attained 97% PCP degradation after 25 days, but no kinetic degradation data were presented. The dechlorination of PCP requires good contact with the bimetallic particles and is more challenging in soil than in water. Compared to previous results obtained in aqueous phase [7,35,36], our data show high removal efficiency and decay rate constant in soil-aqueous phases: more than 90% PCP removal efficiency was achieved and a decay rate constant of 0.08 d^{-1} was attained already after 21 days of treatment.

4.3.3 pH and ORP trend

The pH-value in the soil-aqueous solution was monitored during the reaction. Figure 4.6 shows a slight increase in pH-value reached after 21 days of treatment, from 8.28 to 8.68.

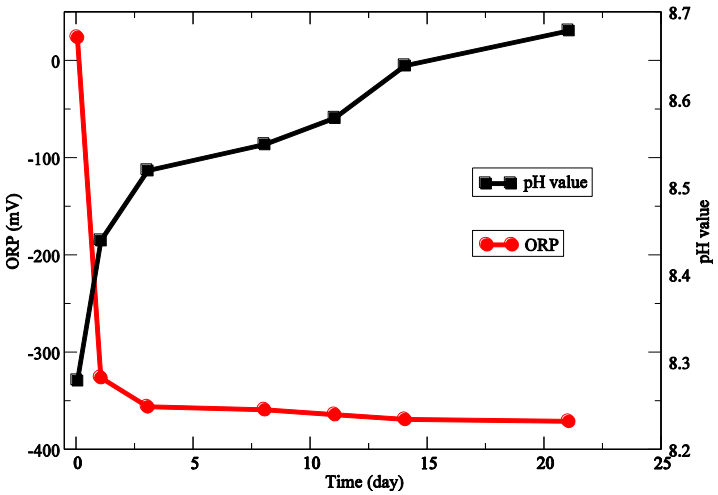

Figure 4.6 Changes in ORP and pH values after 21 days of treatment with 600 mg of BioCAT slurry

The solution pH initially increased steeply and more gradually after that. However, compared to the application of nZVI on lindane [37], pyrene [38] and during atrazine removal [39] the pH range in this study is still low, because the gelling agent in BioCAT composition harbors a local micro pH around the catalyst particle surface. The increase in pH is mainly due to the consumption of protons by hydrodechlorination (Eq 3) and reduction of H_2O in the soil (Eq 4)

$Fe^0 + RCl + H^+ \rightarrow Fe^{2+} + RH + Cl^-$ **Eq 3**

$Fe^0 + 2H_2O \rightarrow Fe^{2+} + H_2 + 2OH^-$ **Eq 4**

$2Fe^0 + 4H^+ + O_2 \rightarrow 2Fe^{2+} + 2H_2O$ **Eq 5**

In contaminated soil with low organic matter and alkaline conditions (pH>8), the bulk of PCP is in an ionized pentachlorophenolate form and interacts mainly with mineral surface [40]. For alkaline pH-values of the soil/water system, metallic/bimetallic particles are easily oxidized and thus covered by oxide and hydroxide, while pentachlorophenolates are chemisorbed on iron oxide surface via inner-sphere coordination. Once the pH reaches basic conditions an oxide or hydroxide film quickly forms on the iron surface and decreases surface reactivity, resulting in lower rates of dechlorination.

According to Eqs 3 and 5, a characteristic increase in pH and decline in solution redox potential (E_H) should accompany any iron-mediated reactions [41]. A reducing environment (E_H

< 0) is created through the rapid consumption of oxygen and of other potential oxidants and by production of hydrogen. Figure 4.6 shows that the ORP quickly dropped during the first 8 days from +25 mV to -360 mV and then slowly declined further to -370 mV, reached towards the end of treatment. Other studies regarding the anaerobic biodegradation of PCP, based upon the release of chloride ions from PCP, indicate that anaerobic (or low redox-potential) conditions are essential for biological PCP dechlorination by microorganisms [42].

4.3.4 Chloride release and accumulation of lower chlorinated intermediates in system

The chloride release is analyzed to determine dechlorination efficiency. This dechlorination efficiency of PCP was defined as the ratio of free chlorides measured to free chloride produced theoretically by complete dechlorination of PCP [8] and can be written as equation (concentration in mM)

$$\text{Dechlorination efficiency (\%)} = \frac{[Cl^-]*100}{5*[PCP]_o} \qquad \textbf{Eq 6}$$

Figure 4.7 shows that the concentration of Cl^- released increases with time and remains close to the concentration of PCP removed at a dosage of 600 mg BioCAT.

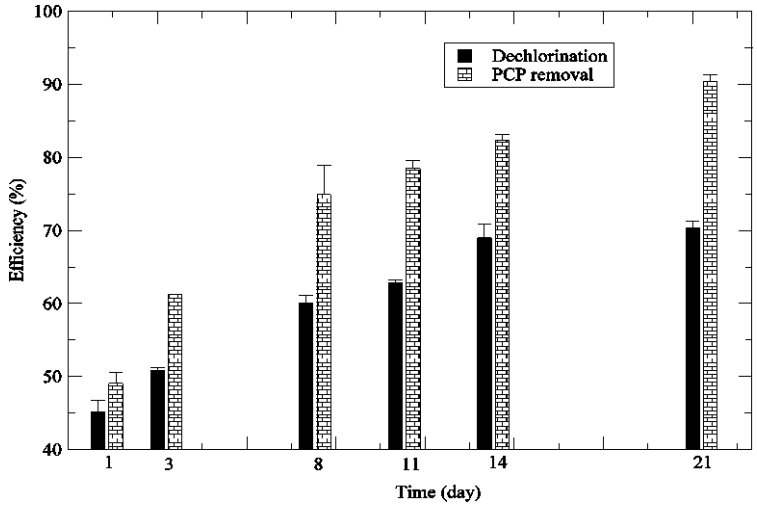

Figure 4.7 Removal and dechlorination efficiency of PCP as a function of time at a dosage of 600 mg BioCAT

On the basis of the stoichiometry of chloride substitutes in the PCP molecule, 70 % of chloride was released after 21 days of treatment with 90 % PCP removal. The 20% remaining removal efficiency is attributable to sorption of PCP on Pd/Fe surface following the reaction: $S\,(\text{sorption site}) + RCl \leftrightarrow S-RCl$ or to sorption of PCP onto soil. In addition, this remaining efficiency may also be attributed to incomplete dechlorination of PCP. These results show that the mechanism of PCP removal is mainly based on reductive dechlorination.

Additionally, other experimental results support the conclusion that the release of chloride ions from PCP was really due to reductive dechlorination by BioCAT slurry, since dechlorinated intermediates were observed during PCP degradation: these intermediates including TeCP, TrCP, DCP, MCP and end-product phenol were mainly found in the liquid phase (Figure 4.8).

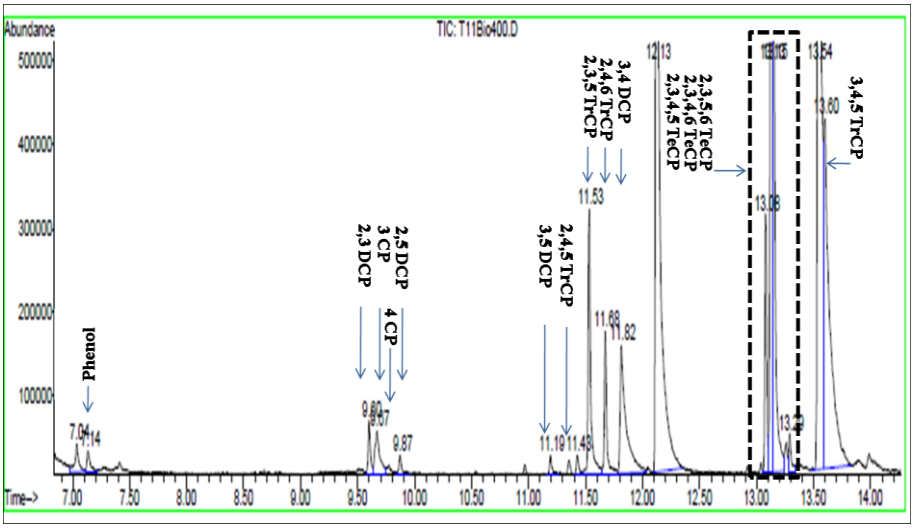

Figure 4.8 Gas chromatographic (GC) analysis of intermediate products at day 11 at a dosage of 400 mg BioCAT slurry/kg-soil

Figure 4.8 demonstrates that BioCAT could efficiently catalyze dechlorination reactions and enhance reductive dechlorination towards completion, i.e. down to phenol. The dechlorinated products of PCP in soil phases and liquid phases were extracted and identified using GC/MS. Due to the poor detection limits of GC/MS for low levels of dechlorinated phenols, it is advantageous to consider peak area to estimate the different levels of lower chlorinated phenols and the initial parent PCP [27]. Thus, the sum of peak areas of each group of CPs is reported.

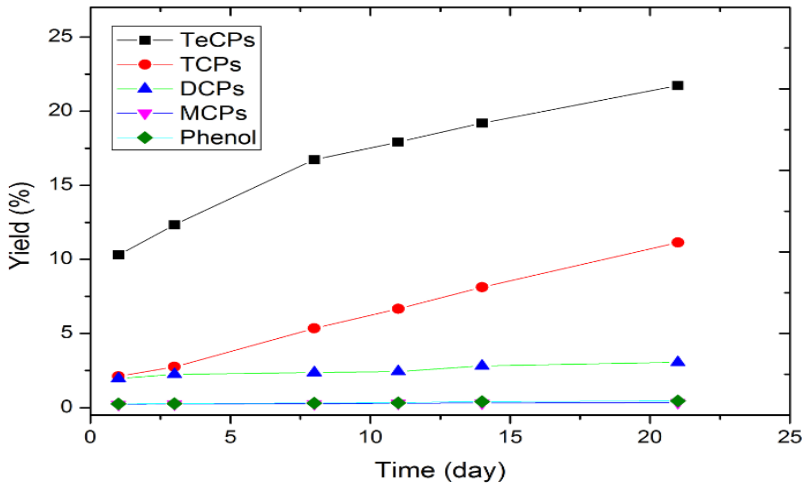

Figure 4.9 Accumulation of lower chlorinated intermediates

Figure 4.9 shows the distribution of intermediates; especially TeCPs, TrCPs, and DCPs, increases linearly with time with very good correlation coefficient of 0.963, 0.973, and 0.959, respectively, while MCPs and the end product of phenol are only found at trace levels. This trend is in good agreement with the accumulation of dechlorination products from reduction of PCP using Pd/Fe found by [7]. The extent of dechlorination becomes more significant as the concentration of lower chlorinated phenol increases. TeCPs are dominant congeners, contributing more than 60 % of total intermediates. Phenol and some lower chlorinated phenols could form volatile phenols in the headspace of the reaction system and be lost for analysis.

4.3.5 Mechanism and degradation pathways

The dechlorination rate of CPs by bimetallics depends on the degree of chlorination of the organic compound [43]. A tentative explanation of this phenomenon is that the energy required to break the C-Cl bond differs for penta-, tetra-, tri-, di- and mono-chlorophenols [43]. Since the rate and extent of dechlorination in bimetallic systems decreases with increase in the number of chlorine atoms on the ring, i.e., the order for the rates of degradation is MCP > DCP > TrCP > TeCP > PCP [6,10,44], the mechanism of dechlorination would be based on carbocations. This mechanism is based on the assumption that dechlorination occurs in two steps. The first step is the cleavage of the C-Cl bond resulting in the formation of a transient electron-deficient carbocation on the phenol ring; the second is the bonding of the carbocation with an electrophile, such as a hydrogen atom derived from the metal hydrides formed on the iron surface, to complete its octet configuration [10,43]. A greater number of chlorines on the phenol ring intensify the positive charge arising from C-Cl cleavage, which destabilizes the carbocation; thereby, lowering the rate of dechlorination [10,43].

Under anaerobic conditions, the bimetallic catalyst generates hydrogen gas at the reactive iron surface (Eq 7) which is converted to reactive hydrogen radicals by the palladium co-catalyst (Eq 8). The radical H* , one of the strongest reductants, attacks pentachlorophenol to replace chlorine and form lower chlorinated phenols and the chloride ions by hydrodechlorination (Eq 9). [14-16, 45]

On an (anoxic) iron surface: $Fe^0 + 2\ H^+ \rightarrow Fe^{2+} + H_2$ (pH < 7) **Eq 7**

On a palladium surface:

$$H^+ + e^- \xrightarrow{Pd} H^* \qquad \textbf{Eq 8}$$

$$C_6HCl_5O \xrightarrow{H^*} C_6H_2Cl_4O \xrightarrow{H^*} C_6H_3Cl_3O \xrightarrow{H^*} C_6H_4Cl_2O \xrightarrow{H^*} C_6H_5ClO \xrightarrow{H^*} C_6H_6O \qquad \textbf{Eq 9}$$

Palladium could promote dechlorination through formation of strong Pd–Cl bonds, thereby accelerating the dissociation of chlorinated hydrocarbons [46]. Furthermore, the hydrogen gas produced is adsorbed on palladium and dissociated into atomic H, one of the strongest reducing

agents in dechlorination [26]. The presence of the less active palladium on the iron surface certainly creates many galvanic cells, in which iron acts as anode and palladium as cathode [26]. Electrons transferred from iron to palladium contribute to the conversion of chlorine atoms to chloride ions [45,47,48]. Hence, dechlorination of PCP by Pd/Fe probably occurs on the palladium surface [16].

The proposed intermediates in the sequentially reductive dechlorination of PCP by BioCAT and the related pathways are illustrated in Figure 4.10.

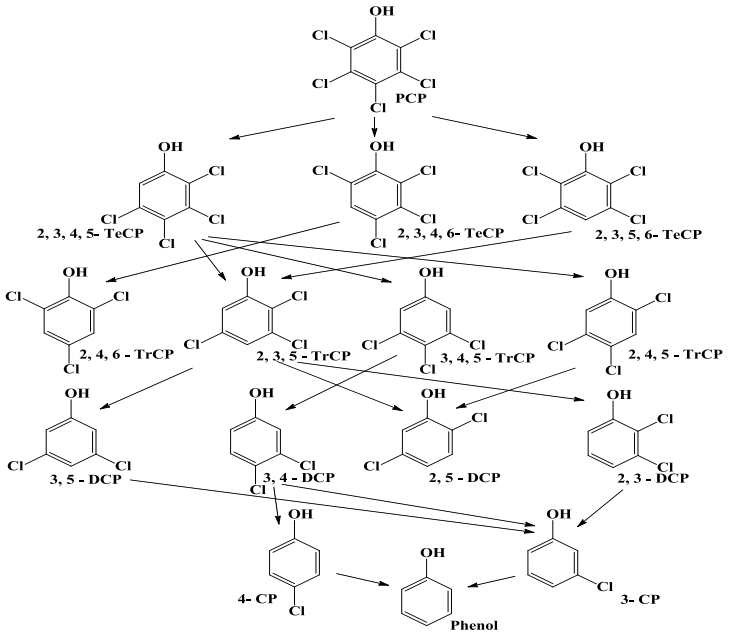

Figure 4.10 General reaction pathways for PCP dechlorination by BioCAT

It indicates that the first step in reductive dechlorination is the loss of one chlorine atom, resulting in all three tetra-chlorophenol (TeCPs) identified as 2,3,5,6-TeCP, 2,3,4,5-TeCP and 2,3,4,6-TeCP. TeCPs continue their dechlorination to form four identified tri-chlorophenol (TrCPs) including 2,4,5-TrCP, 3,4,5 -TrCP, 2,3,5-TrCP, 2,4,6-TrCP. The lower intermediates identified are four di-chlorophenols (DCPs) such as 3,4-DCP, 3,5-DCP, 2,3-DCP, 2,5-DCP and two mono-chlorophenols (MCPs) i.e. 3-CP, 4-CP. Finally, the end product of reductive dechlorination is phenol. The dechlorination of PCP by BioCAT thus occurs through a stepwise reductive dechlorination mechanism. This sequential dehalogenation was also observed during the degradation of hexachlorobenzene [19] and polychlorinated biphenyls [49] with zero-valent iron particles. The toxicity of CPs increases with the degree of chlorination, but decreases with the degree of their dissociation [50]. After reductive dechlorination, the intermediates are less toxic than PCP. Furthermore, lower chlorinated phenols and phenol could be biodegraded more easily than PCP in the environment [51].

4.4 Conclusions

After 21 days of treatment, PCP removal efficiencies of 68.1%, 78.4% and 90.4% were attained with a BioCAT dosage of 200 mg, 400 mg and 600 mg, respectively. This signals a marked improvement in comparison with the blank test. The degradation of PCP by BioCAT follows first order kinetics. The decay rate constant of PCP increased linearly from 0.042 to 0.08 d^{-1} with increasing dosage of BioCAT. On the basis of the stoichiometry of chloride substitution in the PCP molecule, 70% of the chloride released into the water phase was effectively observed. The major mechanism for degradation of PCP in soil-water system by BioCAT was reductive dechlorination. The evidence for reductive dechlorination: the intermediate products (TeCPs; TrCPs; DCPs; MCPs; phenol) were found as well as chloride. Additionally, increase of pH values and strong decrease of ORP values during the reaction also evidenced the reductive dechlorination of PCP. Stepwise dechlorination pathways of PCP with BioCAT were proposed in this study. The results from this study could be applied to remediate PCP-contaminated soil in the field with BioCAT.

It would be interesting if the headspace of the reaction system was analyzed for PCP and end products for closing the mass balance since phenol and some lower chlorinated phenols could also be present as volatile phenols in the headspace. Additionally, we often find an important mass of degradation products accumulating in the headspace, such as phenol, benzene, etc. The same procedure and operating conditions for treating PCP-spiked sandy soil, using a BioCAT slurry, could be adapted for further treatment of soil collected from An-Shun Site. In future work, we will investigate the treatment of OCDD- spiked sandy soil and then apply the findings for simultaneous treatment of PCP and OCDD in real contaminated soil.

References

1. Fisher B (1991) Pentachlorophenol: toxicology and environmental fate. J Pesticide Reform 11:1−5
2. http://www.epa.gov/superfund/accomp/factsheets04/haver.htm (Accessed 10 June 2016)
3. http://www.epa.gov/reg3hwmd/npl/MDD980704852.htm (Accessed 25 Aug 2014)
4. http://www.epa.gov/region4/superfund/sites/npl/florida/escwprefl.html (Accessed 10 June 2016)
5. Environmental Protection Bureau of Tainan City (2004) The pollution survey of two-ninth paths of Tainan City. Report Number 2004-09-25
6. Morales J, Hutcheson R, Cheng IF (2002) Dechlorination of chlorinated phenols by catalyzed and uncatalyzed Fe^0 and Mg^0 particles. J Hazard Mater B90: 97–108
7. Kim YH, Carraway ER (2000) Dechlorination of pentachlorophenol by zero valent iron and modified zero valent irons. Environ Sci Technol 34:2014–2017
8. Zhang W, Quan X, Wang J, Zhang Z, Chen S (2006) Rapid and complete dechlorination of PCP in aqueous solution using Ni–Fe nanoparticles under assistance of ultrasound. Chemosphere 65:58–64
9. Ko SO, Lee DH, Kim YH (2007) Kinetic studies of reductive dechlorination of chlorophenols with Ni/Fe bimetallic particles. Environ Technol 28:583–593
10. Patel UD, Suresh S (2007) Dechlorination of chlorophenols using magnesium-palladium bimetallic system. J Hazard Mater 147:431–438
11. Chen LH, Huang CC, Lien HL (2008) Bimetallic iron-aluminum particles for dechlorination of carbon tetrachloride. Chemosphere 73:692–697
12. Wang X, Chen C, Liu H, Ma J (2008) Characterization and evaluation of catalytic dechlorination activity of Pd/Fe bimetallic nanoparticles. Ind Eng Chem Res 47: 8645–8651
13. Wang CB, Zhang WX (1997) Synthesizing nanoscale iron particles for rapid and complete dechlorination of TCE and PCBs. Environ Sci Technol 31:2154–2156
14. Liu YH, Yang FL, Yue PL (2001) Catalytic dechlorination of chlorophenols in water by palladium/iron. Water Res 35:1887–1890
15. Wei JJ, Xu XH, Wang DH (2004) Catalytic dechlorination of o-chlorophenol by nanoscale Pd/Fe. J Environ Sci 16:621–623
16. Cheng IF, Fernando Q, Korte N (1997) Electrochemical dechlorination of 4-chlorophenol to phenol. Environ Sci Technol 31:1074–1078
17. Lien HL, Zhang WX (2007) Nanoscale Pd/Fe bimetallic particles: Catalytic effects of palladium on hydrodechlorination. Appl Catal B: Environ 77:110–116

18. He F, Zhao D (2008) Hydrodechlorination of trichloroethene using stabilized Fe/Pd nanoparticles: Reaction mechanism and effects of stabilizers, catalyst and reaction conditions. Appl Catal B: Environ 84:533–540
19. Shih YH, Chen YC, Chen MY, Tai YT, Tso CP (2009) Dechlorination of hexachlorobenzene by using nanoscale Fe and nanoscale Pd/Fe bimetallic particles. Colloids and Surfaces A Physicochem Eng Aspects 332:84–89
20. Shih YH, Chen MY (2010) Effect of cations on degradation of pentachlorophenol by nanoscale Pd/Fe bimetallic particles. Sustain Environ Res 20:333–339
21. Shih YH, Chen MY, Su YF (2011) Pentachlorophenol reduction by Pd/Fe bimetallic nanoparticles: Effects of copper, nickel, and ferric cations. Appl Catal B: Environ 105: 24–29
22. Muftikian R, Fernando Q, Korte N (1995) A method for the rapid dechlorination of low molecular weight chlorinated hydrocarbons in water. Water Res 29:2434–2439
23. Gui L, Gillham RW (2002) Evaluation the performance of palladium-plated granular iron for reductive dechlorination of TCE. Proceedings Conference on Groundwater Quality 275:403–408
24. Gillham RW (2003) Discussion of nanoscale iron for dehalogenation. Ground Water Monit Rem 23:6–8
25. Zhang WX, Wang CB, Lien HL (1998) Treatment of chlorinated organic contaminants with nanoscale bimetallic particles. Catalysis Today 40:387–395
26. He N, Li P, Zhou Y, Ren W, Fan S, Verkhozina VA (2009) Catalytic dechlorination of polychlorinated biphenyls in soil by palladium–iron bimetallic catalyst. J Hazard Mater 164:126–132
27. Ngo TT, Chang MB (2012) Investigation of the degradation of pentachlorophenol in sandy soil via low-temperature pyrolysis. J Hazard Mater 229–230:411–418
28. Windt WD, Aelterman P, Verstraete W (2005) Bioreductive deposition of palladium (0) nanoparticles on *Shewanella oneidensis* with catalytic activity towards reductive dechlorination of polychlorinated biphenyls. Environ Microbiol 7:314–325
29. www.bioremengineering.com (Accessed 10 June 2016)
30. Windt WD, Boon N, Bulcke JVD, Rubberecht L, Prata F, Mast J, Hennebel T, Verstraete W (2006) Biological control of the size and reactivity of catalytic Pd(0) produced by *Shewanella oneidensis*. Antonie van Leeuwenhoek 90:377–389
31. He Y, Xu J, Wang H, Zhang Q, Muhammad A (2006) Potential contributions of clay minerals and organic matter to pentachlorophenol retention in soil. Chemosphere 65: 497–505

32. Johnson TL, Scherer MM, Trantnyek PG (1996) Kinetics of halogenated organic compound degradation by iron metal. Environ Sci Technol 30:2634–2640
33. Zhou HY, Xu XH, Wang DH (2003) Catalytic dechlorination of chlorobenzene in water by Pd/Fe bimetallic system. J Environ Sci 15:647–651
34. Chen JL, Al-Abed SR, Ryan JA, Li Z (2001) Effects of pH on dechlorination of trichloroethylene by zero-valent iron. J Hazard Mater 83:243–254
35. Kim YH (1999) Reductive dechlorination of chlorinated aliphatic and aromatic compounds using zero valent metals: Modified metals and electron mediators (Ph. D. Dissertation). Texas A&M University, College Station, TX.
36. Gunawardana B, Singhal N, Swedlund P (2012) Dechlorination of pentachlorophenol by zero valent iron and bimetals: effect of surface characteristics and bimetal preparation procedure. Proceedings of the Annual International Conference on Soils, Sediments, Water and Energy 17:68–81
37. Elliot DW, Lien HL, Zhang WX (2009) Degradation of lindan by zero-valent iron nanoparticles. J Environ Eng 135:317–324
38. Chang MC, Kang HY (2009) Remediation of pyrene-contaminated soil by synthesized nanoscale zero-valent iron particles. J Environ Sci Health A 44:576–582
39. Satapanajaru T, Anurakpongsatorn P, Pengthamkeerati P, Boparai H (2008) Remediation of atrazine-contaminated soil and water by nanozerovalent iron. Water Air Soil Pollut 192:349–359
40. Dela Cruz ALN, Gehling W, Lomnicki S, Cok R, Dellinger B (2011) Detection of environmentally persistent free radicals at a superfund wood treating site. Environ Sci Technol 45:6356–6365
41. Zhang WX (2003) Nanoscale iron particles for environmental remediation: an overview. J Nanoparticle Res 5:323–332
42. Kennes C, Wu WM, Bhatnagar L, Zeikus JG (1996) Anaerobic dechlorination and mineralization of pentachlorophenol and 2,4,6-trichlorophenol by methanogenic pentachlorophenol-degrading granules. Appl Microbiol Biotechnol 44:801–806
43. Gunawardana B, Singhal N, Swedlund P (2011) Degradation of chlorinated phenols by zero valent iron and bimetals of iron: a review. Environ Eng Res 16:187–203
44. Hoke JB, Gramiccioni GA, Balko EN (1992) Catalytic hydrodechlorination of chlorophenols. Appl Catal B: Environ 1:285–296
45. Graham LJ, Jovanovic G (1999) Dechlorination of *p*-chlorophenol on a Pd/Fe catalyst in a magnetically stabilized fluidized bed; implications for sludge and liquid remediation. Chem Eng Sci 54:3085–3093

46. Bodnariuk P, Coq B, Ferrat G, Figueras F (1989) Carbon–chlorine hydrogenolysis over PdRh and PdSn bimetallic catalysts. J Catal 116:459–466
47. Wei JJ, Xu XH, Liu Y, Wang DH (2006) Catalytic hydrodechlorination of 2,4-dichlorophenol over nanoscale Pd/Fe: reaction pathway and some experimental parameters. Water Res 40:348–354
48. Xu XH, Zhou HY, Zhou M (2006) Catalytic amination and dechlorination of *para*-nitrochlorobenzene (*p*-NCB) in water over palladium–iron bimetallic catalyst. Chemosphere 62:847–852
49. Lowry GV, Johnson KM (2004) Congener-specific dechlorination of dissolved PCBs by microscale and nanoscale zero valent iron in a water/methanol solution. Environ Sci Technol 38:5208–5216
50. Titus MP, Molina VG, Banos MA, Gimenez J, Esplugas S (2004) Degradation of chlorophenols by means of advanced oxidation processes: a general review. Appl Catal B: Environ 47:219–256
51. Shen DS, Liu XW, Feng HJ (2005) Effect of easily degradable substrate on anaerobic degradation of pentachlorophenol in an upflow anaerobic sludge blanket (UASB) reactor. J Hazard Mater B119:239–243

Chapter 5 Conclusions and recommendations for future research

5.1 Conclusions

With a large number of PBDE data across Japan, we successfully elucidated the factors influencing atmospheric PBDEs and demonstrated the usefulness of the Tobit model on censored data. We found that all PBDE-congener concentrations that originate from different locations in Japan have exhibited a decrease during 2009−2012. The different behaviors of atmospheric PBDEs are revealed as follow:

- Different temperature effects: higher BDE-47 and -99 concentrations with higher temperature; higher BDE-183 and -209 concentrations with lower temperature
- Different ABL effects: ABL has shown a strong inverse relationship with BDE-47, -99, and -183; however, BDE-209 was less affected by ABL
- Different indoor emission mechanism: mainly volatilization process for BDE-47 and -99; mainly abrasion process for BDE-183 and -209
- Different distribution particle size: mainly associated with fine particles for BDE-47, -99, and -183; associated with fine and coarse particles for BDE-209

By using a population balance model, we estimated that decreasing rates of penta-, octa-, and deca-BDEs (following the pattern: penta > octa > deca) contained in products in use are consistent with the declining rates of the measured concentrations in ambient air. This agreement suggests that the policy and technological control measures for commercial PBDEs in Japan have been implemented effectively to date. In addition, the implication of policy measures on reducing in-use stocks of deca-BDE in Japan in near future was also evaluated. If commercial deca-BDE were used as is, the current (2013) and future (until 2040) stocks of in-use deca-BDE containing products would be an ongoing source of deca-BDE emissions to the environment. On the other hand, if commercial deca-BDE were discontinued after 2020, it is estimated that most of the deca-BDE would be phased out by 2040. Therefore, drafting appropriate policy measures to reduce the emissions of deca-BDE nationally is important, even though significant effects would only be apparent after approximately a decade.

By the means of nanomaterial technology, we effectively treated PCP-contaminated sandy soil by using a commercial preparation of bimetallic iron (Trade name BioCAT). After 21 days of treatment a PCP removal efficiency of 90% was achieved, along with 70% dechlorination efficiency, for a dosage of 600 mg BioCAT slurry/ kg soil. Degradation of PCP by BioCAT follows first order kinetics in PCP. Stepwise dechlorination is the main pathway of PCP elimination from soil slurries contacted with BioCAT. These findings indicate that BioCAT could be applied for field treatment of PCP-contaminated soil under ambient conditions.

The main findings from this thesis play an important role in enhancing the integrated framework for waste prevention of these compounds based on the scientific ground, in adapting

to the Stockholm Convention.

5.2 Recommendations for future research

As discussed above, the combining monitoring data in air and statistical analysis is a crucial pathway for tracking the PBDE emission to the environment and the humans. These tools tell us whether policy and technological control measures on PBDEs have been effective or not. In addition, by extensively analyzing the air data and the related meteorological data (temperature, rainfall rate, ABL), we can gain insight into the atmospheric fate and behavior of PBDEs. Consequently, the regular air monitoring plan is needed to track the POP emission, in order to adapt to the Stockholm Convention. In other aspects, statistical analysis on atmospheric PBDE data would not provide any mechanism on the atmospheric fates and behaviors of PBDEs. In our future work, by combining the ABL values and the particle size distribution of PBDEs, we aim to develop an environmental fate indoor-outdoor model, incorporating the emission strength in indoor air and environmental processes in outdoor media, to elucidate the seasonality of atmospheric PBDEs.

Since the information on emission factors for the new POP (e.g., PCP) and candidate POP (e.g., deca-BDE) have not been available yet, the emission inventory is difficult to estimate. Hence, combining monitoring air and environmental fate model (e.g., reverse model or back-calculate model) offers an opportunity to estimate POP concentration in air and emission inventory.

For developing countries (e.g., Southeast Asian countries), the regular air monitoring plan is costly and difficult to implement. Consequently, the alternative strategies could be based on the existing monitoring data and existing emission factor, by using back-calculate model, to estimate POP concentration in air and then promote emission inventory.

Although the waste phase and material recycling flow of deca-BDE containing–products do not likely affect the deca-BDE stocks in use, environmental emissions could potentially occur if waste management were inappropriate. Therefore, material recycling will be incorporated in our future estimation of the stocks and flows of PBDEs in products from use to waste in Japan.

The same procedure and operating conditions for treating PCP-spiked sandy soil, using a BioCAT slurry, could be adapted for further treatment of soil collected from contamined site (e.g., An-Shun site). The simultaneous treatment of PCP and co-related OCDD in real contaminated soil would be a good challenge in future study.

The policy and technological control measures for PCP and deca-BDE are important to prevent and reduce their exposure to the environment and the humans. Since PCP and deca-BDE have been considered as new and candidate POPs, respectively, PCP and deca-BDE should be treated like other POPs (PCB, PBDE) in BAT and BEP.

Appendix

✧ Tobit regression model with typical assumptions

When there are several observations at the limit y_0 (such as 0 or < LOD) and y_0 varies with year, this feature destroys the linearity assumption so that the least squares method is clearly inappropriate (Tobin, 1958; Amemiya, 1984). The Tobit model was defined as follows (Tobin, 1958):

$y_i^* = \beta_0 + \beta x_i + \varepsilon_i$ (1)

where the subscript i = 1,…, n indicates the observation; β_0 is an intercept; y_i^* is an unobserved ("latent") variable; x_i is a vector of explanatory variables; β is a vector of unknown parameters, ε_i is a disturbance term.

if $y_i^* > y_0, y_i = y_i^*$ (2)

if $y_i^* \leq y_0, y_i = y_0$

The parameters of the model are estimated by using a Maximum Likelihood (ML) method. The assumptions for the Tobit model are that is follows a Linear Regression Model and that ε_i is assumed to follow a normal distribution with mean 0 and variance σ^2 $[N(0, \sigma^2)]$.

The log-likelihood function was given by

$$\log L = \sum_{i=1}^{n} [I_i^{y_0} \cdot \log \Phi\left(\frac{y_0 - \beta \cdot x_i}{\sigma}\right) + (1 - I_i^{y_0}) \cdot (\log \phi\left(\frac{y_i - \beta \cdot x_i}{\sigma}\right) - \log \sigma)]$$

where $\phi(.)$ and $\Phi(.)$ denote the probability density function and the cumulative distribution fuction, respectively, of the standard normal distribution; $I_i^{y_0}$ is the indicator function (Kronecker's delta function) with $I_i^{y_0} = \begin{cases} 1 \; if \; y_i = y_0 \\ 0 \; if \; y_i > y_0 \end{cases}$

✧ The results of paired t-tests on natural logarithm of BDE-47 and BDE-209

```
t.test(lnSBDE47,lnWBDE47,paired=TRUE)
        Paired t-test
data:  lnSBDE47 and lnWBDE47
t = 12.1524, df = 144, p-value < 2.2e-16
alternative hypothesis: true difference in means is not equal to 0
95 percent confidence interval:
 0.7083506 0.9835347
sample estimates:
mean of the differences
              0.8459427
```

```
> t.test(lnSBDE209,lnWBDE209,paired=TRUE)
        Paired t-test
data:  lnSBDE209 and lnWBDE209
t = -5.1812, df = 144, p-value = 7.31e-07
alternative hypothesis: true difference in means is not equal to 0
95 percent confidence interval:
 -0.5280036 -0.2363936
sample estimates:
mean of the differences
             -0.3821986
```

✧ **Confirmation of Tobit model (Wooldridge, 2009)**

Wooldridge (2009), in his classic textbook " Introduction Econometrics: A modern approach" (Chapter 17: Limited dependent variable models and sample selection corrections; specification issues on Tobit models; page 595), stated that one way to informally evaluate whether the Tobit model is appropriate is to estimate a probit model where the binary outcome (w) follows w = 1 if the concentration y_i > max(LOD_i), and w = 0 if y_i <= max(LOD_i). Then, from P($y_i = 0|x_i) = 1 - \Phi(x_i\beta/\sigma)$, w follows a probit model, where the coefficient on x_j is $\gamma_i = \beta_j/\sigma$. This means we can estimate the ratio of β_j to σ by probit, for each j. If the Tobit model holds, the probit estimate, $\hat{\gamma}_i$, should be "close" to $\hat{\beta}_j/\hat{\sigma}$, where $\hat{\beta}_j$ and $\hat{\sigma}$ are Tobit estimates. For example, if $\hat{\gamma}_i$ is significant and negative, but $\hat{\beta}_j$ is positive, the Tobit model may not be inppropriate . Or, if $\hat{\gamma}_i$ and $\hat{\beta}_j$ are the same sign, but $|\hat{\beta}_j/\hat{\sigma}|$ is much larger or smaller than $|\hat{\gamma}_i|$, this could be also indicate problems. These will never be identical because of sampling error, but we can look for certain problematic signs. We should not worry too much about sign changes or magnitude differences in explanatory variables that are insignificant in both models.

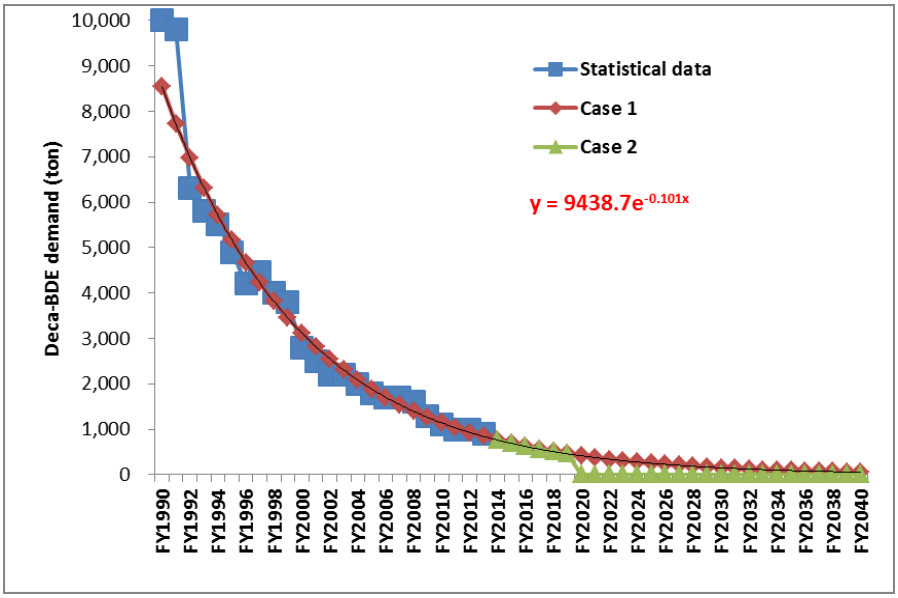

Figure A3.1 Forecasting the domestic demand of deca-BDE in Japan from 1990 to 2040, with Case 1 where deca-BDE is used as is and Case 2 where deca-BDE is discontinued after 2020

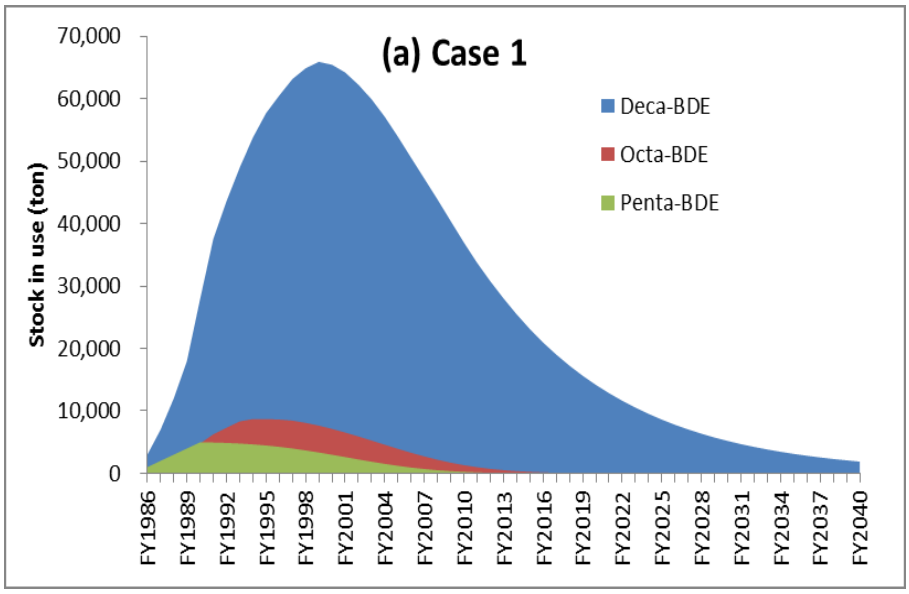

Figure A3.2 Estimating the stock of PBDEs in use in Japan (1986−2040), with (a) Case 1 where deca-BDE is used as is, and (b) Case 2 where deca-BDE is discontinued after 2020

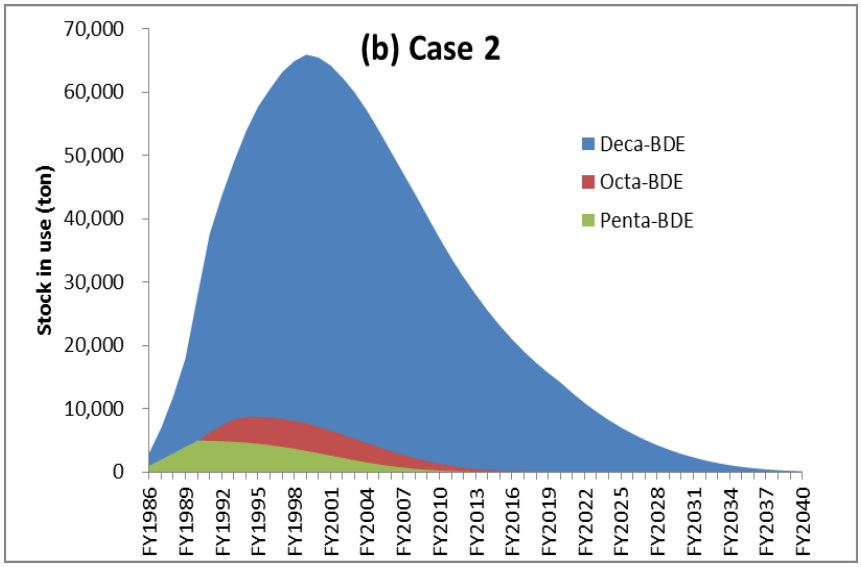

Figure A3.2 Estimating the stock of PBDEs in use in Japan (1986−2040), with (a) Case 1 where deca-BDE is used as is, and (b) Case 2 where deca-BDE is discontinued after 2020

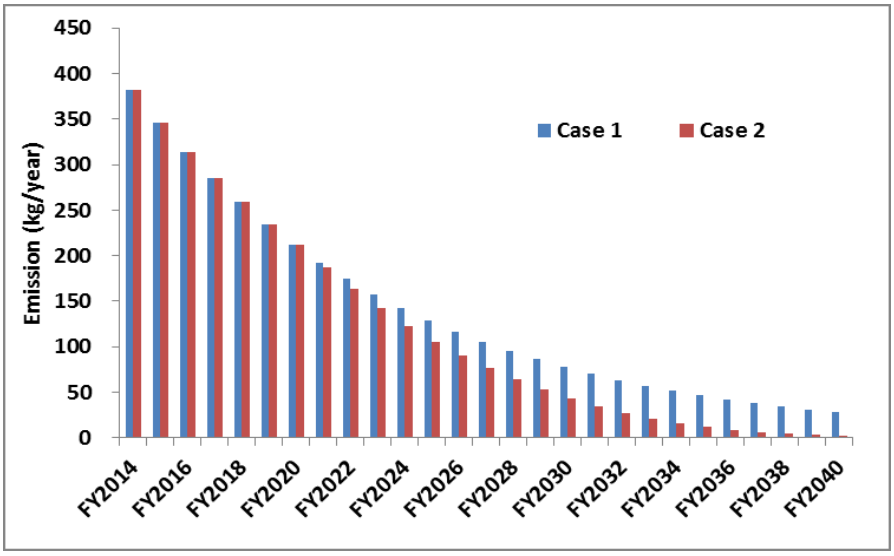

Figure A3.3 Estimating the atmospheric emissions of deca-BDE in Japan (1914−2040), with Case 1 where deca-BDE is used as is, and Case 2 where deca-BDE is discontinued after 2020, by using the air emission factor of 1.5×10^{-5} (median value; Sakai et al., 2006)

Acknowledgement

First and foremost, I would like to express my sincere gratitude to my supervisor, Professor Shin-ichi Sakai for all great support, inspiration and patience during my study. He kindly offered me lots of opportunities to improve my research by attending the scientific conferences. He has trained me how to cooperate in research and to develop the original article as well. I would gratefully acknowledge to him for all supports.

I am deeply indebted to my second supervisor, Associate Professor Yasuhiro Hirai, for his great guidance. Through the regular meeting, I have learnt so many research skills and received lots of insightful comments from him. He inspired me an outlook of research and provided me various research frameworks.

I gratefully acknowledge Professor Moo Been Chang from National Central University, Taiwan for his great supervision on Pentachlorophenol research (Chapter 4 of this thesis). Thank you so much for his supports in the past, present and future.

Besides my supervisors, I would like to thank the rest of my dissertation committee: Professor Minoru Yoneda for his encouragement, insightful comments, and hard questions.

I would like to thank Professor Martin Scheringer from ETH Zurich, Switzerland for his great advice on my research. I got a lot of benefit when attended a short internship in his Institute. Through this intership, I can apply what I learnt for my study.

Many sincerely thanks to Assistant Professor Junya Yano for his kindly supports. He is always willing to help and give his best suggestion to improve my study.

To Associate Professor Misuzu Asari who always give a comfort atmosphere to foreign students including me. Particularly, she has organized and inspired students to various activities regarding environmental education.

I would like to thank all my labmates and members in the Environment Preservation Research Center (EPRC), Kyoto University. Being a foreign student, there were many new things for me, their sincerely help and encouragement have given me a motivation to overcome some troubles in daily life and research. Many thanks to Ms. Shoko Imamura for helping me during three years study at EPRC.

Without Mr. Guochang Xu, Mr. Myo Min Win, and Mr. Raju Poudel, I might not have a wonderful time at Student room. Above all, we have shared the friendship, knowledge, and

encouragement that I will never forget. Many good comments and suggestions, during the Monday seminar, give me an opportunity to improve the study.

I would like to acknowledge financial support from Japanese government scholarship (MEXT). My research would not have been completed without the scholarship. Many thanks to Nong Lam University-Vietnam for open conditions to my study at higher education.

My gratefulness goes to Global Center for Education and Research on Human Security Engineering in Asian Mega Cities, Kyoto University for their excellent program and support for my research.

I would like to send a massive thank to my family who always encourage and believe in me. Their boundless love gives me a motivation to could be able to achieve more successes.

A special thank to my wife - Van Thi Thu Trang. She always shares with me happiness and difficulties with her love and encouragement during our time in Japan.

A big thank to all my dear friends who have shared and encouraged me a lot.

NGUYEN THANH DIEN
August 25, 2016